

PROJECT PERIODIC REPORT

Grant Agreement number: 288869

Project acronym: NAVOLCHI

Project title: Nano Scale Disruptive Silicon-Plasmonic Platform
for Chip-to-Chip Interconnection

Funding Scheme: Collaborative Project

Date of latest version of Annex I against which the assessment will be made:

2011-06-03

Periodic report: 2nd

Period covered: from 2013-05-01 to 2015-07-31

Name, title and organisation of the scientific representative of the project's coordinator¹:

Prof. Dr. Manfred Kohl
Karlsruhe Institute of Technology
Tel: +49-721-608 22798
Fax: +49-721-608 23848
E-mail: manfred.kohl@kit.edu

Project website² address: www.navolchi.eu

¹ Usually the contact person of the coordinator as specified in Art. 8.1. of the Grant Agreement.

² The home page of the website should contain the generic European flag and the FP7 logo which are available in electronic format at the Europa website (logo of the European flag: http://europa.eu/abc/symbols/emblem/index_en.htm logo of the 7th FP: http://ec.europa.eu/research/fp7/index_en.cfm?pg=logos). The area of activity of the project should also be mentioned.

Declaration by the scientific representative of the project coordinator

I, as scientific representative of the coordinator of this project and in line with the obligations as stated in Article II.2.3 of the Grant Agreement declare that:

- The attached periodic report represents an accurate description of the work carried out in this project for this reporting period;
- The project (tick as appropriate) ¹:
 - has fully achieved its objectives and technical goals for the period;
 - has achieved most of its objectives and technical goals for the period with relatively minor deviations.
 - has failed to achieve critical objectives and/or is not at all on schedule.
- The public website, if applicable
 - is up to date
 - is not up to date
- To my best knowledge, the financial statements which are being submitted as part of this report are in line with the actual work carried out and are consistent with the report on the resources used for the project (section 3.4) and if applicable with the certificate on financial statement.
- All beneficiaries, in particular non-profit public bodies, secondary and higher education establishments, research organisations and SMEs, have declared to have verified their legal status. Any changes have been reported under section 3.2.3 (Project Management) in accordance with Article II.3.f of the Grant Agreement.

Name of scientific representative of the Coordinator: Manfred Kohl



.....
Date: ...September.. / .23.. / .2015.....

For most of the projects, the signature of this declaration could be done directly via the IT reporting tool through an adapted IT mechanism and in that case, no signed paper form needs to be sent

Contents

1	Introduction.....	4
2	NAVOLCHI Final Summary	5
3	Core of the Report.....	9
3.1	Project Objectives for the Period.....	9
3.2	Work Progress and Achievements during the Period.....	11
3.2.1	Work Package 1: Project Management.....	11
3.2.2	Work Package 2: Definitions and Specifications.....	11
3.2.3	Work Package 3: Plasmonic Transmitter.....	19
3.2.4	Work Package 4: Plasmonic Receiver	38
3.2.5	Work Package 5: Optical and Electrical Interfaces	56
3.2.6	Work Package 6: Integration, Characterising and Testing	71
3.2.7	Work Package 7: Exploitation and Dissemination	77
3.3	Project Management (Work Package 1).....	89
3.3.1	Request for Amendment	89
3.3.2	Administrative Boards and Decisions.....	89
3.3.3	Management Deliverables.....	90
3.3.4	Communication: Meetings and Phone Conferences	91
3.3.5	New Delivery Dates for Deliverables and Milestones.....	91
3.3.6	Legal Status.....	92
3.3.7	WEB-site.....	92
3.3.8	Management Summary	92
3.4	Deliverables and Milestones Tables.....	93
3.4.1	Deliverables	93
3.4.2	Milestones	95
3.5	Explanation of the Use of the Resources and Financial Statements	98
3.5.1	Manpower	98
3.5.2	Finances	99
4	Attachments	103
4.1	Detailed Explanation of the Use of the Resources and Financial Statements.....	103

1 Introduction

The report here present summarizes the results and achievements during the months 19 to 45 of the NAVOLCHI project. It is the Second Periodic Activity Report out of a list of five major reports during the project:

- First Intermediate Report after 9 months,
- First Periodic Activity Report after 18 months,
- Second Intermediate Report after 27 months and
- Third Intermediate Report after 36 months and
- Second Periodic Activity Report after 45 months.

Additionally, a final report will follow in the end of the project.

As usual for periodic reports, this document contains a section ‘Summary’ which can be published by the EC. Details about the results reached so far, including the achievement of deliverables and milestones, are located in the section ‘Core of the Report’, where each work package is discussed separately. Man power and financial situation of the beneficiaries are attached at the end of the report.

2 NAVOLCHI Final Summary

The Project

The NAVOLCHI project explores, develops and demonstrates a novel nano-scale plasmonic chip-to-chip and system-in-package interconnection platform to overcome the bandwidth, foot-print and power consumption limitations of today's electrical and optical interconnect solutions. The technology exploits the ultra-compact dimensions and fast electronic interaction times offered by surface plasmon polaritons to build plasmonic transceivers with a few square-micron footprints and speeds only limited by the RC constants. Key elements developed in this project are monolithically integrated plasmonic lasers, modulators, amplifiers and detectors on a CMOS platform. The transceivers will be interconnected by free space and fiber connect schemes. The plasmonic transceiver concept aims at overcoming the challenges posed by the need for massive parallel interchip communications. Yet, it is more fundamental as the availability of cheap miniaturized transmitters and detectors on a single chip will enable new applications in sensing, biomedical testing and many other fields where masses of lasers and detectors are needed to e.g. analyze samples. Economically, the suggested technology is a viable approach for a massive monolithic integration of optoelectronic functions on Si substrates as it relies to the most part on the standardized processes offered by the silicon industry. In addition, the design and production cost of plasmonic devices are extremely low and with the dimension 100 times smaller over conventional devices they will require much lower energy to transfer data over short ranges of multi-processor cluster systems. The project is disruptive and challenging, but it is clearly within the area of expertise of the consortium. It actually builds on the partners prior state of the art such as the demonstration of the first nano-scale plasmonic pillar laser. This project has the potential to create novel high-impact technologies by taking advantage of the manifold possibilities offered by plasmonic effects.

Project Status

The second period and extension up to month 45 of the NAVOLCHI project included the fabrication and characterization of all plasmonic devices, in particular:

- metallo-dielectric laser
- absorption, phase and Mach-Zehnder modulators
- receiver, subdivided into the amplifier and QD-photodetector
- passive plasmonic components (optical gratings, optical filters and plasmonic couplers)

In addition, a plasmonic chip-to-chip interconnect prototype has been fabricated, tested and evaluated.

Due to the project extension, most of the targeted objectives for the plasmonic devices could be fulfilled. In particular, outstanding results are achieved by plasmonic phase modulators exceeding

the objectives with respect to speed and size. The highest risk has been the development of the metallo-dielectric laser. Within the time of the project, lasing has not been achieved, yet relatively high on-chip external quantum efficiency and output power has been observed compared to state-of-the-art nanoscale LEDs.

Due to the reduced engagement of the industrial partner ST in the final demonstration of chip-to-chip interconnection, the project had to be reorganized and a new partner ETH was added to the consortium. A contingency plan has been successfully implemented, which comprises a dense plasmonic modulator array operating at 4×36 Gbit/s, an external laser source and Si-Ge photodiodes. The core tasks and detailed results are discussed for each work package 2-6. The various dissemination activities are summarized in the section of work package 7.

WP1 (Project Management) Summary

In the second period of the project, the consortium faced severe difficulties caused by the pullback of ST. The EC accepted an amendment of the projects Grant Agreement containing the admittance of ETHZ as new partner and an extension of the project up to month 45.

As all relevant objectives for the second period have been achieved, the project partners are keen to present a well operating demonstrator device. Based on intense communication between the project partners, no further critical situations occurred.

On the NAVOLCHI-WEB-Site www.navolchi.eu further information can be obtained.

WP2 (Interconnect Specifications) Summary

WP2 investigates the new plasmonic device technology for chip-to-chip interconnection. In the context of WP2, the requirements and needs for chip-to-chip interconnects have been reviewed. In view of the benchmarking review, industrial partner's ST input and all partner's contributions, targeted specifications have been set for the system in order for the plasmonic interconnect to be competitive and, eventually, outperform competing technologies. A simulation platform has been implemented for the design space exploration and the extraction of the sub-system specifications. The simulation platform has been realized with the commercial VPI Photonics software. Three scenarios have been identified for the integration, demonstration and performance evaluation of the NAVOLCHI system: In the first scenario the transmitter is based on the direct modulation of metallo-dielectric laser while in the second and third scenario the transmitter is based on the external laser with a plasmonic based, phase/amplitude MZ modulator respectively. In all cases the collector is based on either a conventional Si/Ge photodetector, or a plasmonic Schottky one. Finally, the interfaces of the plasmonic modules have been defined and the required electronic systems for the transceivers have been implemented and evaluated.

Furthermore, technoeconomical evaluation of chip interconnects with respect to the cost efficiency and power consumption has been performed. The implemented plasmonic-based architecture is evaluated and compared against alternative technologies like photonic and electronic interconnects.

The comparison study is based on the latest data available from NAVOLCHI partners and literature, and is divided in two sections: In the first section, a comparison between conventional electronic CMOS, photonic and the NAVOLCHI project interconnect approach is attempted, on the fields of energy efficiency and implementation details, at present and up to a long term time scale. In the second section, the comparison is specified at the device module level of an interconnect system, for both active (transmitters, receivers) and passive modules (waveguides, couplers), in terms of energy and cost efficiency.

WP3 (Plasmonic Transmitter) Summary

- The main objectives of WP3 are: (1) to investigate via simulations the transmitter which consists of a plasmonic/metallic laser and a plasmonic modulator, and (2) to develop the technology required their fabrication.
- The modelling of both, a Fabry Perot plasmonic laser and a metallo-dielectric nanolaser was carried out.
- The fabrication of the waveguide-coupled metallo-dielectric nanocavities was completed in a III-V membrane on silicon platform.
- Modelling of both, a plasmonic phase modulator and a plasmonic absorption modulator was performed.
- The fabrication of a plasmonic phase modulator has been carried out in a silicon on insulator platform.

WP4 (Plasmonic Receiver) Summary

From previous and new measurements the peak gain of HgTe QDs is of the order of 400 dB/cm for a closed-packed film of this material, indicating that 10 dB gain under optical pumping is feasible. However, results on both closed-packed QD and QDs dispersed on PMMA does not seem to reach such a net gain, possibly because of the HgTe QD photostability. In parallel, the two concepts of hybrid-plasmonic amplifiers incorporating QDs (using polymer and SiN waveguides) have been fabricated and characterized by using CdSe QDs emitting at visible and HgTe QDs emitting at NIR wavelengths. Metal waveguides (planar and ridges) have been fabricated and used to investigate the observed increase of the SPP propagation length by optical pumping of QDs, even if net gain cannot be achieved by the available material.

In the case of photodetectors based on quantum dots important advances have been reached along the project: i) **reproducible** and optimized conductive films of PbS QDs prepared by Dr. blading were achieved along several series of devices, and ii) the best value for the responsivity in Schottky-heterostructure photodetector was very close to **2 A/W** at 1550 nm (and close to 0.5 A/W at 1300 nm). In microgap photoconductors the QD-solid is created by the QD-ink dropping/dispensing on top of prepatterned electrodes and ligand exchange. After the device encapsulation to assure stability, good responsivities (0.1 – 1 A/W under illumination at 1500 nm in the range 1 - 100 nW) are measured by using appropriate bias voltages (15-30 V for 10-20 μm gaps, less than 10 V for 2-5 μm gaps). Nanogap plasmonic detectors are under current work.

WP5 (Optical and Electrical Interfaces) Summary

WP5 focuses on realizing the optical and electrical interfaces for the plasmonic interconnection platform. KTH demonstrated an optimized version of the couplers between silicon and plasmonic waveguides. Through process and design improvements the losses are now below 1dB. In parallel also the simulation of a side coupler was carried out. IMEC carried out simulations and fabrication of a new type of ultracompact grating coupler, aiming at coupling light from QD-devices to the a microscopy system. ST developed a new PHY adapter, and integrated it with the models developed in WP2.

WP6 (Integration, Characterising and Testing) Summary

This work package was under responsibility of ST, which declared to stop work on the work package in the beginning of 2014 (project month 26). From that time on, this work package was led by ETH Zurich who became new partner. During the last reporting period, individual plasmonic components were fabricated, characterized and tested. Furthermore, a concept for a chip-to-chip interconnect link demonstration was developed following the contingency plan according to NAVOLCHI's description of work. The optical interconnect is based on the plasmonic phase modulators of WP3 arranged in a Mach-Zehnder configuration. A modulator array of four channels spaced at 50 μm is fed by an external laser source. The modulator array is packaged into a transmitter including electronic RF amplifiers on a PCB board. On the receiver side, IMEC's Si-Ge photodiodes (PDs) are used with the same channel spacing of 50 μm . The receiver consists of the PDs wire bonded to a PCB board which includes transimpedance amplifiers and driving electronics for the PDs. The optical link between transmitter and receiver was realized using a multicore fiber with a channel spacing of 50 μm . The receiver was successfully tested for operation at 4×28 Gbit/s, the receiver at 3×28 Gbit/s. In first experiments, the full link including transmitter, interconnect and receiver demonstrated to operate successfully at 1×28 Gbit/s.

WP7 (Exploitation and Dissemination) Summary

NAVOLCHI partners have been very active disseminating and promoting the activities and results of the project. The following list summarizes the related activities of the project.

- 37 journals to highly ranked journals
- 74 conference publications disseminating the project have been published by NAVOLCHI partners,
- in addition, a cover article on plasmonic communications has been publish in the May 2013 issue of Optics & Photonics News.
- a white paper on the innovation potential of plasmonic interconnects has been published online,
- communication has been established with plasmonics-related EU-funded project PLATON (<http://www.ict-platon.eu>),
- the project website is up and running with useful information on the project,
- a brochure on NAVOLCHI activities and goals has been issued.

3 Core of the Report

3.1 Project Objectives for the Period

WP1 (Project Management) Objectives

- Performing common project management tasks
- WEB-site preparation and continuous update,
- Intermediate progress reports after month 27 and 36.
- Amendment of Grant Agreement containing ETHZ as new partner and extension of the project run time by 9 months.

WP2 (Interconnect Specifications) Objectives

- Detailed design space exploration of the architectures and extraction of the sub-system specifications
- Integrated system modeling of three architectures based on the developed module's features
- Techno-economic evaluation of the NAVOLCHI architecture and comparison with competitive technologies (conventional electronic CMOS and photonics)

WP3 (Plasmonic Transmitter) Objectives

- Fabricate the plasmonic modulator in a SOI platform
- Fabricate the metallo-dielectric nanolaser in a III-V membrane layerstack bonded to silicon
- Carry out the characterization of both devices (modulator and nanolaser)“

WP4 (Plasmonic Receiver) Objectives

Plasmonic Amplifier:

- IR Quantum Dots (HgTe) with gain.
- Plasmonic Amplifier concept by using polymers incorporating those IR QDs (optical injection).
- Si based Plasmonic Amplifier platform incorporating those IR QDs (optical electrical injection).

Photodetectors using QDs and metal nanostructures

- PbS quantum dots absorbing light at telecom wavelengths and conductive films based on them.
- Photodetectors based on these films reaching responsivities above 0.1 A/W at telecom wavelengths: Schottky/heterostructure vs nanogap/microgap devices.

- Fabrication of nano-gap waveguide photoconductors.

WP5 (Optical and Electrical Interfaces) Objectives

- Fabrication and characterization of the metallic taper photonic-to-plasmonic mode converters
- More comprehensive theoretical study of the MMI based photonic-to-plasmonic mode converters
- Design of second generation grating couplers
- Implement new PHY adapter integrated with developments in WP2

WP6 (Integration, Characterising and Testing) Objectives

- The characterization and testing of the particular active and passive plasmonic devices.
- Its integration with the plasmonic interconnect modules, representing the physical layer (PHY) of such a communication structure and
- The System in Package characterization and testing

WP7 (Exploitation and Dissemination) Objectives

- Dissemination through paper submission to high quality and high impact scientific journals, magazines and white papers.
- Promotion of the project outputs through the participation in conferences and symposia.
- Interaction with other EU-funded and national projects.
- Generation of intellectual property (patents portfolio).
- Theses at the partners' institutes on NAVOLCHI technology.
- Maintenance of the project web site for information and result dissemination purposes.
- Work Progress and Achievements

3.2 Work Progress and Achievements during the Period

3.2.1 Work Package 1: Project Management

Please refer to chapter 3.3 for a detailed description of the activities concerning the project management.

3.2.2 Work Package 2: Definitions and Specifications

This work package investigates the new plasmonic device technology for chip-to-chip interconnection.

Task 2.2 Modelling of devices and system for communications applications

The aim of this task was to give device specifications for the novel disruptive plasmonic Si-photonics devices and its application in the chip-to-chip interconnection environment.

A simulated model has been implemented that it is used for the design space exploration and the definition of the sub-system specifications. The simulation platform has been realized with the commercial VPI Photonics software.

Three scenarios have been identified for the integration, demonstration and performance evaluation of the NAVOLCHI system:

In the first scenario the transmitter is based on the direct modulation of metallo-dielectric laser, a directly modulated laser (DML) - based system in which the data are applied directly on the driving current of the metallo-dielectric laser source.

In the second and third scenario the transmitter is based on the external laser with a phase/amplitude modulator respectively. Specifically, in the second scenario, system consists of a differential phase shift keying (DPSK) transmitter, utilizing the plasmonic MZM driven by the external laser source in continuous wave (CW) mode and with differential phase shift keying (DPSK) detection based on a passive delay line interferometer (DLI) at the receiver. In the third scenario system consists of an intensity modulation transmitter(OOK) utilizing the MZM and the laser source in CW mode, with direct detection at the receiver. In all cases the collector is based on either a conventional Si/Ge photodetector, or a plasmonic Schottky one.

Scenario-1:direct modulation of metallo-dielectric nanolaser(DML)

In the directly modulated laser (DML) - based system, the data are applied directly on the driving current of the metallo-dielectric nanolaser source. Concerning DML laser we have used a VPI DFB laser model and we have set its parameters in such a way so that its output pulse profile to match

exactly the sample data pulse profile we have received from our Navolchi partner, TU/e. Laser structure updated parameters, given as feedback by TU/e, are showed in Table WP2-1 and Table WP2-2.

Metallo-dielectric Nanolaser Characteristics Table	
Parameter	Expected value
Wavelength	1.4 – 1.55 μm
Driving Voltage	> 2V
Current	> 0.5mA (Threshold current = 120 μA)
Device Length	< 1 μm^2
Output Power	Up to 40 μW

Nanolaser Characteristics Table 2-More data given as feedback	
Parameter	Expected value
Confinement factor Γ	0.33
Differential gain	3.768e-16 cm^2
Carrier lifetime	1.256 ns
Differential efficiency	0.16
Optical efficiency	0.34
Coupling efficiency	0.47
Active region volume V	0.042 μm^3
Active region L, h, w	400nm, 300nm, 350nm
Threshold gain	815 cm^{-1}

Table WP2-1 and Table WP2-2: Nanolaser characteristics

External driving electronics would electrically pump the nanolaser, which will be coupled to a conventional fiber interconnection, before sending the signal to the receiver chip (Figure WP2-1). An attenuator is placed between transmitter and receiver in order to simulate overall end to end system losses, mainly those come from conventional fiber interconnection. The photodetector could be either a conventional Si/Ge Photonics detector (IMEC feedback data) or a Plasmonics detector (UVEG feedback data). Finally, at the end of the system a BER tester is used for measuring the system's BER performance.

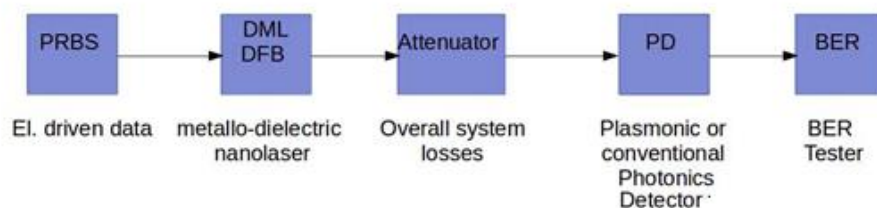


Figure WP2-1: DML scenario

Scenarios 2 and 3: external laser with a phase/amplitude modulator(EML)

In the externally modulated laser (EML) - based system the transmitter is based on the external laser with a phase/amplitude modulator respectively. Specifically, in the second scenario, system consists of a differential phase shift keying (DPSK) transmitter, utilizing the plasmonic MZM driven by the

external laser source in continuous wave (CW) mode and with differential phase shift keying (DPSK) detection based on a passive delay line interferometer (DLI) at the receiver (Figure WP2-2).

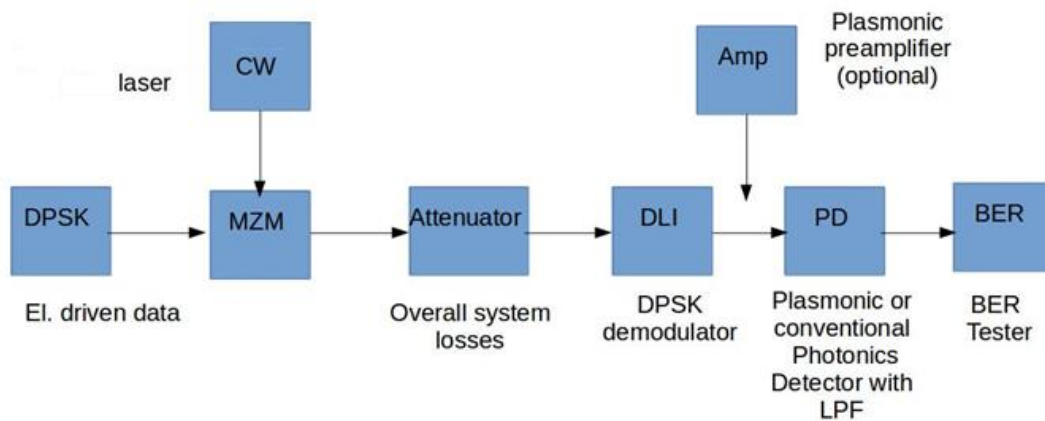


Figure WP2-2: EML DPSK scenario

In the third scenario, system consists of an intensity modulation transmitter(OOK) utilizing the MZM and the laser source in CW mode, with direct detection at the receiver (Figure WP2-3).

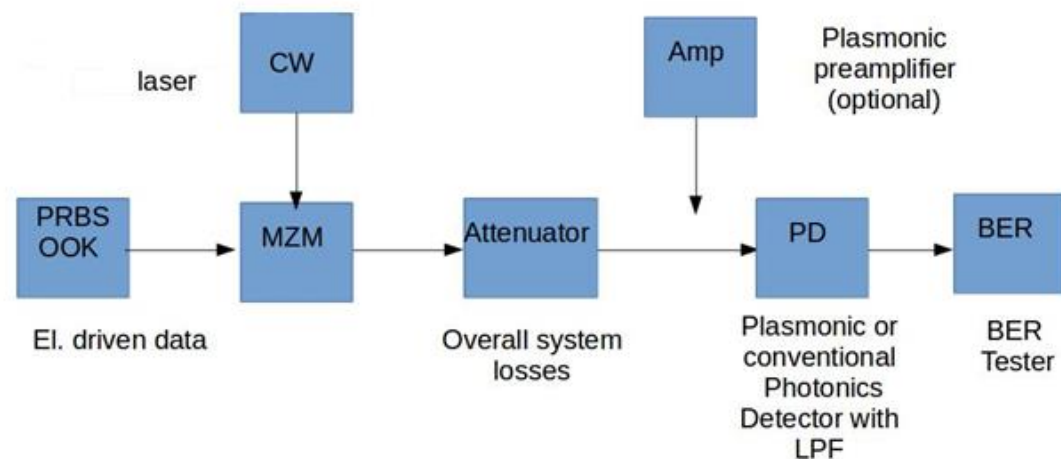


Figure WP2-3: EML OOK scenario

The Bit Error Rate has been calculated for each case, as a system performance means of measurements by sweeping parameters such as the received power or the laser output power or the MZM losses, or amplifier Noise Figure, or receiver sensitivity for default system bitrate (7.2Gbps), and at higher or lower bitrates. Other parameters such as MZ extinction ratio, or laser's linewidth, or receiver's dark current, to name but a few, have been tried out as well, but they didn't seem to affect system BER behavior.

Directly modulated (DML) scenario shows poor BER performance at NAVOLCHI bitrate (7.2Gbps) for such low typical operating nanolaser powers (20-70uW), and at typical conventional receiver's operating responsivities, while at plasmonic typical responsivities, it doesn't seem to operate properly. However, the DML system shows good BER performance at lower bit rates (1Gbps).

On the contrary, both EML simulation scenarios have been extensively carried out, since MZM plasmonic device, has been fully characterized, and hence there is a much more accurate view on system behavior. Obviously, external laser scenarios with MZM show better BER performances than DML but they can be significantly improved by reducing MZM total losses (up to 12dB), especially when system is to be operated at higher than default bit rate (7.2Gbps). Moreover, external laser scenario performance can be greatly enhanced by placing an optical amplifier prior to detector, extending system total loss margins.

The detailed study of the updated simulation model is reported in M39 "Concept for System Integration".

Task 2.5 Technoeconomical evaluation with respect to the cost efficiency and green aspects

In this task, AIT performed a thorough techno-economic study on the plasmonic systems that has been developed in NAVOLCHI. In this study, we have compared the optical and the electronic technologies with the plasmonic technologies and specifically with the developed plasmonic components. A comparison between the aforementioned interconnect technologies and their possible future trends is studied, to find out which technologies are more appropriate for implementing future high speed and energy efficient on-chip and off-chip interconnects. The focus of this study, which is based on the latest available literature tries to identify application areas for the different technologies and their impact on the possible future evolution. Optical interconnects utilizing nanophotonic and plasmonic technology interconnects can implement energy efficient on/off chip interconnects that could successfully meet long term energy requirements for selected HPC and DC applications. Plasmonic based interconnects modules, can be even more cost efficient than photonic ones, building active transmitter and receiver chip modules, usually interconnected with silicon photonic waveguides. The main results of the techno-economic analysis are shown in the following table. The detailed analysis of this report is presented in D2.5 "Technoeconomical evaluation with respect to the cost efficiency and green aspects". The following figure shows also the comparison of the plasmonic devices compared with the nanophotonics devices in terms of energy consumption.

Year	Node techn (nm)	Energy efficiency in pJ/bit				Optical technology roadmap	
		Navolchi (hybrid)	IBM optical	STmicro optical	CMOS convent. (ITRS projected)	Navolchi (hybrid)	Optical
2013	28	10-20	<25	15	30-40	Cu/VCSEL for Backplane	AOC and VCSEL Backplane
2015	24						Si Ph for Backplane
2016-2017	22/20	~5	5	4.4	11-8		Si Ph for interposer and Board
2018	18					Cu/VCSEL and Si Ph. for Backplane	
2019-2020	17/15	~1-2	~1	<1.7	4.5-3		Si Ph on chip
2021-2024	14-11					Cu/VCSEL and Si Ph. for Board	
2025	10	~0.5			1.3	Si Ph. Onto chip	
beyond	9-5	~0.05			0.8		

Table WP2-3: Energy efficiency.

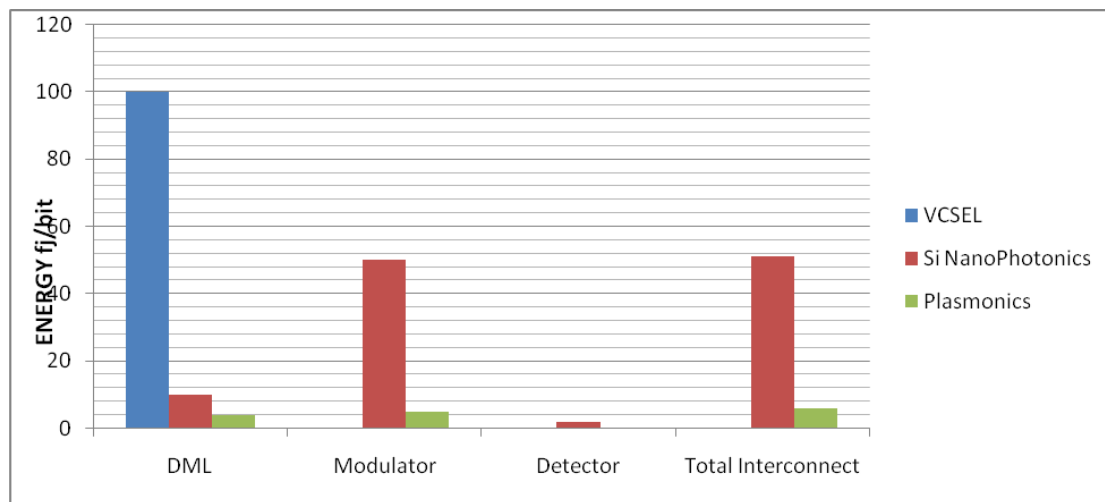


Figure WP2-4: Chip interconnect energy comparison at device module level

Furthermore, a brief analysis has been done for new applications and their opportunities of the developed NAVOLCHI modules. D2.6 (Report on new applications and their opportunities) reports on the new applications of the developed systems in the NAVOLCHI projects. The document presents the main advantages of the developed systems for the plasmonic interconnects and presents their possible application and opportunities in other fields. Specifically, the document describes how the plasmonic laser could be utilized in other applications like sensor systems and biomedical applications. Also the plasmonic amplifier could be utilized to realize more complicated and more efficient sources (e.g. disk lasers coupled to waveguides), albeit optically pumped. Alternatively the developed systems could be used for wavelength conversion. The approach followed for the development of the plasmonic amplifier enables all-optical wavelength conversion at rates matching state-of-the-art converters in speed, yet with significantly cheaper materials

Task 2.5 work progress: VHDL modelling of plasmonic interconnect and CMOS interface circuits [M10-M24]

The objective of this task is the implementation of behavioral models of the plasmonic devices (emitter, detector, modulator, transmission medium) and the CMOS mixed analog/digital circuits responsible for interfacing the digital modules with the plasmonic devices.

The task has been completed on time.

A Verilog-A training has been followed by Alberto Scandurra (ST) on January the 30th/31st 2013 at the Agrate site of STMicroelectronics; Verilog-A is a Hardware Description Language (HDL) extending the classical Verilog language, specific for VLSI digital system, with capabilities for modeling analog electronic devices, as well as photonic, mechanical and thermal systems. This language was supposed to be used for modeling the plasmonic devices in terms of both functionality and physical effects conditioning their behavior (such as temperature variation impact on performance, etc.), and the analog electronic components allowing the digital electronic system to interact with the plasmonic devices, such as emitter/modulator driver, Trans-Impedance

Amplifier (TIA), voltage level adjusters, and so on. However, while carrying out the task, it has been realized that using VHDL for modeling both plasmonic and analog parts at behavioral level was simpler and faster, in particular for what concerns co-simulation with the designed digital parts.

The modeling activity has been carried out between July and October 2013 exploiting a post graduate stage.

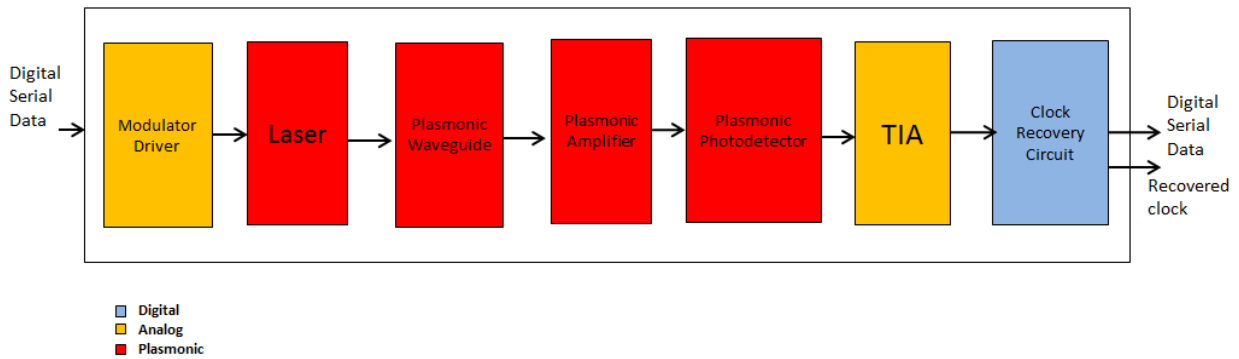


Figure WP2-5: Plasmonic Interconnect Block Diagram (Top-level)

As far as the interface circuits are concerned, they are the digital building-blocks that in the demonstrator will be mapped onto an FPGA in order to have a fast prototype available for plasmonic chip to chip interconnect characterization. These blocks are the serializer and the deserializer already developed last year, bi-synchronous FIFOs to store data and decouple the different clock domains (the slow one of the processing electronics and the fast one of the chip to chip communication) and a set of encoders and decoders allowing to minimize the power consumption (Optical Bus Inverter, Bus Inverter).

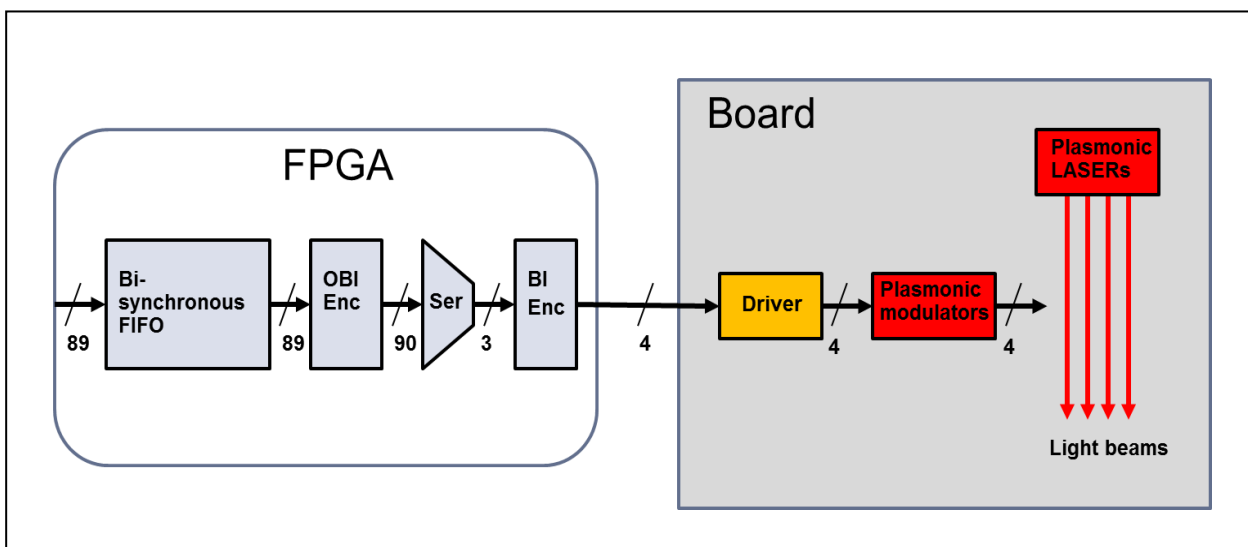


Figure WP2-6: NAVOLCHI demonstrator PHY adapter transmitter

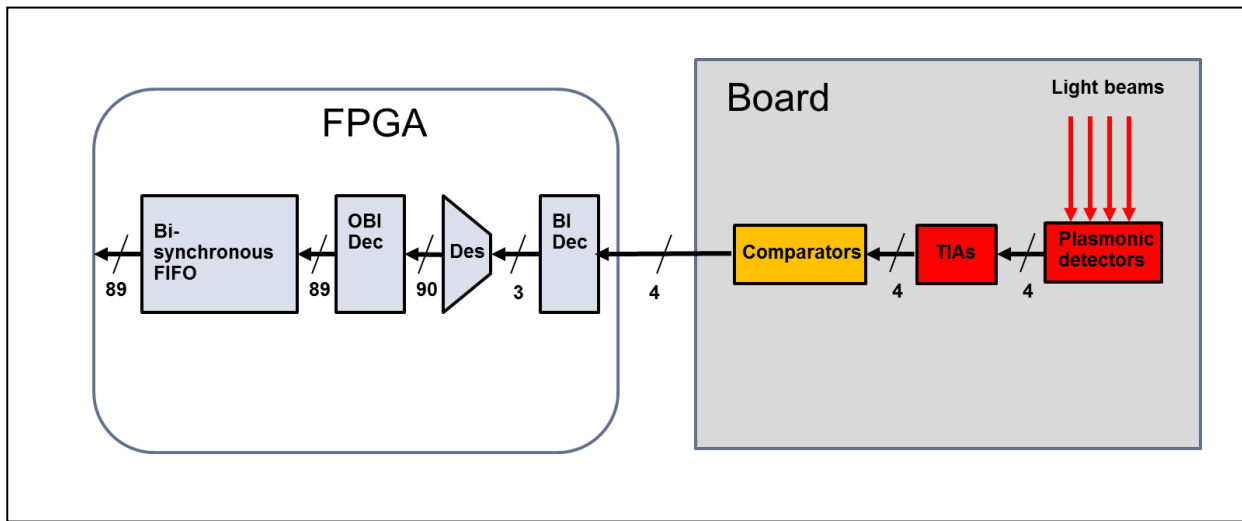


Figure WP2-7: NAVOLCHI demonstrator PHY adapter receiver

3.2.3 Work Package 3: Plasmonic Transmitter

A summary of each WP3 task is presented below. The full description of the modelling results can be found in D3.1 and D3.2, whereas the developed fabrication technology is reported in detail in D.3.3 and D3.4.

Task 3.1. Modelling of plasmonic laser and its coupling

It is one of the aims of WP3 to develop a waveguide-coupled laser with a metallic nano-cavity. This section describes the design of a plasmonic and a metallo-dielectric laser, both coupled to an InP waveguide. An extensive study of the laser modelling has been reported in deliverable 3.1.

Fabry-Perot plasmonic laser

The laser structure proposed is shown in Figure WP3-1, which is based on previously reported plasmonic lasers [1]. The laser consists fundamentally of a MISIM (metal-insulator-semiconductor-insulator-metal) waveguide forming a Fabry Perot resonator coupled to a dielectric waveguide, fabricated on an InP-membrane. The top n-contact and the lateral p-type contact provide the electrical pumping for the InGaAs active medium, which has a bandgap of $1.65 \mu\text{m}$.

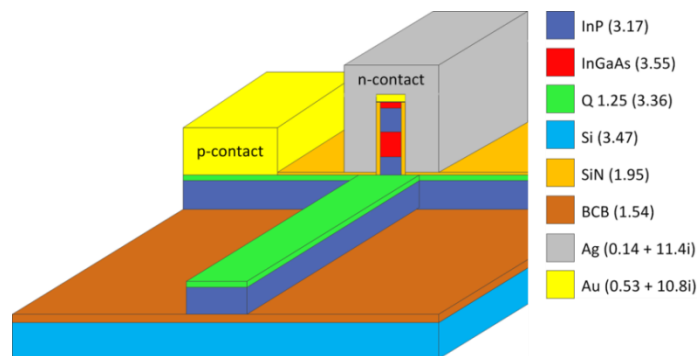


Figure WP3-1: Schematic representation of a plasmonic laser coupled to a dielectric waveguide. The refractive index of each material at $1.55 \mu\text{m}$ is shown in parenthesis. Optical absorption in InGaAs has been neglected for the simulations.

As it can be seen in Figure WP3-2, there is a thin insulating layer of SiN between the semiconductor layer stack and the metal cladding, which serves to insulate the structure horizontally and therefore allow a top-down current flow. The quaternary ($Q\ 1.25$) layer acts as the ohmic contact layer for the p-contact. The back side of the Fabry Perot cavity is completely terminated by metal to achieve a strong reflection, whereas it has an open facet at the frontal end to improve the coupling.

The intensity distribution of the hybrid surface plasmon polariton mode with lowest loss in the cavity is shown in Figure WP3-2b. Due to its plasmonic nature, it has a dominant E_x component and is mainly confined within the insulation layer, which leads to a poor overlap with the active

region. The structure geometry shown in Figure WP3-2a was optimized for a low modal loss and high waveguide coupling efficiency.

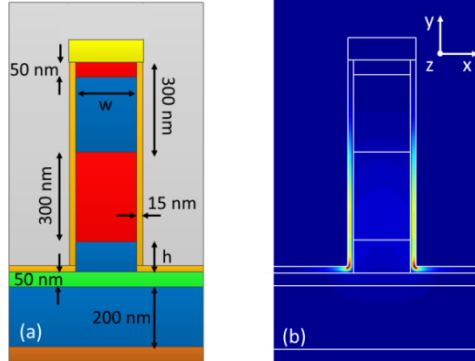


Figure WP3-2: (a) Cross section of the plasmonic laser cavity with the dimensions used for the simulations. (b) Optical intensity of the plasmonic mode at 1.55 μm. Blue: low intensity. Red: high intensity.

To estimate the threshold material gain g_{th} shown in Figure WP3-3, we obtained via simulations the propagation loss α , the confinement factor Γ , and the facet reflectivities R_1 and R_2 . Lasing in a cavity with length L is achieved when

$$g_{th}\Gamma = \alpha + \frac{1}{2L} \ln\left(\frac{1}{R_1 R_2}\right).$$

Figure WP3-3 shows both, optical and differential quantum efficiencies, as well as the threshold gain required to overcome losses. For example, assuming a laser length of 50 μm and considering a cavity with $w = 200$ nm and $h = 100$ nm, it gives $\alpha = 0.16$ dB / μm, $\Gamma = 0.23$, $R_1 = 0.65$ and $R_2 = 0.98$, resulting in a threshold gain of $g_{th} = 1796$ cm⁻¹ with only 5% of differential quantum efficiency, which is theoretically possible at room temperature under a high injected carrier density above $6 \cdot 10^{18}$ cm⁻³ [2].

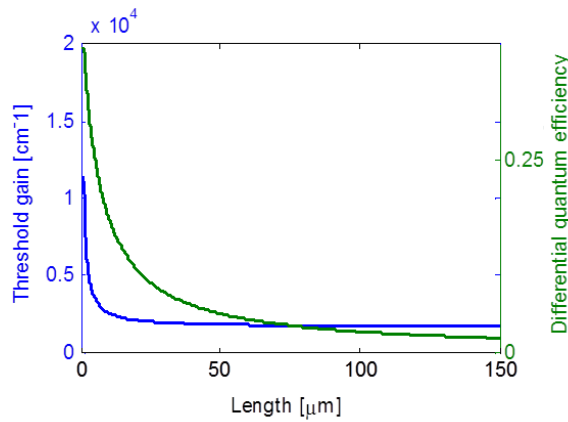


Figure WP3-3: Threshold gain and differential quantum efficiency assuming unity internal quantum efficiency.

Metallo-dielectric nanolaser

In this section, the design of a metallo-dielectric laser with higher performance is summarized. The combination of dielectric and metallic confinement can lead to strong optical confinement of a dielectric mode with relatively low loss, and has been used to demonstrate room-temperature lasing in a subwavelength cavity [3]. Before NAVOLCHI it remained a challenge, nevertheless we achieved waveguide-coupling as reported in MS40.

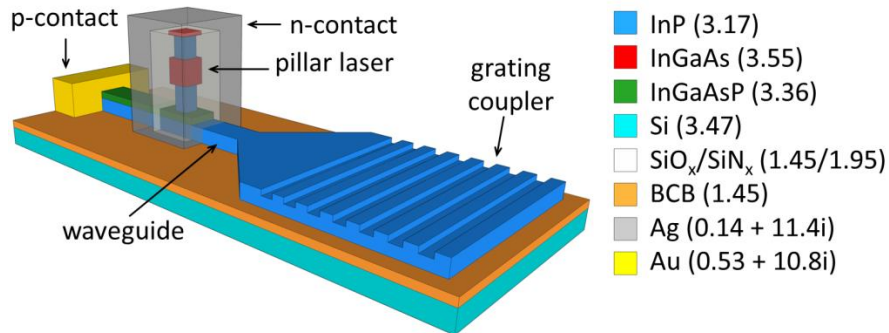


Figure WP3-4: Model of the metallo-dielectric laser coupled to an InP-membrane waveguide. The refractive index of each material at **1.55 μm** is shown in parenthesis.

The proposed laser structure is shown in Figure WP3-4. The semiconductor pillar laser lies on top of a thin InP waveguide and it is insulated with a SiO₂ layer from a metallic cladding. A lateral p-contact is electrically connected to the pillar through a highly p-doped quaternary (InGaAsP) layer. The metallic cladding acts itself as the n-contact allowing a top-down current flow. For simplicity, Figure WP3-4 does not show the ohmic contact layers Ti/Pt/Au, however they were included in the simulation model in order to account for their optical loss.

The optical design of the laser cavity and its coupling to an InP-waveguide was performed with three-dimensional finite-difference time-domain simulations. The cavity supports a TE-polarized mode with high quality factor. The optimized parameters are highlighted in Figure WP3-5a, where **t** is the SiO₂ dielectric thickness, **h** is the height of the InP bottom post and **s** is an undercut. A thick dielectric decreases the absorption into the metal, but also increases the radiative leakage due to a poor confinement. The bottom post controls the Q-factor as well as the coupling to the waveguide. A short post enhances the laser optical efficiency at the expense of a Q-factor decrease. The undercut is introduced to increase the Q-factor, while maintaining a relatively short post to simplify the fabrication process. The optimum values of these parameters were found to be **t = 175 nm**, **h = 400 nm**, **s = 60 nm**. The detailed design is described in [5].

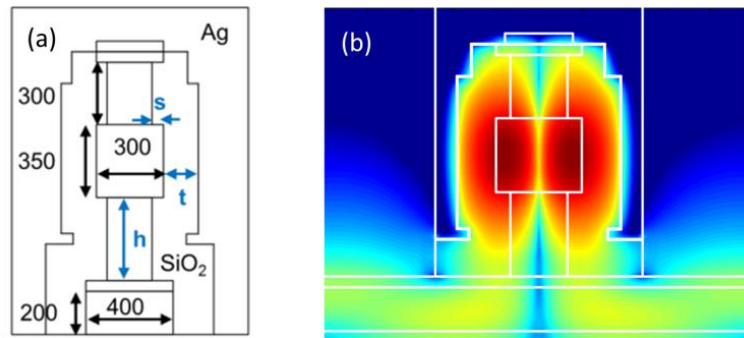


Figure WP3-5: (a) Transversal cross section of the parameterized cavity with dimensions in nanometers. (b) Colour plot of $\log(|E|^2)$ showing the coupling between the lasing mode and the waveguide along the longitudinal cross section.

After the optimization of a symmetric pillar cavity, the longitudinal dimension (along the outcoupling waveguide) of the pillar was increased to enhance the waveguide coupling, which in turns enhances the differential quantum efficiency. The differential efficiency is defined as the number of photons injected into the waveguide divided by the total number of photons generated in the cavity. Furthermore, the resonant wavelength can be adjusted, since it increases linearly with the cavity length. As it can be seen in Figure WP3-6, a cavity length of **400 nm** results in a resonant wavelength near **1.55 μm** , a Q-factor exceeding 500 and a differential efficiency of **0.16**. Considering a confinement factor of **0.33**, the threshold gain is calculated to be **815 cm^{-1}** , which is expected to be achievable at room temperature.

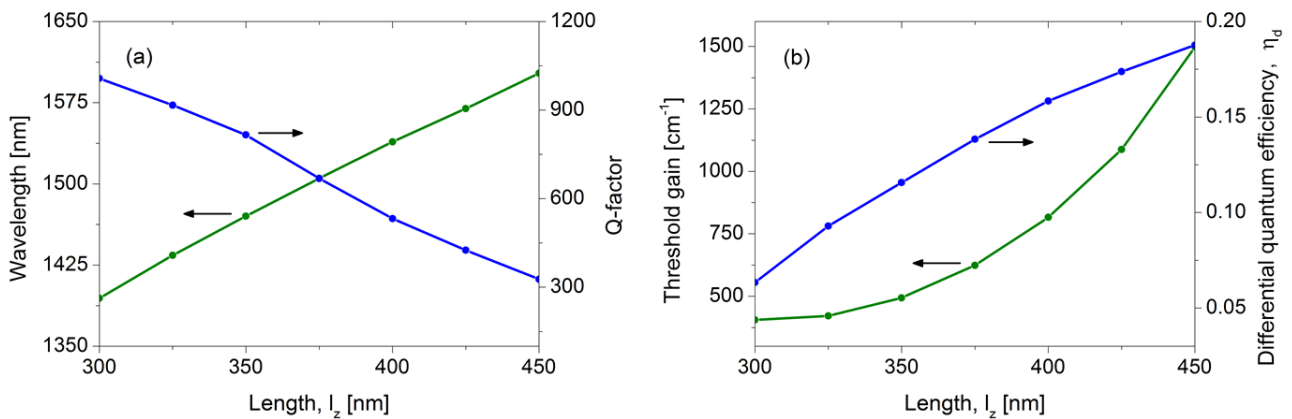


Figure WP3-6: (a) Resonant wavelength and Q-factor as a function of cavity length. (b) Threshold gain and differential quantum efficiency, assuming a unity internal quantum efficiency.

Additionally, electrical and thermal simulations were carried out to determine the expected threshold current and maximum output power due to self-heating. A detailed description of such simulations can be found in [6].

This metallo-dielectric laser device was the design of choice to fabricate since it offers a better performance while maintaining reduced physical dimensions.

Task 3.2. Modelling of Si-plasmonic modulators

Within the framework of NAVOLCHI, two different modulator approaches have been studied. The modelling of these two concepts, direct amplitude modulation employing surface plasmon polariton absorption modulator [7, 8] and phase modulation with plasmonic phase modulator [9], shall be reviewed in the following section. Detailed modelling results can be found in deliverable D.3.2.

Surface Plasmon Polariton Absorption Modulator

Surface plasmon polariton absorption modulator is a device where the absorption coefficient of surface plasmon polariton (SPP) is modulated by an externally applied voltage. The essential parts of the SPPAM are highly conductive metal layers (e.g. Au, Ag) and middle active section consisting of metal oxide (Indium Tin Oxide) and high dielectric strength insulator (SiO₂, HfO) layers, see Figure WP3-7. Such a structure sustains highly confined SPP mode, which represents strong optical field confinement in ultrathin metal oxide layer [7, 8]. Consequently, the dispersion relation of the SPP is predominantly sensitive towards the optical properties of ITO thin film, particularly to its free carrier density. The voltage applied between the two electrodes induces charge accumulation layer in ITO. As a result, the free electron density of ITO is modified by the applied voltage which results in a change of the absorption coefficient of SPP.

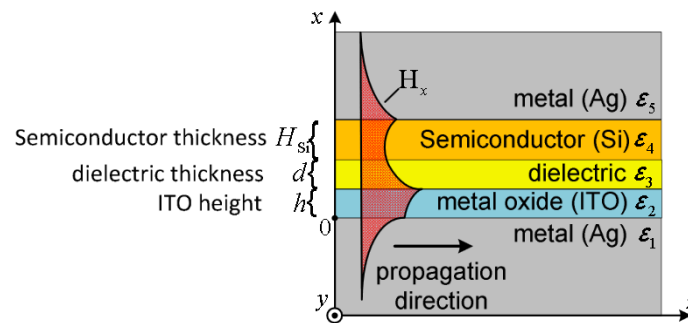


Figure WP3-7: The SPPAM geometrical structure studied in NAVOLCHI. The SPPAM approach reported comprising metal / semiconductor / metal-oxide / dielectric / metal layers.

To estimate the performance of the SPPAM, we have used the combination of the dispersion relation (Section 1.1. in D 3.2) and the accumulation layer (Section 1.2 in D 3.2) solvers. In Figure WP3-7, we show one of the structures which have been considered as possible candidates for the SPPAM.

As optimization parameters, we use the dielectric height d and the ITO height h , as referenced in Figure WP3-7. We define the figure of merit to $FoM = \frac{L_e}{L_{1dB}}$, where L_e is the propagation length of SPP and L_{1dB} is the length necessary for having an extinction ratio of 1dB for the given 4.5Vpp voltage. The larger the FoM, the better is the performance of the modulator, i.e. the lower the propagation losses are for a 1 dB extinction ratio and an applied on-voltage of 4.5 Vpp. Overall the report, the silicon thickness H_{Si} is assumed to be 220 nm, a standard device layer height in Silicon

Photonics. As a result, we see in Figure WP3-8 that an increasing FoM and the least device length are reached for decreasing dielectric layer thickness.

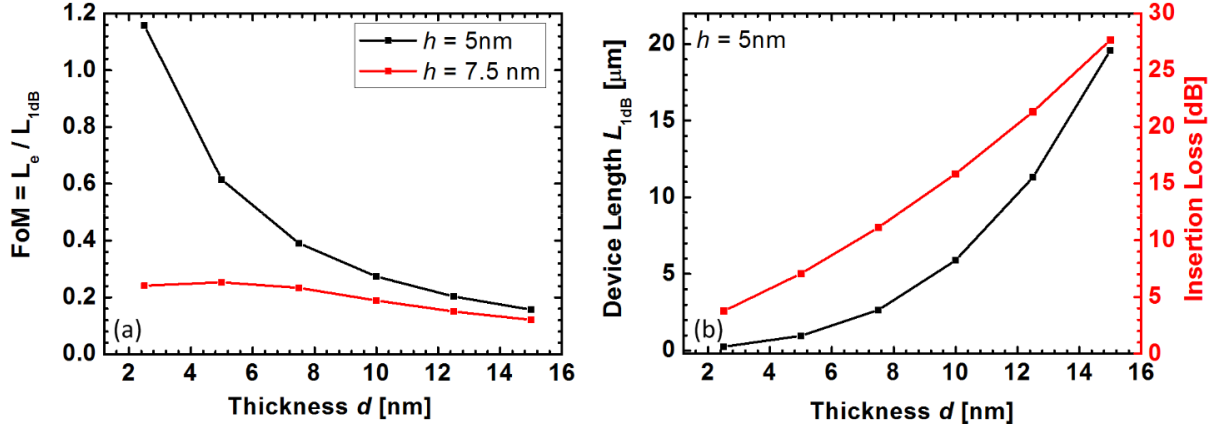


Figure WP3-8: Characteristic quantities of semiconductor based SPPAM. The figure of merit for various silicon dioxide and ITO thicknesses (a) and 1dB device length and insertion loss for 5nm of ITO thickness.

Surface Plasmon Polariton Phase Modulator

SPP based phase modulator [10] can be designed making use of metal-insulator-metal structure and replacing passive insulator layer with linear electro-optically active nonlinear optical (NLO) material, see Figure WP3-9. Externally applied static electric field E_{stat} changes the refractive index of the NLO material, thus changing the phase of the SPP mode. The refractive index change happening in the nonlinear material can be given as [11]

$$\Delta n = \frac{1}{2} r_{33} n_{NLO}^3 E_{stat} = \frac{1}{2} r_{33} n_{NLO}^3 \frac{U}{d}$$

where r_{33} and n_{NLO} are the linear electro-optic coefficient and the refractive index of the nonlinear material, E_{stat} is the strength of the static electric field. Typical NLO materials studied in NAVOLCHI are electro-optic polymers with a typical refractive index n_{NLO} of 1.6 and 1.7. Such NLO material can be synthesised with relatively large nonlinear coefficient thus ensuring the ultra-compact size of the device as well as small driving voltage [10].

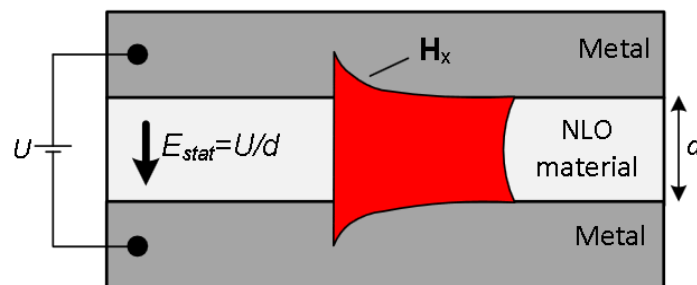


Figure WP3-9: Geometry of the plasmonic phase modulator comprising linear electro-optically active material sandwiched between two metals.

In order to compare various geometries for phase modulators, we define the figure of merit as a ratio of the SPP propagation length L_e over the length L_π necessary for accumulating a phase shift of π relative to the voltage off state: $FoM = \frac{L_e}{L_\pi}$. The larger FoM, the shorter L_π and the longer L_e

are i.e. the smaller the device footprint and the insertion losses are. The first decision that has to be made on the modulator structure is the material system which has to be used, that is the choice on the metal electrodes as well as on the nonlinear polymer. We have assumed commercially available NLO polymer [12] with a refractive index of 1.6 and 1.7. The high conductivity of the metal electrodes ensures the potentially high speed characteristics of the device. Therefore, the choice of the metal only depends on technological aspects as well as on their optical losses. It is well known that silver has the highest conductivity and thus the least optical losses, consequently, the structure employing silver electrodes result in a higher figure of merits. Increasing the refractive index of the insulator – in this case of the polymer - the characteristic surface plasmon frequency reduces resulting in lower group velocity, thus resulting in reduction of the L_π via enhancement of light-matter interaction.

Below, we show the figure of merit calculated for the various polymer heights for the case of both silver and gold. In summary, we can conclude that the performance of the device strongly depends on the polymer thickness d especially in the range of the small values and saturates while increasing the thickness d . Because of the technological challenges in fabrication process, the polymer thicknesses below 50 nm are ignored and the focus has been paid more on the relatively large polymer thickness i.e. above 50 nm.

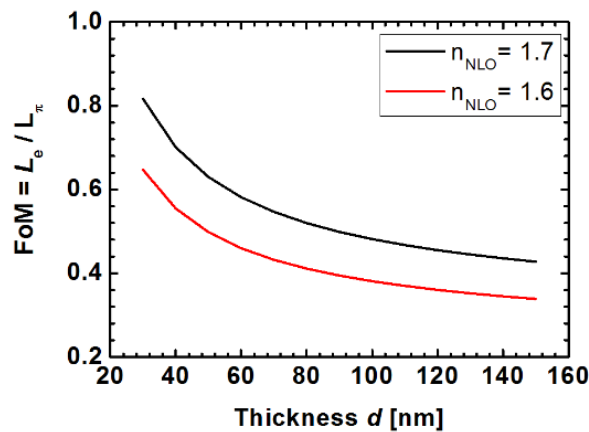


Figure WP3-10: Figure of merits of the device for various nonlinear material size d and for $n_{NLO} = 1.6$ and $n_{NLO} = 1.7$ refractive indices. In the calculation applied voltage is assumed to be 4.5 Vpp. Silver electrodes have been considered.

The plasmonic phase modulator approach is preferred over the SPPAM reported in [7], because of its relatively large figure of merit and easy coupling structure. The decision is also supported by the fact that the plasmonic phase modulator [10] is relatively easier to fabricate comparing to the absorption modulator [7]. Below in the document we give the possible approach for fabricating plasmonic phase modulator.

Further modelling details, e.g. with respect to photonic-to-plasmonic coupling structures and electronic properties can be found in deliverable D.3.2.

Task 3.3. Fabrication of plasmonic/metallic laser

In the following, a summary of the technology developed to fabricate the device is presented. The detailed technology including the process flow was reported in “D.3.3 – Fabrication of plasmonic laser device”.

The fabrication process requires a variety of techniques, such as electron-beam and optical lithography, plasma-enhance chemical vapour deposition of dielectrics, reactive ion etching processes, wet-chemical etching, thermal and electron-beam evaporation of metals, rapid thermal annealing, etc.

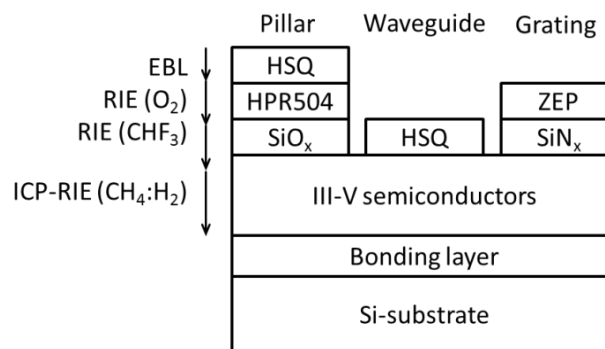


Figure WP3-11: Processing schemes to fabricate the nanostructures. The top layer of each lithographic scheme is always defined by EBL and development.

After epitaxial growth of the layer stack, the fabrication starts with the bonding process of III-V to silicon by means of BCB (Benzocyclobutene). Then, the definition of the nanostructure is carried out by electron-beam lithography (EBL) due to the high resolution required. This is done in three EBL steps using different lithographic masking schemes (depicted in Figure WP3-11). During the first lithography, the nanopillar is defined. Later, an overlay exposure is needed to define the waveguide and, finally, the grating coupler is defined with another overlay exposure. The result is shown in Figure WP3-12a.

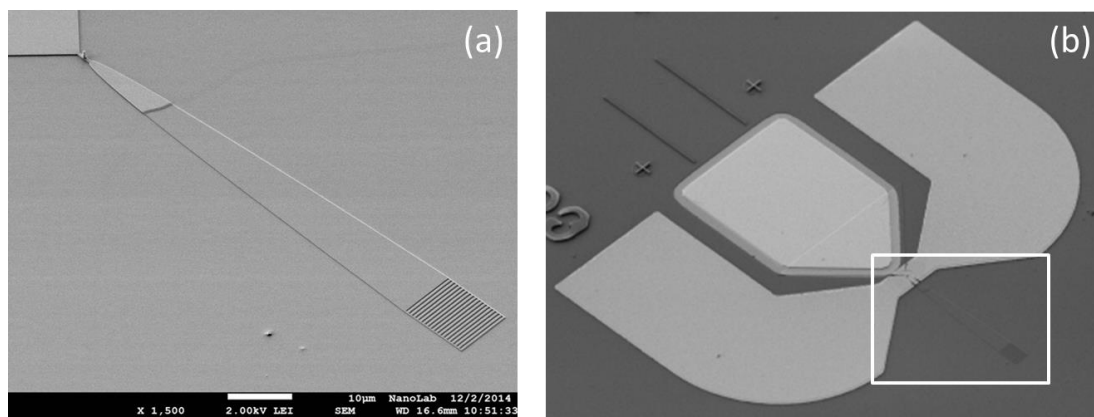


Figure WP3-12: (a) Panoramic view after the pillar, waveguide and grating coupler fabrication by three e-beam lithography steps. This device region corresponds to the region indicated in Fig. 3b with a white square. (b) Panoramic view after metallization of the device.

After the nanostructures have been fabricated with EBL, dielectric and metallic layers are deposited to form the metallo-dielectric cavity and do the metallization of the device in order to complete the fabrication as shown in Figure WP3-12b. This is carried out by means of five optical lithography steps. The fabrication of the waveguide-coupled cavities was completed.

Task 3.4. Fabrication of Si-plasmonic modulators

Plasmonic absorption modulator

The plasmonic absorption modulator as described in deliverable 3.4 was characterized in two steps. First, we studied the quasi-static behavior. We measured the current and the optical transmission while slowly sweeping the applied voltage. In a second step, a MHz modulation was applied to the device. In summary, the device shows optical extinction ratios of 12 dB at 1550 nm wavelength for 10 μm long devices. The operation power is below 200 nW with operating voltages in the range of ± 2 V and currents below 100 nA. Tests with 50 write cycles and sinusoidal modulation in the MHz regime demonstrate excellent repeatability of the switching mechanism.

Static behaviour

We measured the current and the optical transmission as a function of the applied voltage. The voltage was applied between top and bottom electrode. A compliance current of 100 nA was set to protect the device from permanent breakdown. Continuous wave laser light at a wavelength of 1550 nm was coupled to the chip through grating couplers. The transmitted optical signal was measured with a power meter.

The electrical behavior of a 5 μm long device with the laser being turned off is displayed in Figure WP3-13. The applied voltage was swept from -3 V to 3 V and back in steps of 60 mV with a duration of 2 s per step. We observed a sudden increase of the current at a threshold of ~ 2.9 V. Here, the current reached its compliance limit. When scanning back, the current decreased while showing a hysteresis.

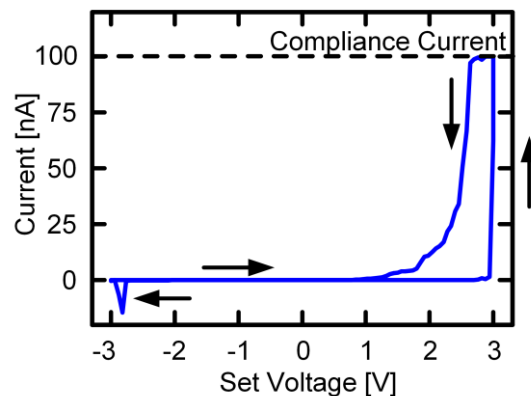


Figure WP3-13: Electrical current-voltage characteristic of the plasmonic absorption modulator. The response indicates a hysteresis. An abrupt increase of the current is found with a threshold around 2.9 V. Note that the set voltage differs from the actual (measured) voltage in the compliance limit.

Figure WP3-14a shows the normalized optical transmission for 50 consecutive measurement cycles below threshold (± 2 V, 20 mV per step, 2 s per step, total duration of 13.3 min per cycle). We started at -2 V in the ON state. While gradually increasing the voltage, the optical signal decreased. When decreasing the voltage, the optical transmission increased again, while being lower than for the forward sweep direction. This hysteresis indicates a memory effect of the switch. The device returned to its initial state after completion of each measurement cycle. This shows excellent repeatability of the switching effect. The difference between the ON and the OFF state (extinction ratio) was 6 dB. The latching extinction ratio between the latched states was 3.5 dB. Since the device was operated below threshold, no significant current was measured and no hysteresis was observed in the I-V curve. Therefore, peak operating power during switching is below 200 nW.

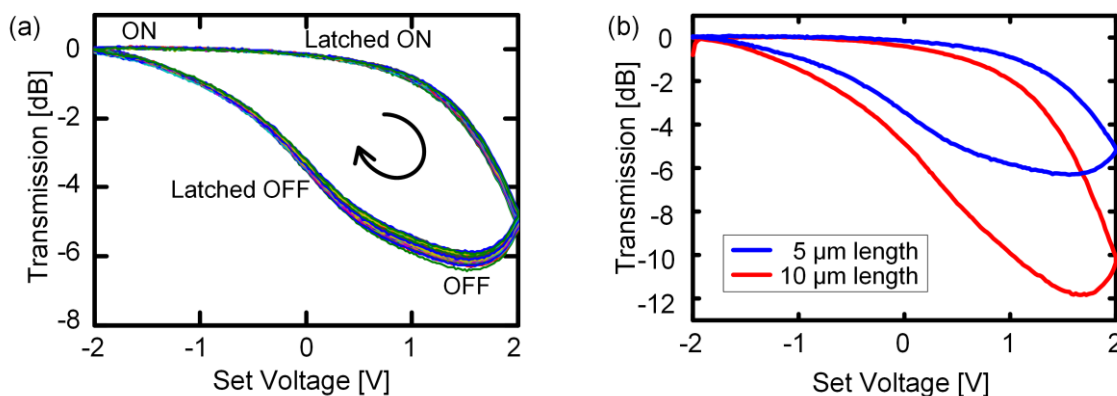


Figure WP3-14: Quasi-static performance of the plasmonic absorption modulator. (a) Latching optical switch behavior for a 5 μm long device: 50 measurement cycles of the normalized optical transmission as a function of the set voltage showing a hysteresis and an extinction ratio of 6 dB. (b) Latching optical switch behavior of a 10 μm long device showing an extinction ratio of 12 dB. During these measurements below threshold, no hysteresis was observed in the I-V curve.

The dependence of the extinction ratio on the device length was investigated as well. From Figure WP3-14b one can see that increasing the length from 5 μm to 10 μm increases the extinction ratio from 6 dB to 12 dB. Thus, the extinction ratio increases with increasing device length. While two

devices with different lengths do not yet provide sufficient statistics the result at least indicates a trend.

Propagation losses in the hybrid waveguide section of 1 dB/ μm and coupling losses between the silicon photonic and the hybrid waveguide of 6.5 dB per interface were determined through cut-back measurements.

Dynamic behaviour

To further assess the device, we studied the dynamic behavior of the switch. Here, a sinusoidal modulation in the MHz regime was applied to the device and detected with a photodiode and a lock-in amplifier. This revealed a relatively flat frequency response between 40 kHz and 10 MHz. The 3 dB bandwidth at an operation with ± 2 V with respect the amplitude at 40 kHz is 30 MHz (see Figure WP3-15, blue triangles).

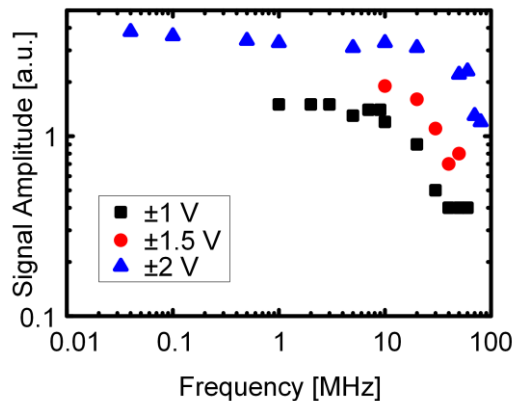


Figure WP3-15: MHz frequency response of the plasmonic absorption modulator. A sinusoidal signal was applied to a 5 μm long device using an arbitrary waveform generator. The optical signal was detected with a photodiode and a lock-in amplifier.

Plasmonic Mach-Zehnder modulators

The plasmonic Mach-Zehnder modulator consists of two high speed plasmonic phase shifters (see Figure WP3-16a, Deliverable 3.2 and Deliverable 3.4) placed in the arms of a Mach-Zehnder interferometer realized on a silicon-on-insulator (SOI) wafer. The interferometer is designed with un-balanced arms and the operation point of the modulator is defined by the operating wavelength, see Figure WP3-16b. Standard photonic multimode interference (MMI) couplers have been used as 3dB optical splitters/combiners. High speed phase modulation is performed by plasmonic phase shifters based on the Pockels effect in an electro-optic (EO) organic material, see Figure WP3-16a. Applying a voltage between the metal electrodes can change the refractive index of the EO-material due to the Pockels effect, and therefore the phase velocity of the plasmonic mode. The photonic-to-plasmonic mode conversion within the arms of the Mach-Zehnder interferometer is accomplished by the metal taper couplers. Scanning electron microscope image of the active plasmonic phase shifter section is give in Figure WP3-16c and Figure WP3-17a-c. To keep the insertion loss of the

modulators in the practical range we use low loss silicon MMI with an insertion loss of less than 0.5dB.

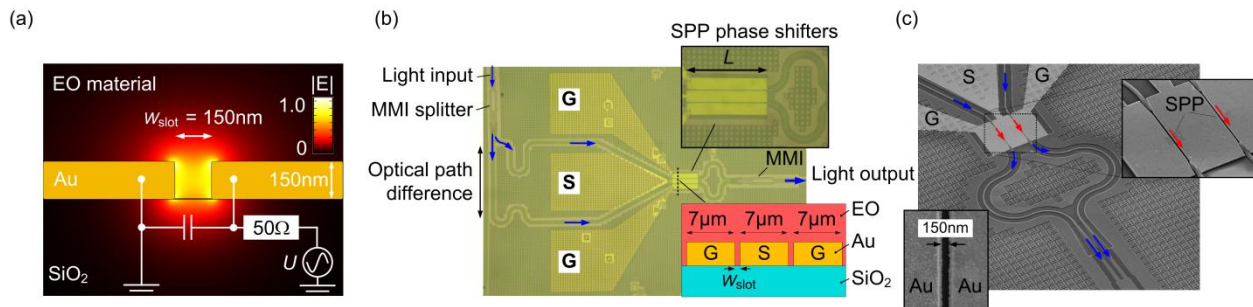


Figure WP3-16: Silicon-plasmonic Mach-Zehnder modulator (MZM) designed and fabricated on a silicon-on-insulator (SOI) platform. (a) Gap surface plasmon polariton (SPP) mode profile in a metal slot filled with an electro-optic (EO) material. The SPP mode is strongly confined to the slot. In addition, a lumped-element equivalent circuit of the modulator is given. Because of the high conductivity of the gold electrodes, the device can be represented by a capacitor ($C_{\text{Device}} \approx 1.5 \dots 3 \text{ fF}$, L dependent). (b) Optical microscope image of the fabricated Mach-Zehnder (MZ) modulator. The MZ interferometer is defined on a passive silicon platform, where light splitting / combing is done by low loss photonic multimode interference (MMI) couplers. The photonic to plasmonic mode conversion is accomplished by metal taper couplers. An optical path difference is implemented in the MZ interferometer design to avoid applying high bias voltages. An optical phase difference between the two arms is modulated by the plasmonic phase shifters. (c) Scanning electron microscope (SEM) picture of the silicon-plasmonic MZM. The modes of the silicon waveguide are coupled to the plasmonic phase shifters, where the phases of the SPPs are modulated. In the end of the phase shifters the SPPs are back converted to photonic modes and then combined within the photonic MMI coupler. Images from [10, 13]

The Mach-Zehnder modulators are fabricated on a silicon-on-insulator (SOI) platform with a buried oxide with a thickness of 2 μm , and a silicon device layer with a thickness of 220 nm. First, the passive silicon photonic circuit is fabricated at IMEC, in the frame work of ePIXfab, by using standard processes such as 193 nm DUV lithography and Si dry etching. The plasmonic high-speed phase shifters with a common signal electrode are defined on gold (Au). The metallic slots with the widths of $\sim 150 \text{ nm}$ slot and the length of 19 μm , 29 μm and 39 μm are defined with e-beam lithography and lift-off process. The slot is filled with an electrooptic material SEO100 (Soluxra, LLC). The electro-optic effect in the EO material is activated through a poling procedure. To avoid electrical breakthroughs, we perform the poling with electrical fields which are lower than the optimum poling field of 100 V/ μm corresponding to the maximum $r_{33} = 110 \text{ pm/V}$.

Characterization results of the photonic-to-plasmonic mode converters

We first characterize the photonic-to-plasmonic mode converters using the fabricated test samples consisting of single metallic slot waveguides interfacing to silicon nanowires through two metallic taper mode converts, see Figure WP3-17a-c. By varying the length L_{MSW} of the metallic slot waveguide between the pairs of taper couplers we can extract the conversion efficiency similar to the standard cut-back measurement. Three devices with metallic slot waveguide lengths of L_{MSW} of 1 μm , 29 μm , and 44 μm , see Figure WP3-17a-c. The slot width is about 140 nm for all three cases.

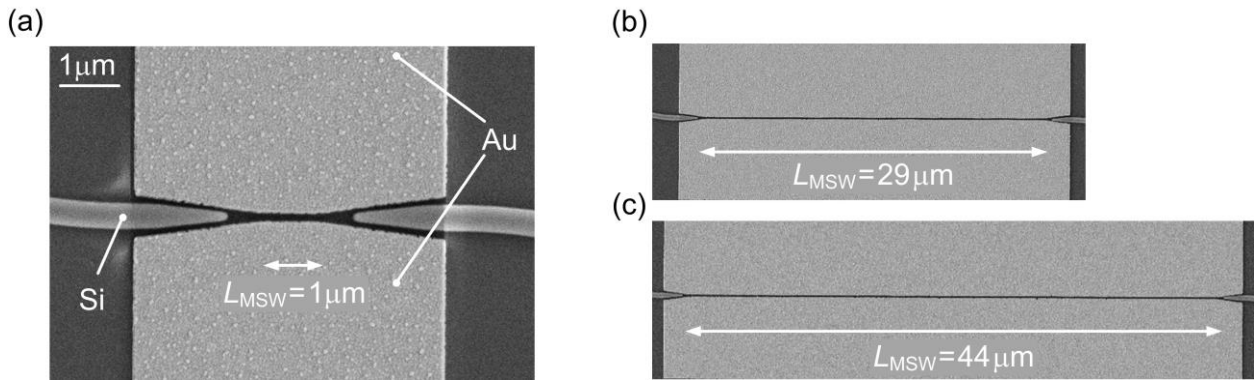


Figure WP3-17: Fabricated metallic tapered mode converters with three different MSW lengths L_{MSW} of (a) 1 mm, (b) 29 mm, and (c) 44 mm. The slot size h is about 140 nm for all three devices.

The measured silicon-to-silicon waveguide transmission spectra for the three different metallic slot waveguide lengths L_{MSW} are given in Figure WP3-18a. The measured transmission spectra are normalized to the measured reference spectra for a silicon strip waveguide without a plasmonic section. As can be seen, the tapered mode converters exhibit large conversion efficiency in a wide operating wavelength range. A total conversion loss of 1 dB is estimated for two transitions. This is in agreement with the theoretically expected conversion efficiency of 2...3 dB. The difference between theoretically calculated and experimentally measured conversion efficiencies is attributed to small differences of the fabricated slot widths and variations of the sidewall roughness of the metallic slots.

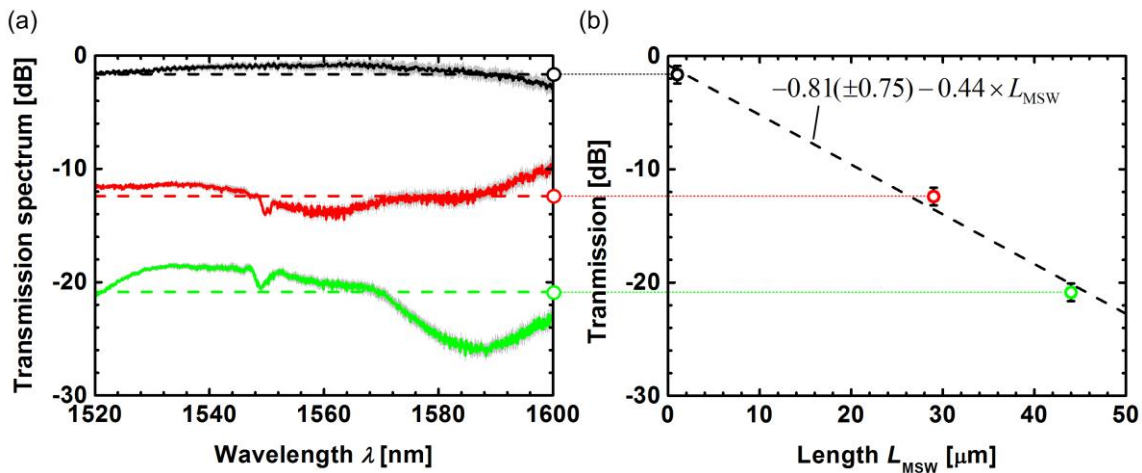


Figure WP3-18: Fabricated metallic tapered mode converters with three different MSW lengths L_{MSW} of (a) 1 mm, (b) 29 mm, and (c) 44 mm. The slot size h is about 140 nm for all three devices.

Static behaviour of plasmonic Mach-Zehnder modulators

Power transmission spectra for all three MZMs are given in Figure WP3-19a. In addition, the transmission spectrum of a reference Mach-Zehnder interferometer is given without a plasmonic phase shifter. It can be seen that, that silicon grating couplers have a big contribution in the total insertion loss of our silicon-plasmonic Mach-Zehnder modulators. With the state of the art fiber to silicon-waveguide couplers with 1dB loss the total insertion loss of the current silicon-plasmonic Mach-Zehnder modulators can be reduced down to 13-20 dB depending on the length of the

plasmonic phase shifters. The extinction ratio and the free spectral range (FSR) vary among the devices because of the uncertainty in defining the width and quality of the metallic slots. The shift of the wavelength corresponding to the minimum transmission with the applied voltage is measured in order to estimate the voltage U_p required for having a phase shift of π . An example of the transmission spectra for voltage off and on states are given in Figure WP3-19b for the MZM with the 39 μm long phase shifters. Measuring the wavelength shift $\Delta\lambda_0$ for the applied voltage of U_0 , we calculate $U_p = \text{FSR} \times U_0 / (2\Delta\lambda_0) \approx 30 \text{ V}$ for MZM with 39 μm long phase shifters and that the $U_p = 37 \text{ V}$ for the MZM with the 29 μm long phase shifter. In particular, we achieve on-chip electro-optic coefficient r_{33} in the range of 70 pm/V. This value is significantly lower than the maximum value of 110 pm/V specified for bulk. These values can further be improved by optimizing the poling procedure of the EO material and improving the fabrication of the metallic slots.

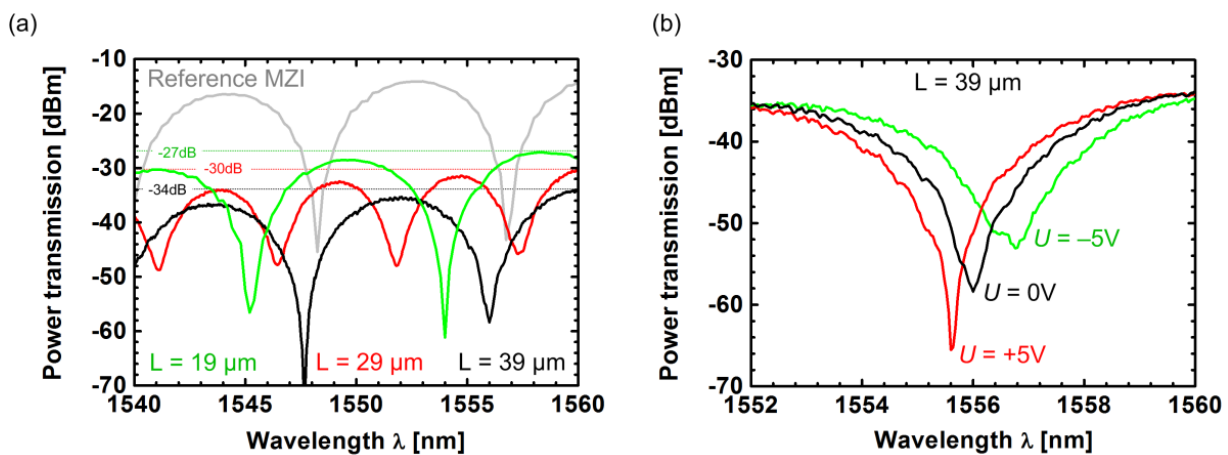


Figure WP3-19: Static characterization results for the Mach-Zehnder modulators. (a) Fiber-to-fiber power transmission is given for the MZMs with the length of 19 μm , 29 μm and 39 μm . In addition, we give the transmission spectrum of a reference Mach-Zehnder interferometer without a plasmonic phase shifters. The plasmonic phase shifters add 13 dB to 20 dB additional optical loss. (b) Transmission spectrum of the 39 μm long device is given for various applied voltages. Analyzing the shift of the wavelength corresponding to the minimum transmission we estimate the voltage U_p required for having a phase shift of π . Images from [13]

Data modulation

Next, data modulation experiments have been performed with the plasmonic MZM using a direct receiver setup as shown in Figure WP3-20a. An electrical non-return-to-zero (NRZ) signal with PRBS pattern length of $2^{31}-1$ and with a peak-to-peak voltage swing of 5 V (measured across a 50 W resistor) is fed to the modulator via a ground-signal-ground (GSG) RF probe. The operating point for the MZM is defined by selecting the operating wavelength. The MZMs are operated in the quadrature points, i.e., the modulator output intensity changes linearly with the relative phase difference of the two arms. The OOK signal after the MZM is detected with a standard pre-amplified direct receiver comprising a single erbium doped fiber amplifier, an optical band-pass filter with a bandwidth of 2 nm, a bit-error-ratio tester (BERT), and a digital communication analyzer (DCA).

We measured the BERs for all three MZMs at a bit rate of 30 Gbit/s in order to find the optimum length for the phase modulators. During the experiment, the EDFA of the receiver is operated in constant output power mode. The input optical power to the modulator is varied from +10 dBm to +23 dBm. This varies the input power to the receiver, i.e., the optical signal-to-noise power ratio (OSNR) at the photodiodes. The optimum length of the PS is defined by a compromise between insertion loss and modulation index — making the device too short results in small optical modulation amplitude, while a too long phase modulator section decreases the receiver’s input power. We find that in our case ($U_{pp} = 5$ V, SPP propagation losses of ~ 0.4 dB / μm , $r_{33} = 70$ pm/V) the optimum performance can be achieved with 29 μm long phase modulators, see Figure WP3-20b. A better BER can be achieved by either increasing the optimum PM length L by improving the slot quality (decreasing optical losses), or by reducing the effective PM length by increasing the electro-optical coefficient and reducing the slot (increasing the optical modulation amplitude). The eye diagrams measured after the MZM with 29 μm long PM sections for bit rates of 30 Gbit/s (BER = 2×10^{-5}), 35 Gbit/s (BER = 3×10^{-5}) and 40 Gbit/s (BER = 6×10^{-4}) are given in Figure WP3-20c. These BER are well below the threshold of 4.5×10^{-3} for hard-decision FEC codes with 7% overhead. The driving voltages and the optical insertion losses can be further reduced by, first, optimizing the poling procedure and thereby achieving higher electro-optic coefficients, second, reducing the slot size, and third, by using silver instead of gold.

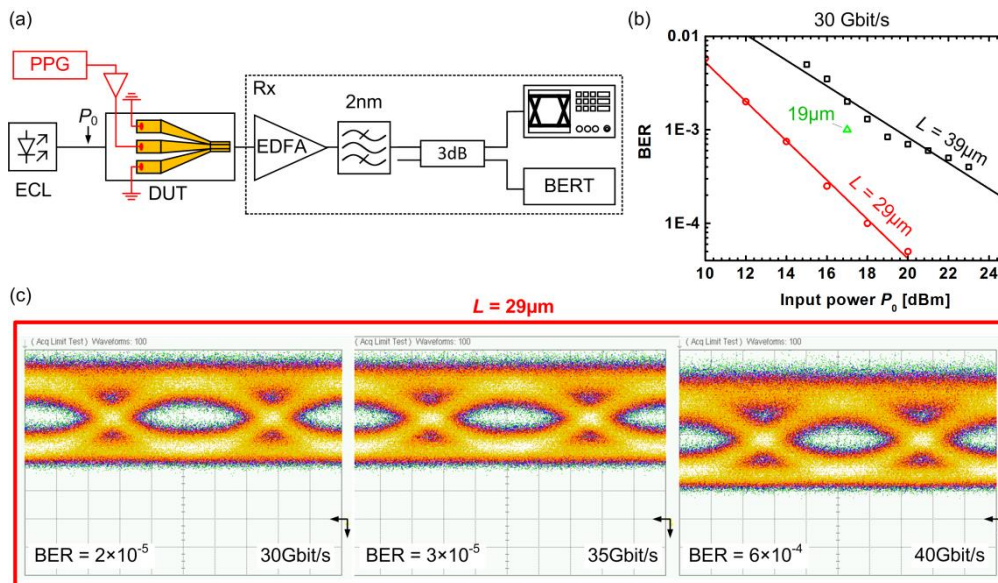


Figure WP3-20: Modulation experiments with plasmonic silicon-organic MZMs with PM lengths of 19 μm , 29 μm and 39 μm . (a) Direct receiver setup used for detecting on-off keyed signal after the plasmonic MZMs. (b) Bit error ratios measured for the MZMs with plasmonic phase modulator sections having lengths of 19 μm , 29 μm and 39 μm . To find the optimum phase shifter length, we vary the input power to the modulators and measure the BER. A compromise between the optical loss and the modulation index can be achieved by using a MZM with a PM length of 29 μm . (c) Eye diagrams measured at bit rates of 30 Gbit/s (BER = 2×10^{-5}), 35 Gbit/s (BER = 3×10^{-5}) and 40 Gbit/s (BER = 6×10^{-4}) for a MZM with 29 μm long PM sections at an input optical power of 20 dBm and at an operating wavelength of 1556.8 nm. The difference in the DC levels for data rates of 35 Gbit/s and 40 Gbit/s is attributed to the thermal drift of the operating point as a consequence of the large optical input power. Images from [13]

All-plasmonic Mach-Zehnder modulators

The plasmonic MZ modulators use external silicon photonic multimode-interference couplers (MMI) to split the optical power and distribute it to the respective arm of the MZI. However, the great size reduction enabled by Plasmonics is partly lost again, as still comparably large silicon photonic components are needed. This situation can be overcome by expanding the design to an all-plasmonic device [14]: 3D metallic patterning enabled the fabrication of an integrated all-plasmonic MZM incorporated in a photonic waveguide. A record small footprint for a MZM that comprises splitters integrated within the photonic-to-plasmonic converters and the phase-modulator sections. A colorized scanning electron microscopy (SEM) image depicts the fabricated device (Figure WP3-21). The total configuration is 10 μm long and its width is as narrow as the silicon access waveguide. The device consists of three sections. In a first photonic-plasmonic interference (PPI) section, incident laser light from the silicon waveguide is converted into SPPs. Subsequently, the SPPs are split up between the two arms of the plasmonic phase shifters (second section). The phase shifters are designed as metal-insulator-metal plasmonic slot waveguides formed by gold contact pads and a gold island. The island is contacted through a suspended bridge. The operation principle is similar to the previous plasmonic phase modulators: The slots are filled with DLD-164, a highly nonlinear $\chi^{(2)}$ -material. When a voltage is applied between the island and the outer electrodes, SPPs propagating in the slots change their phase due to the linear electro-optic effect. Finally, another PPI section transforms the relative phase relations of the SPPs in the two arms into an amplitude modulation.

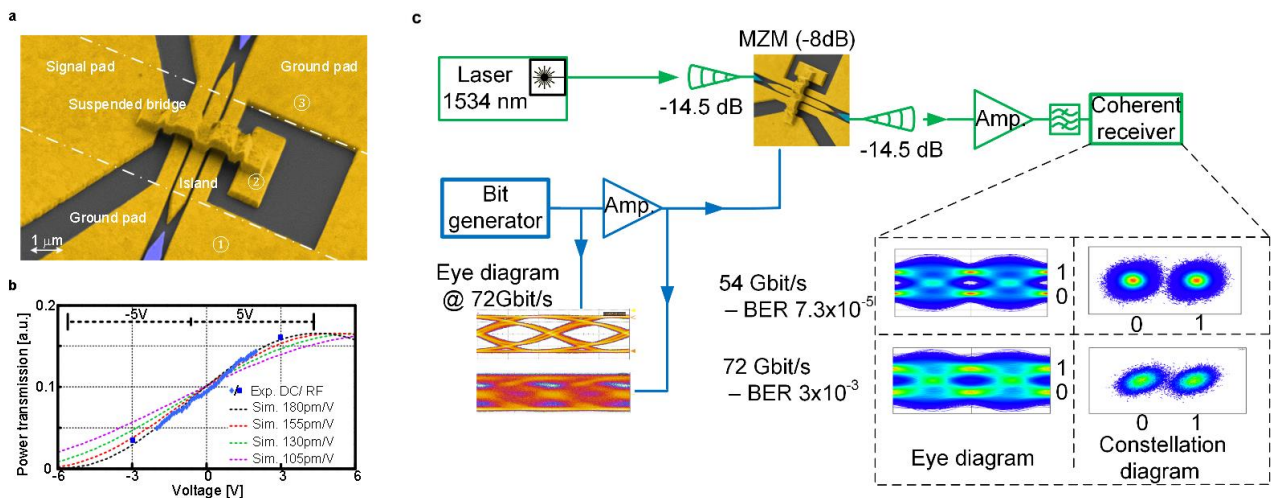


Figure WP3-22: **Plasmonic circuit realizing a Mach-Zehnder modulator (MZM) and experimental high speed setup.** (a), Colorized SEM image of the MZM components. The suspended bridge enables the electrical control of the device. (b), Measured (dots) and simulated (dashed) optical power transfer function versus applied voltages. The simulations indicate a best fit for a material with a nonlinear coefficient of 180 pm/V. (c) The all-plasmonic MZM encodes electrical signals at 54 and 72 Gbit s⁻¹ onto a laser signal at 1534 nm. The respective eye diagram at 72 Gbit/s before and after the electrical amplifier as well as the received eye diagrams are shown at the bottom. The BERs at the receiver are 7.3x10⁻⁵ and 3x10⁻³ for bit rates at 54 Gbit s⁻¹ and 72 Gbit s⁻¹, respectively. The performance at 72 Gbit s⁻¹ is diminished by the limited electrical bandwidth of the transmitter as can be seen from the degraded eye diagram at the input. Still, the nonlinear transfer function of the MZM converts the 72 Gbit s⁻¹ signal into a received eye diagram with BER above the FEC limit. Images from [14]

The device's high-speed performance has been tested by data experiments. A schematic representation of the experimental setup together with the results are given in WP3-23(c). Laser light was coupled to and from the chip by grating couplers and after amplification detected by a coherent receiver. The amplifier was used to compensate losses of the grating couplers. A two-level electrical signal was amplified and fed to the device to perform data transmission experiments at rates of 54 Gbit s⁻¹ and 72 Gbit s⁻¹. Bit-error ratios (BERs) of 7x10⁻⁵ and 3x10⁻³ have been found at 54 Gbit s⁻¹ and 72 Gbit s⁻¹, respectively, after applying post-processing equalization with a 9 tap delay filter, which was provided by the Agilent receiver. Both BERs are below the forward error correction (FEC) limit with a 7% overhead²⁵. The increased BER at 72 Gbit s⁻¹ was caused by the limited bandwidth of the transmitter's electrical amplifier, higher SNR requirements at higher bit-rates and by working at bandwidth limits of our receiver setup. It was operated above its specified bandwidth as can be seen from the eye diagrams before and after the electrical amplifier. The modulator's electrical energy consumption is estimated to be ~25 fJ bit⁻¹ for its capacitance of 2.8 fF driven with ±3 V_{peak} for up to 54 Gbit s⁻¹ and beyond²⁶. Due to the flat frequency response of the device the energy consumption should not change with the bit-rate. However, the low pass characteristic of the electrical amplifier at 72 Gbit s⁻¹ led to a pattern dependence so that the exact energy consumption cannot be stated.

References:

- [1] M. T. Hill: Status and prospects for metallic and plasmonic nano-laser, J. Opt. Soc. Am. B, 27(11), pp. 36-44, 2010.
- [2] C. Y. Lu, , *et al.*, "A surface-emitting 3D metal-nanocavity laser: proposal and theory", Optics express, 19(14), pp. 13225-44, 2011.
- [3] M. P. Nezhad, A. Simic, O. Bondarenko, B. Slutsky, A. Mizrahi, L. Feng, V. Lomakin, and Y. Fainman, "Room-temperature subwavelength metallo-dielectric lasers", Nature Photonics, 4(4), 2010.
- [4] M. K. Kim, *et al.*, "Efficient waveguide-coupling of metal-clad nanolaser cavities", Optics express, 19(23), pp. 23504–12, 2011.
- [5] V. Dolores-Calzadilla, D. Heiss, A. Fiore, and M. Smit, "Metallo-dielectric nanolaser coupled to an InP-membrane waveguide", Proceedings of the 17th Annual Symposium of the IEEE Photonics Society Benelux Chapter, (2012).
- [6] D. Heiss, V. Dolores-Calzadilla, A. Fiore, and M. Smit, "Design of a waveguide-coupled nanolaser for photonic integration", Proceedings of the Integrated Photonics Research, Silicon and Nano-Photonics, 2013.
- [7] A Melikyan, N. Lindenmann, S. Walheim, P. M. Leufke, S. Ulrich, J. Ye, P. Vincze, H. Hahn, T. Schimmel, C. Koos, W. Freude, and J. Leuthold, "Surface plasmon polariton absorption modulator.," Optics express, vol. 19, no. 9, pp. 8855–69, Apr. 2011.
- [8] E. Feigenbaum, K. Diest, and H. a Atwater, "Unity-order index change in transparent conducting oxides at visible frequencies," Nano letters, vol. 10, no. 6, pp. 2111–6, Jun. 2010.
- [9] S.-I. Inoue and S. Yokoyama, "Numerical simulation of ultra-compact electro-optic modulator based on nanoscale plasmon metal gap waveguides," Electronics Letters, vol. 45, no. 21, p. 1087, 2009

- [10] A. Melikyan, L. Alloatti, A. Muslija, D. Hillerkuss, P. C. Schindler, J. Li, R. Palmer, D. Korn, S. Muehlbrandt, D. Van Thourhout, B. Chen, R. Dinu, M. Sommer, C. Koos, M. Kohl, W. Freude & J. Leuthold, “High-speed plasmonic phase modulators” *Nature Photonics* 8, 229 – 233 (2014)
- [11] Robert W. Boyd, “Nonlinear Optics” (Academic, 2008), Third Edition
- [12] “GigOptix”, retrieved <http://www.gigoptix.com/>
- [13] Melikyan, A.; Koehnle, K.; Lauermann, M.; Palmer, R.; Koeber, S.; Muehlbrandt, S.; Schindler, P. C.; Elder, D. L.; Wolf, S.; Heni, W.; Haffner, C.; Fedoryshyn, Y.; Hillerkuss, D.; Sommer, M.; Dalton, L. R.; Thourhout, D. V.; Freude, W.; Kohl, M.; Leuthold, J.; Koos, C. Plasmonic-organic hybrid (POH) modulators for OOK and BPSK signaling at 40 Gbit/s *Opt. Express* 23, 9938--9946 (2015)
- [14] C. Haffner, W. Heni, Y. Fedoryshyn, J. Niegemann, A. Melikyan, D. L. Elder, B. Baeuerle, Y. Salamin, A. Josten, U Koch, C. Hoessbacher, F. Ducry, L. Juchli, A. Emboras, D. Hillerkuss, M. Kohl, L.R. Dalton, C. Hafner, J. Leuthold, “All-plasmonic Mach-Zehnder modulator enabling optical high-speed communication at the microscale”, *Nature Photonics* 9, 525 – 528 (2015)

Deliverables (all completed during Month 1-45)

Deliverable	Name of deliverable	Responsible partner	Delivery date
D3.1	Report on studies of optimized structure for metallic/plasmonic nano-laser and its coupling to Si waveguide	TU/e	10/2012
D3.2	Report on modelling of the modulator structure	KIT	10/2012
D3.3	Fabrication of plasmonic laser device	TU/e	07/2014
D3.4	Report on fabrication of modulators	KIT	10/2013

Milestones (all completed during Month 1-45)

Milestone	Name of milestone	Responsible partner	Delivery date
MS8	Decision on an optimized structure for metallic/plasmonic nano-laser and its coupling to Si waveguide	TU/e	04/2012
MS9	Decision on an optimized structure for plasmonic modulator.	KIT	04/2012

M10	Grown wafer structure for plasmonic lasers	TU/e	10/2013
M11	Fabrication of plasmonic modulator on a SOI platform	KIT	01/2013
MS12	Decision on an optimized structure for plasmonic modulator with a maximum loss of 20dB	KIT	04/2013
MS14	Initial testing and characterization of plasmonic modulators	KIT	07/2013
MS15	Initial testing of bonded plasmonic laser	TU/e	10/2013

Use of resources

Use of resources has been according to plan. The table below gives a review of each partners contribution.

Partner	Person months	Main contribution
TU/e	31.7	Modelling and fabrication of metallo-dielectric nanolaser; Bonding of III-V wafer to silicon wafer with IMEC
KIT	27.3	Modelling and fabrication of plasmonic modulator

3.2.4 Work Package 4: Plasmonic Receiver

Task 4.1 Design and modeling of plasmonic pre-amplifier

a) Polymer based version

Task completed.

b) Hybrid silicon plasmonic amplifier

Task completed.

Task 4.2 Modelling of plasmonic QD polymer based photodetectors

Task completed.

Task 4.3 Colloidal quantum dots with optimized gain and electrical injection scheme

a) “Flash” CdSe/CdS QDs

The QD used below to test amplification devices are different types of the recently developed (UGENT) “flash” CdSe/CdS core-shell colloidal quantum dots (QDs). These types of dots have large CdS shells, which create an improved surface passivation, while on the other hands they also have alloyed interfacial layers, which provide more smooth wave functions of electrons and holes. The smooth wave function created by the alloyed interfacial layer weakens the Auger recombination. We performed pumping experiments for drop casted compact layer on glass substrates and under pulsed, high power laser pumping (1kHz repetition rate @ 20mW) the QD compact layer shows amplified spontaneous emission (ASE). Figure WP4-1 shows a typical emission spectrum under the pulsed laser pumping, showing spectral narrowing and ASE peaks both at 600nm (S-S transition) and at 530nm (P-P transition).

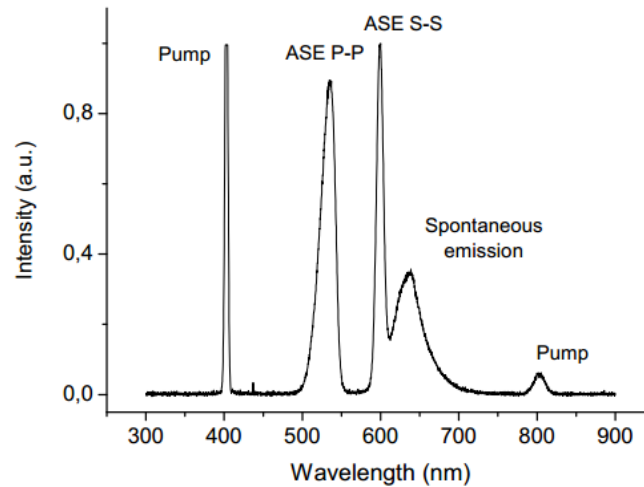


Figure WP4-1: Emission spectrum of drop cast compact layer of “flash” QDs under pulse laser pumping

b) HgTe QDs material

For operation in the telecom wavelength range, we further optimized the synthesis of the HgTe QDs earlier reported. We now achieved mono-disperse QDs with wavelength ranging from 1000 nm to 1800 nm. Optical gain in dispersions of HgTe QDs with average exciton numbers per nanocrystal $\langle N \rangle$ as low as 0.005 were measured. Intrinsic gain coefficients of about 500 cm^{-1} (around 100 cm^{-1} for a close packed film) were demonstrated and the extrapolated gain lifetime corresponds to the single exciton lifetime. This almost thresholdless gain is attributed to stimulated emission between the lowest conduction band level and shallow, empty surface states near the first valence band level, thus creating a nearly thresholdless, effective 3-level system. Since the gain characteristics meet the requirements for DC electrical pumping, this result shows that the use of effective 3-level systems is the way forward for developing performing QD-based gain media. To translate these exciting properties (low threshold, long gain lifetime and large gain magnitude) to an actual integrated amplifier or laser (see a proof of concept in Milestone 24), eventually using electrical injection, we should process the QDs into thin films. Employing the same transient absorption routine as outlined above, we observe a decreased performance of HgTe QDs in the thin spincoated films used in these experiments. Although gain is still observed at exciton densities below unity, the thresholds are substantially higher (up to 1 order of magnitude) and the cross sections are smaller. We attribute such a decrease in gain cross section to increased photocharging, which is attributed to charge accumulation due to surface traps and clustering of the QDs. More results obtained on HgTe QDs and thin films based on them can be found in Milestone 24. The observed limitations could be solved in the future by working on most appropriate surface functionalization of QDs in order to avoid clustering.

Task 4.4 Fabrication and characterization of QD-based (plasmonic) amplifiers

a) Polymer based version

Different plasmonic waveguides were fabricated, planar and linear (100 – 1000 nm wide), after the work developed in task 4.1, which were covered by a polymer-QD nanocomposite or bi-layer (PMMA cladding a QD close packed layer). These structures were characterized by using a novel method consisting on the excitation of the PL of the QDs at a wavelength of 533 nm with a monomode bare fiber ended with a sharp round tip and the analysis of waveguided PL signal at the nearest edge of the sample (see Figure WP4-2a). The small diameter of the tip allows a reduced excitation area (down to $5 \mu\text{m}^2$) selectively on the top of Au layers/stripes. In these conditions, the PL of the QD-material can be coupled into the TE_0 mode and the LR-SPP TM mode that are allowed in the investigated waveguides. With the present method the propagation length, L_p , of those optical modes may be easily measured in a direct way by recording the PL signal as a function of the distance between the tip and the edge of the sample. In a second step we have studied the possible enhancement of the L_p when the QD-nanocomposite is optically pumped. For this purpose a pump beam at 450 nm was coupled in the structure along the dielectric planar waveguides integrated on the left and on the right of the Au stripe, as illustrated in Figure WP4-2b. In order to separate the PL signal used in the probe from that of the pump we have modulated the probe at a frequency < 1 kHz and measured the influence of the optical pumping of the QD-nanocomposite on that modulated signal (using a lock-in amplifier). In this way, we can extract L_p from the probe signal decay as a function of the optical pumping power.

When a plasmonic waveguide is pumped with the fiber tip (see Figure WP4-2a) the PL signal (600 nm if used CdSe QDs) can be coupled to the modes allowed in the structure, whose dependence on the distance between the tip and the edge of the sample will exhibit two exponential decays (see red and blue curves in Figure WP4-3a):

$$I_{\text{PL}} = A_1 \cdot e^{-z/L_{p1}} + A_2 \cdot e^{-z/L_{p2}} \quad (1)$$

where A_1 and A_2 are constants and L_{p1} and L_{p2} the propagation lengths of the modes in regions 1 (Au-stripes) and 2 (PMMA-left/right sides), respectively. The shortest propagation length, L_{p1} , would correspond to LR-SPP and TE_0 modes under TM and TE polarizations, respectively. The longest propagation length, L_{p2} , shows a negligible dependence with polarization and corresponds to the planar waveguide as a whole.

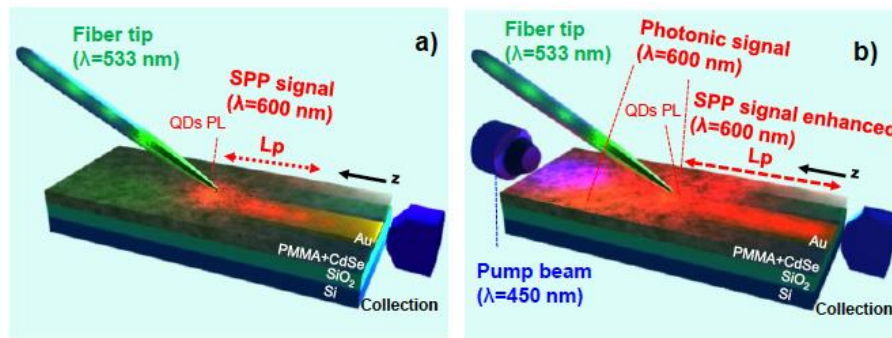


Figure WP4-2: a) SPP excitation with a fiber tip. The tip provides a small spot on the sample at a wavelength (533 nm) smaller than the QD band-gap (600 nm). Then the PL is coupled to the waveguide modes (LR-SPP mainly) and the L_p of the modes is characterized by measuring the intensity as a function of the distance between the tip and the edge of the sample. b) Loss compensation by coupling a pump beam (450 nm) at the input edge of the sample. This light can propagate through the dielectric waveguides outside the stripe and excite light emission from QDs.

Results plotted in Figure WP4-3a (data symbols) refers to a stripe of $w=10 \mu\text{m}$, where L_{p1} in TM polarization is fitted with values in the range $10 - 17 \mu\text{m}$ (red line), in agreement to calculated values for the LR-SPP mode ($11.4 \mu\text{m}$, see Deliverable 4.1). The fit for TE polarization (blue line) gives a longer propagation length ($L_{p1}=40 - 67 \mu\text{m}$), given that this mode is centred at the dielectrics (QD-PMMA nanocomposite) and not at the metal stripe. On the other hand, the longest propagation length, L_{p2} , results around $370 \mu\text{m}$ independently of the polarization (TE and TM) and corresponds to the light travelling out of the metal stripe (PMMA-left/right sides). The images inserted in Figure WP4-3a illustrate the behaviour described above by comparing waveguided light at $z=0$ and $z=200 \mu\text{m}$ under both polarizations. Clearly, at $z=0$ the plasmonic and photonic modes are present, but for long distances ($z=200 \mu\text{m}$) the LR-SPP is lost (TM polarization) and the TE_0 is attenuated by the scattering with the gold stripe, hence only photonic modes travelling along the dielectric waveguides are preserved in the structure.

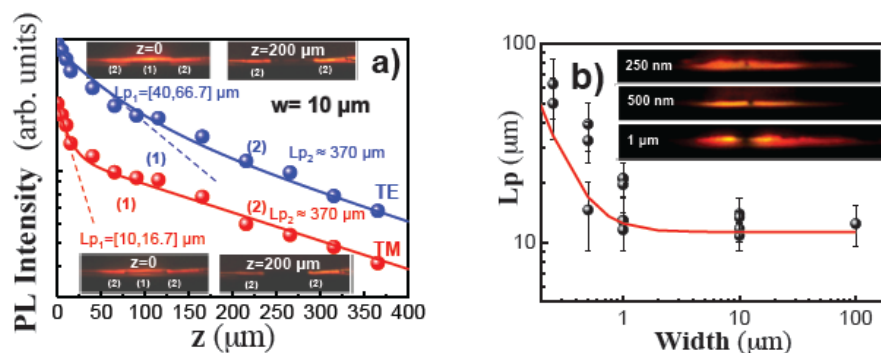


Figure WP4-3: a) PL intensity as a function of the distance between the tip and the edge of the sample under TE (blue) and TM (red) polarizations. Symbols correspond to the experimental data and red-blue continuous lines to the fitting using a two exponential decay from which L_{p1} and L_{p2} are deduced. The images inserted in the figure refer to the near field distribution at $z=0 \mu\text{m}$ and $z=200 \mu\text{m}$ for both polarizations. b) Propagation length of the LR-SPP mode measured (data symbols) and calculated (red continuous line) in waveguides whose width varies from 250 nm and 100 μm (planar waveguide). Calculations were made by using the effective index method. The inset corresponds to images of the waveguided signal in TM polarization at the output of 250, 500 and 1000 nm wide Au-strips.

When the width of the Au-stripe is reduced, the analysis of the structure with the effective refractive index method predicts lower propagation losses (longer propagation lengths) of the LR-SPP due to the delocalization of the mode to the dielectric surrounding the metal, as observed in Figure WP4-3b (red continuous line). The experimental values of L_p measured in several fabricated Au stripes (ebeam lithography followed by lift-off of a deposited gold layer) with widths of 250 nm, 500 nm and 1 μm follow the predicted behaviour (data symbols in Figure WP4-3b): L_p increases from 11 to 50-60 μm when reducing the stripe width down to 250 nm.

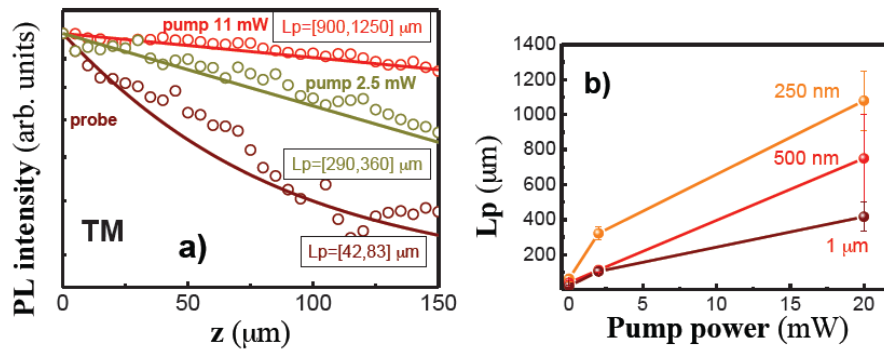


Figure WP4-4: a) PL intensity as a function of the distance between the tip and the edge of the sample in TM and a waveguide width of 250 nm for a probe beam (wine) and under two pumping conditions (dark yellow and red). Clearly L_p improves with the pump. Symbols correspond to the experimental data and straight lines to the fitting b) L_p as a function of the pump power for 1 μm , 500 nm and 250 nm wide Au-stripes.

When a 450 nm pump beam is end fire coupled to a 250 nm wide Au-stripe the propagation length of the LR-SPP significantly increases, as shown in Figure WP4-4a for two pump powers (dark yellow and red symbols). The value of L_p increases from 40 μm to more than 1 mm (after fitting to Eq. 1, continuous lines in Figure WP4-4) when using a laser pumping power of 20 mW, in comparison to the case of the 1000 nm wide Au-stripe where L_p increases from 11 μm to 400 μm (\approx 35 times enhancement), as observed in Figure WP4-4b. This experimental behaviour is also corroborated by simulations of light propagation along the Au-stripe with an active three dimensional beam propagation method.

The propagation length was also characterized at telecom wavelengths in symmetric and asymmetric planar plasmonic structures (see deliverable 4.1). For this purpose PMMA was doped with HgTe QDs exhibiting emission in the 1400-1500 nm wavelength range with good efficiency (see deliverable 4.2). Preliminary results using available HgTe QD material (in a concentration on PMMA of around 1%) one year ago was used to investigate planar plasmonic waveguides. The characterization of waveguided PL as a function of z in TM polarization also exhibits two propagation lengths (Figure WP4-5). The shortest propagation length ($L_p = 20 \mu\text{m}$) is attributed to the LR-SPP mode, while the longest one ($L_p = 67 \mu\text{m}$) to an hybrid plasmonic-photonic mode due to a refractive index asymmetry between the top (HgTe-PMMA) and bottom (PMMA) dielectric layers cladding this planar plasmonic waveguide. When a pump beam is coupled into the waveguide (propagating along the bottom PMMA cladding) a weak compensation of losses is also observed (Figure WP4-6): $L_p = 25 \mu\text{m}$ for the SR-SPP and $L_p = 100 \mu\text{m}$ for the hybrid plasmonic-photonic mode.

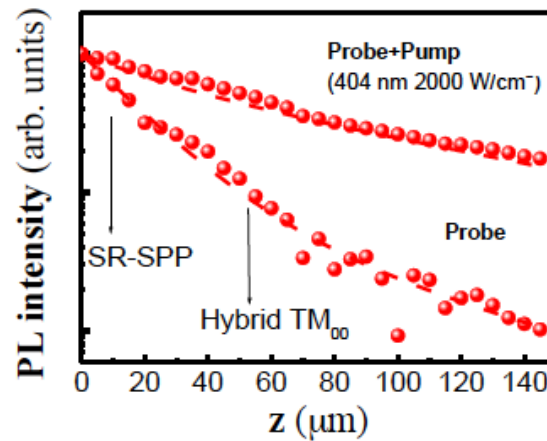


Figure WP4-5: TM waveguided PL intensity as a function of z for both probe and pump+probe excitation conditions.

As a first conclusion from results described and discussed above we can say that QD-nanocomposites, even if they do not exhibit amplification of spontaneous emission under standard excitation conditions (continuous and ns-pulsed lasers), we observe an enhancement of the propagation length that was noticeable when using CdSe QDs (visible wavelengths), up to a factor 25-35, possibly due to their higher quantum yield as compared to HgTe QDs. Experiments using au-stripes covered with new HgTe QDs will be developed in brief in order to corroborate our conclusions.

To gain further knowledge of the mechanism that gives rise to an increase of the propagation length of plasmonic optical modes, we focused our attention to use an active material exhibiting stimulated emission. Recently, we have combined our previous experience along the project to combine polymer waveguides with other solution processed active materials. Particularly, we demonstrated amplification of the spontaneous emission at around 780 nm, by combining Lead Halide Perovskites (HPVK) with a PMMA cladding, as shown in Figure WP4-6 [I. Suárez, E. J. Juárez-Pérez, I. Mora-Seró, J. Bisquert and J. P. Martínez-Pastor, *Polymer/perovskite amplifying waveguides for active hybrid silicon photonics*, *Advanced Materials*, in press (2015)]. These materials are very promising for active photonics in silicon platforms, eventually combined with QDs to obtain different emission wavelengths, as recently probed by Sargent and co-workers [Z. Ning *et al.*, *Quantum-dot-in-perovskite solids*, *Nature* **523**, 324 (2015)].

When the HPVK was integrated in a planar plasmonic waveguide similar to the ones previously explored in the present project stimulated emission is still observed for the TM mode, as shown in Figure WP4-6e. The threshold pumping energy in the plasmonic waveguide is higher than in the dielectric one, other than a larger linewidth of the amplified PL signal, probably due to the most important ohmic losses in the first case because of the metal layer beneath the active material, as expected, but this result is very promising to investigate the effect of an active medium exhibiting stimulated emission on the SPP amplification along its propagation (under current investigation).

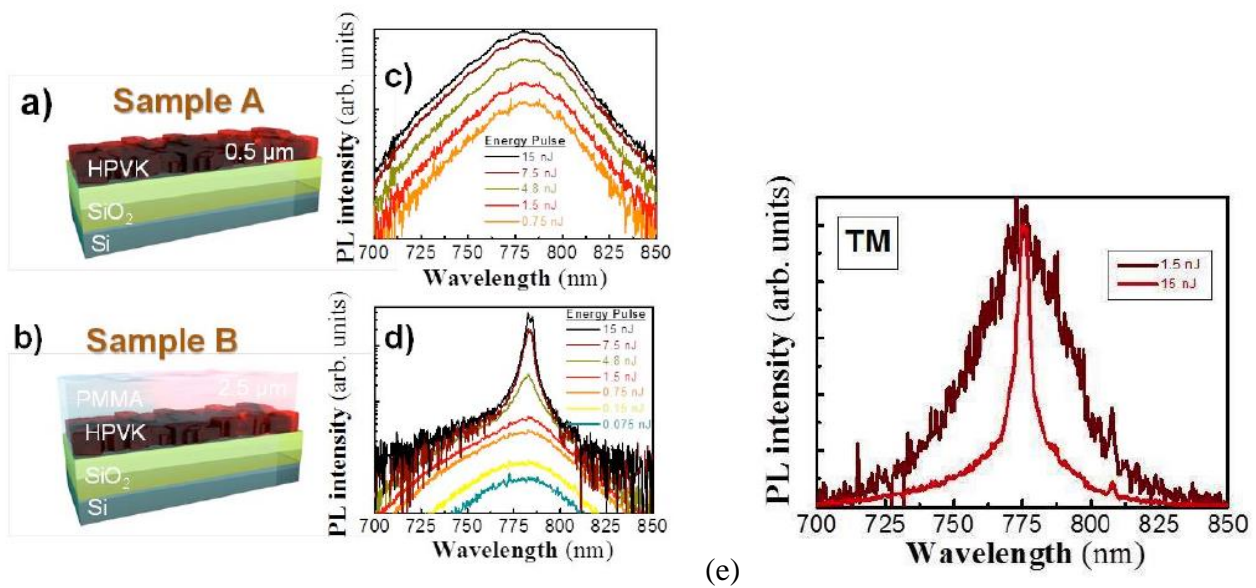


Figure WP4-6: (a) Sample A structure: A thin layer of $\text{CH}_3\text{NH}_3\text{PbI}_3$ (500 nm) is deposited by spin coating on a Si/SiO₂ substrate, a previous buffer of TiO₂ was deposited on SiO₂ to enhance the HPVK adherence. (b) Sample B structure: similar to sample A, but adding a PMMA cladding layer (2.5 μm) on top of the HPVK. (c) and (d) PL spectra for different pump powers in sample A and B, respectively. (e) Waveguided PL spectra at the output of a plasmonic waveguide covered with a PMMA- $\text{CH}_3\text{NH}_3\text{PbI}_3$ bilayer for two pump powers, below and above the threshold of stimulated emission..

b) Hybrid silicon version

SiN-based photonics was found to be the ideal solution to integrate QDs into a Si-platform after first investigations to integrate into direct silicon photonic structures, even if the combination with plasmonics is not straightforward. In this way, several devices have been designed, fabricated and tested along the last months, particularly disk resonators and linear waveguides. Finally, this section will end by including results on electrical injection devices.

Disk resonators

The design of the SiN-QD disk with vertically coupled waveguide is shown in Figure WP4-7. The bus waveguide is defined on a silicon wafer with a 3 μm SiO₂ layer and is also sideways embedded in SiO₂. An amorphous silicon (aSi) pillar supports the SiN disk with the embedded QD layer. The height of the aSi pillar determines the vertical coupling gap between the disk and the waveguide. The undercut distance d is chosen sufficiently large to prevent leakage of the fundamental transverse electric (TE) modes to the aSi pillar. To tune the coupling strength, the horizontal offset between the center of the bus waveguide and the edge of the disk is adjusted from -400 nm to +400 nm, with positive offsets denoting a bus waveguide closer towards the centre of the disk.

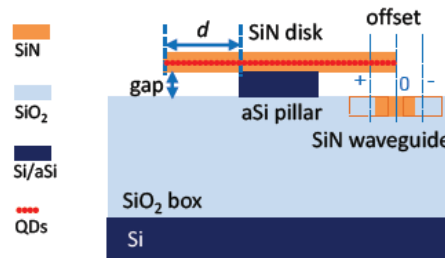


Figure WP4-7: Cross-sectional schematics of device design.

From finite-difference time-domain simulations, we choose a height of ~ 135 nm for the bus waveguide, guaranteeing single mode operation at a wavelength of 625 nm, the peak PL wavelength of the QDs employed. The disk height was set at ~ 180 nm to ensure low-loss for the TE-like disk modes. The width of the bus waveguide and the diameter of the SiN disk were varied to study their influence on the disk-waveguide coupling. The vertical coupling gap was fixed at ~ 200 nm. Note that there are two main advantages to our vertical coupling configuration. First, it allows for an on-chip waveguide-coupled free-standing disk and therefore to achieve high quality (Q) whispering gallery modes (WGM) with low radiation loss, even for relatively small diameters. Second, because of the separation of the fabrication steps for waveguide and disk, we can integrate the QDs exclusively in the disk and not in the access waveguides. This allows to study the coupling of the QD emission to disk modes without background interference, which would not be possible if also the waveguides contain QDs as would be unavoidable in a lateral coupling scheme.

The fabrication starts with the deposition of a ~ 135 nm PECVD SiN layer onto a wafer with a $3 \mu\text{m}$ thermal SiO₂ box layer. Next the bus waveguide is patterned using contact lithography and RIE etching to form a strip waveguide. Both the contact lithography and the RIE process were optimized to be able to define a low-loss waveguide supporting only a single TE-like mode at the operating wavelength. This ensures only the TE-like disk modes are coupled out efficiently. After waveguide fabrication, a 800 nm PECVD SiO₂ cladding is deposited and a chemical mechanical polishing step is applied down the top of waveguide layer to planarize the surface, as shown in Figure WP4-8. Next, the vertical coupling gap is defined by depositing a 200 nm thick PECVD aSi layer. The SiN-QD composite layer is prepared by first depositing a ~ 90 nm SiN layer, then spin-coating a layer of QDs, and then depositing another ~ 80 nm SiN layer on top of the QDs. These latter ones consist in 10 nm CdSe/CdS core/shell QDs prepared according to the “flash” synthesis procedure. The disk is defined using the same process as used for the waveguides. Finally an alkaline based wet etch is utilized to undercut the aSi and to realize the free-standing SiN-QD disk schematically depicted in Figure WP4-7. The microscope and SEM pictures of Figure WP4-8 show that the designed structure is accurately realized.

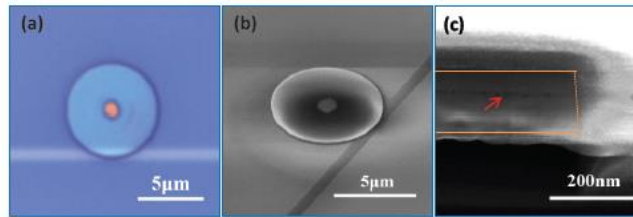


Figure WP4-8: (a) Optical and (b) scanning electron microscope images of one fabricated device with a 7 μ m diameter disk. (c) Cross section of the etched profile of disk with the red arrow indicating the embedded QDs.

To study possible lasing of these devices, we also developed processes for integration of a thicker QDs layer. The design and fabrication are similar to that described above except for the pillar part. Here the top disk is supported on the planarized SiO₂ surface. The presently developed process allows for integrating thick QDs (30-100nm) within SiN disk and in Figure WP4-9 we show the fabricated device with ~55nm thick CdSe/CdS core/shell QDs embedded in SiN disk. We used a focused beam (spot size ~100 μ m diameter) to pump the disk from the top and collected PL from the cleaved facet of the access waveguide using microlensed fibers. The location of QDs is perfectly aligned with the maximum of the light field in the disk, resulting in an efficient coupling of the QD emission into the whispering gallery modes (WGM) of the disk with a negligible PL background. In Figure WP4-10a we show the PL spectra of the disk of 15 μ m diameter pumped with different laser powers. We observe a narrowing feature that could be attributed to a certain contribution of amplification of the spontaneous emission. On the other hand, the intensity of the spectra shows evident sensitivity to the pump power and it increases rapidly from 0.02 to 0.03mW pump power while decreases when further increasing the pump power to 0.15mW, as observed in WP4-10b. These preliminary results show a possible lasing effect in QD-SiN disk and detailed measurement at low pump power (below 0.03mW) is needed to confirm whether lasing occurs at a certain threshold pump power. At higher pump power region a saturation output power is expected while a reduction of PL is actually observed. This could be attributed to heating effect of the disk when increasing the pump power; however it still needs further investigation.

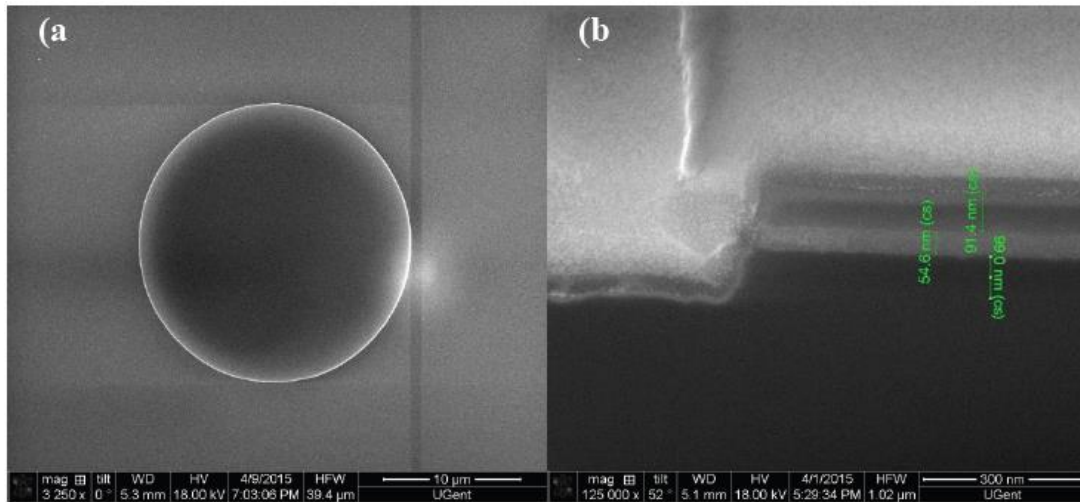


Figure WP4-9: (a) SEM image of the top view of fabricated disk with a diameter of 20 μm and (b) cross section of the etched profile of disk with $\sim 55\text{nm}$ thick QD layer embedded in SiN disk.

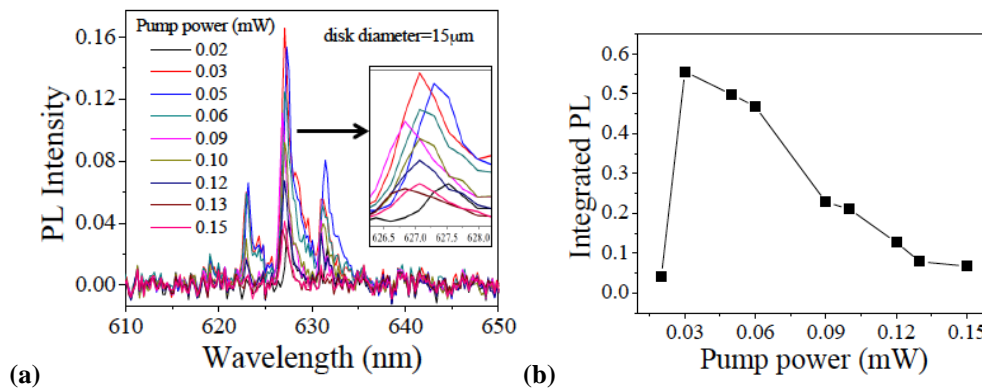


Figure WP4-10: PL spectra under different pump power of TOPAS. (b) Integrated PL intensity as a function of pump power.

In-line amplifiers

Next to the resonator devices we also investigated straight waveguides with embedded QDs. Again we first used PECVD to deposit 100 nm high temperature low frequency SiN layer on top of SiO₂. The measurement shows this type of SiN has quite low optical losses which is the reason we choose it as the under layer. Then we spin-coated a layer of “flash” QDs on top of that SiN layer. The layer thickness can be controlled by the concentration of the QDs solution and the spin-coating speed. Here we used a 50 nm thick and uniform QD compact layer. Then we deposited another 100 nm high temperature mixed frequency SiN on top of the QD layer. We choose this type of SiN because the stress of the layer is more or less compatible with the QDs layer underneath and hence peeling of the layer is avoided in these larger structures. Other types of SiN have different stress compared with QDs layer, which will cause the up layer crack after deposition. After one step of etching through the QDs layer, we can have the waveguide with embedded QDs in between.

We performed a measurement evaluating the excitation power dependence with this sandwich waveguide sample. A cylindrical lens is used to form a narrow line beam to pump along the

waveguide. The emission is collected by a lensed fiber, the collected light has been measured by power meter and spectrum analyzer separately to obtain the power and spectrum information. Figure WP4-11a shows the spectrum information of the collected light. The emission is around 520nm, which is consistent with the ASE P-P from the dropcast sample. Figure WP4-11b shows the result of excitation power dependence of this waveguide with embedded QDs in between. There is a clear non-linear power dependence of the ASE, but also saturation at higher pump powers. Quantitative analysis of these results to extract a modal gain is currently under way.

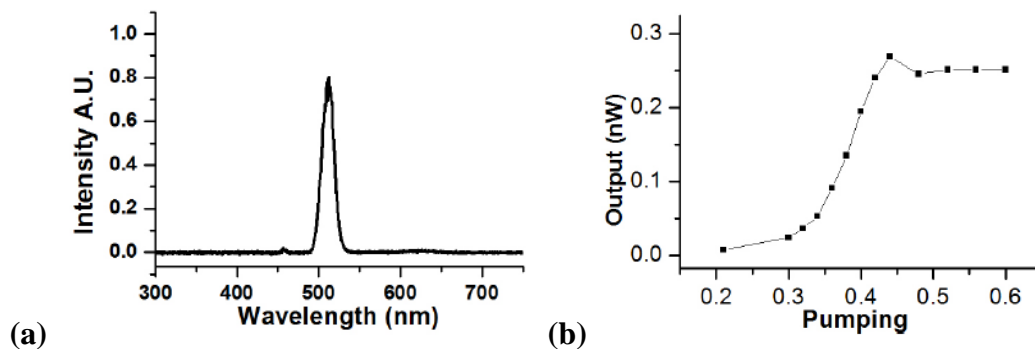


Figure WP4-11: a) Spectrum of emission from waveguide facet. The small peak around 450nm comes from the pumping laser. b) Excitation power dependence measure

Electrical injection devices

To make integrated QD-based light sources viable on-chip light sources, electrically driven QD light emitting devices are needed and integration on chip must be demonstrated. Electrically driven light emission by colloidal quantum dots requires the formation of electron-hole pairs in the quantum dots, for example by direct injection of electrons and holes, that subsequently emits light by radiative recombination. Although this is possible utilizing separate electron and hole contacts, a relatively straightforward approach that is readily amenable to down-scaling and photonics integration is based on sandwiching three or more quantum dot layers in between two insulators to form a quantum dot capacitor. When driving this capacitor using a sufficiently high, alternating voltage, electron injection from the valence band to the conduction band between quantum dots in successive layers occurs and the resulting electron-hole pairs in the central quantum dot layers emit light (as shown in Figure WP4-12a).

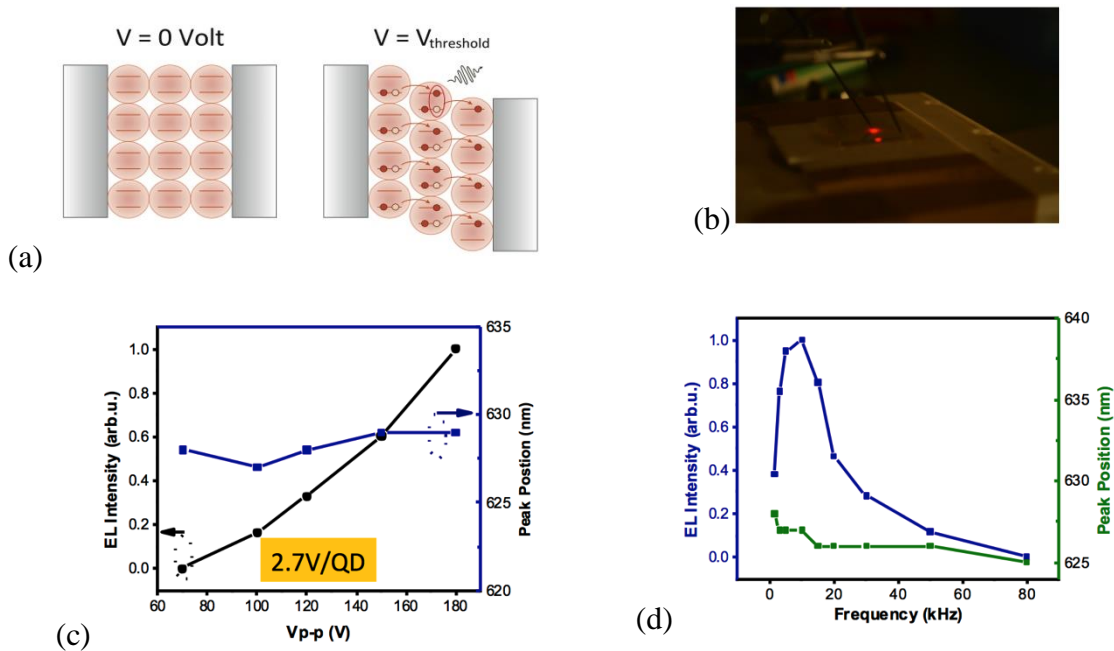


Figure WP4-12: (a) Operation principle of AC driven QD-capacitor. (b) EL from the AC driven sandwich structure: ITO-SiN-QDs-SiN-M. (c) EL intensity vs. Vpp. (d) EL intensity vs. modulation frequency AC voltage

The sandwich-structure used to demonstrate electroluminescence consist of: a glass substrate with an ITO layer, a SiN layer is deposited on top, followed by a spin-cast CdSe/CdS core-shell QDs layer and another SiN layer, and finally metal contacts. Using metal probe needles an AC voltage can be applied over the QDs (see Figure WP4-12b). EL intensity as a function of Vpp over the stack, and frequency is shown in Figure WP4-12c and 12d, respectively. By using a broad range of driving voltage and analysing the time-dependent displacement current and light emission we will try to understand the details of the operation mechanism of this light emitting quantum-dot capacitor.

Task 4.5 Fabrication of plasmonic polymer QD based photodetectors

a) Schottky-heterostructure photodiodes

Along the project we have optimized the synthesis of PbS QDs with absorption/emission at wavelengths around 1550 nm (Figure WP4-13a), as also the deposition (+ ligand exchange) of thin films in the thickness range 300-500 nm by means of a Dr.Blading technique. These QD-solid films exhibit a reasonable uniformity throughout the sample (see the SEM transversal view of a Schottky structure in Figure WP4-13b). Layers with completed ligand exchange have a typical resistivity around $10^5 \Omega\text{cm}$, a hole concentration larger than 10^{15}cm^{-3} and mobilities smaller than $0.065 \text{cm}^2/\text{Vs}$, as estimated from Hall measurements (very difficult to obtain good values due to the extremely high resistivity).

In the case of the most recent generation of devices we have obtained peak responsivities of 0.48 and 0.18 A/W at around 1300 and 1500 nm (blue and green lines in Figure WP4-15c) for 500 and

250 nm thick PbS-QD films as active layers, respectively. The time response of these photodiodes working in photocurrent mode is estimated to be around 100 ns, very similar to values reported in literature. The photovoltage noise was measured to be of the order of 85 nV/Hz^{1/2} at 1 kHz for the photodiode based in the 500 nm thick PbS QD film, whereas the photocurrent was perfectly linear over more than three orders of magnitude (constant responsivity). The experimental detectivity is estimated to be in the range 10¹² - 10¹³ Jones. These photodiodes, even if not made with an optimized architecture to be used as a solar cell, when illuminated under AM1 solar conditions, open circuit voltages (V_{oc}) of 200-300 mV were measured in the best photodiodes of the examined generations and short circuit currents (J_{sc}) as high as 10-20 A/cm², respectively, which are also in the range of the best expected and reported values using PbS QDs of smaller size as the base for solar cell structures. It is also worth noting that photodiodes fabricated without encapsulation are stable in air during several weeks, even if electrical parameters degrade progressively (after one month in air the responsivity decreased a factor two), possibly due to the protecting effect of the top metal electrode (Ag).

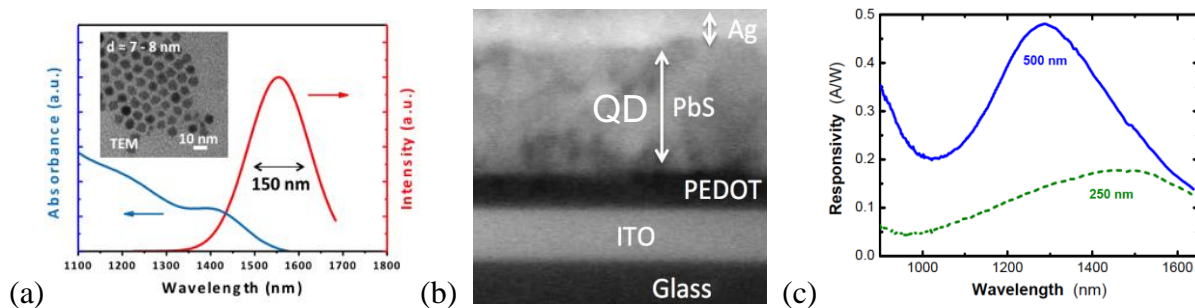


Figure WP4-13: (a) PL (red curve) and absorbance (blue curve) of PbS QDs optimized for photodetectors working at telecom wavelengths; in the inset a TEM image is shown with indication of the QD diameter. (b) Transversal SEM image of a complete Schottky photodiode. (c) Responsivity measured in the best fabricated photodiodes using the same PbS QDs to deposit 250 (green dashed line) and 500 nm (blue continuous line) thick films.

b) QD-solid based microgap/nanogap photoconductors

The Schottky concept is a very convenient device to be integrated in SOI technology, because photocurrent or photovoltage can be directly measured without needing of polarization or used as input for a transimpedance amplifier. However, microgap and nanogap photoconductive devices would offer the most ideal geometry to be integrated in a planar geometry of the final plasmonic chip targeted in NAVOLCHI, other than smaller footprints, faster time response and the possibility to add plasmonic effects in the case of the nanogap photoconductor. Within this task we have developed several series of microgap and interdigitated electrodes (Figure WP4-14a-b, respectively), whose results are discussed below. In the case of nanogap devices two series have been developed until now, a first one using a very ITO-layer (to produce a better focusing during ebeam patterning) on a quartz substrate and a second one using a Si/SiO₂ substrate with a more complicated layout of fabrication (Figure WP4-14c shows the sample containing 65 nanogap photoconductor devices); these devices are under current investigation.

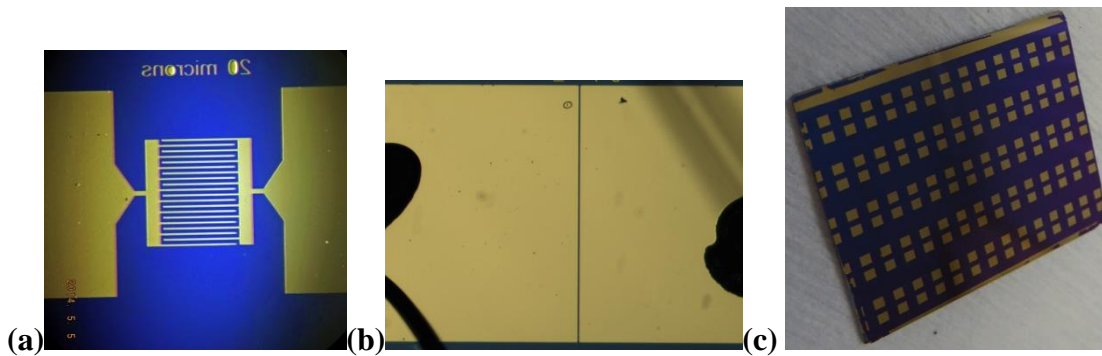


Figure WP4-14: Photographs of interdigitated (20 μm gap) (a), single microgap (10 μm gap) (b) photoconductors and processed piece of wafer with $1 \times 1 \text{ mm}^2$ pads containing waveguide-nanogap (50-150 nm gaps) devices (c).

As an starting point we fabricated photoconductive devices (200 μm gap) by depositing Ag electrodes on top of a DrBlading film (500 nm thick) with ligand exchange procedure (similarly to the case of Schottky photodiodes) on a glass substrate. For these photoconductors we arrive to photocurrents $\approx 30\text{-}50 \text{ nA}$ (responsivities very close to 0.1 A/W) in the wavelength range 1200-1500 nm at 200 V bias, despite the big distance between electrodes, over a reasonably low dark current (49 nA).

In the case of single microgap and interdigitated photoconductors the electrodes are patterned on the Si/SiO₂ wafer and created by using lift-off processing. For this reason the QD-solid films should be created in a subsequent step by dropping the QD solution, previous to the ligand exchange procedure and curing. This method is not ideal, because the reduced control of the QD-solid thickness and the formation of important granularity. Another technique that is being optimized is the controlled dispensation of the QD solution by using a microplotter, because it should be the optimal method to create a QD-film on nanogap devices.

The results obtained on the best microgap-based photoconductors are summarized in Figure WP4-15. In Figure WP4-15a the photocurrent as a function of the applied bias is recorded under solar-AM1 illumination (the incident power is 100 mW/cm^2 , giving different collected light in the three devices because of their different active area: 200 and 20 - 10 μW in the interdigitated and 20 - 10 μm gap photoconductors, respectively). The poorest results are observed is the interdigitated photoconductor, possibly due to the inhomogeneity in the QD-film over it largest active area as compared to the case of single microgap photoconductors; on the contrary the interdigitated device would offer the possibility to work with smaller applied bias, given the high number of fingers. For the best device, the 10 μm gap photoconductor, for which we measure a photocurrent around 40 nA at 1300 nm under a bias of 100 V, which is translated in a responsivity of around 1.6 A/W. It is important to mention that microgap devices degraded faster with exposure to ambient than Schottky photodiodes.

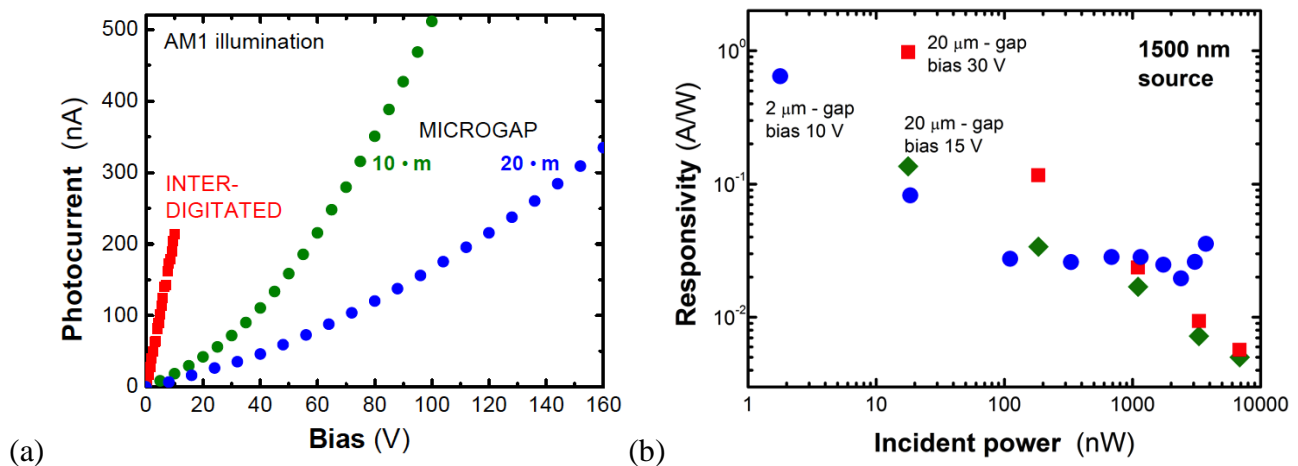


Figure WP4-15: (a) Photocurrent measured in a 20 μm gap interdigitated device (red symbols) as compared to 10 (green symbols) and 20 (blue symbols) μm gap photoconductors as a function of applied bias under AM1-solar illumination. (b) Responsivity measured in 2 and 20 μm gap photoconductor devices as a function of the incident power using a 1500 nm laser source; the applied bias is indicated in the plot.

For that reason a polymer encapsulation of photoconductor devices was performed after the final ligand exchange and curing processing that allows a stable operation with time. It is important to note that microgap photoconductors have a more important responsivity for lower incident powers, contrary to the case of Schottky devices, as shown in Figure WP4-15b for a 20 μm gap photoconductor after encapsulation, decreasing by near two orders of magnitude from 20 nW to 7 μW of incident power. The measured responsivity at 1500 nm was around 0.14 and 1 A/W under 15 and 30 V bias over dark currents of 12 and 18 nA, respectively. For a 2 μm gap photoconductor the observed phenomenology is similar, with a responsivity around 0.7 A/W under 2 nW illumination, even if the responsivity stabilizes at 0.02 A/W above 100 nW.

Plasmonic effects are expected if the distance between electrodes in a gap-waveguide photoconductor (metal-insulator-metal) is smaller than 100 nm: coupling of light both under normal and in-plane incidence and enhancement of the electric field in the nanogap region. The fabrication of these photoconductor devices (Figure WP4-16a) on Si-SiO₂ was not simple, because involving several processing steps to define the millimeter size gold pads, micrometer wide (from 0.5 to 2 μm) aluminum electrodes and the opened nanogap on them by using RIE after an ebeam patterning on PMMA (Figure WP4-16b). The QD-layer deposition and characterization of these devices are under way.

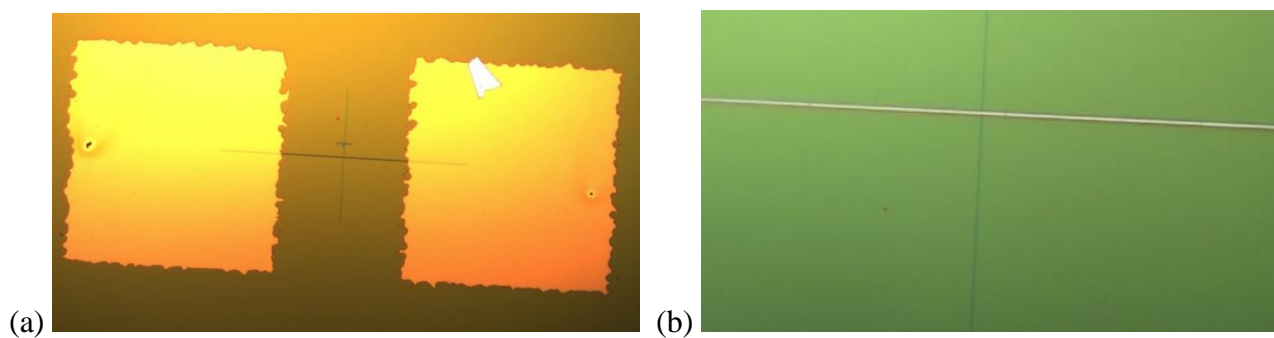


Figure WP4-16: (a) Nanogap devices fabricated on a Si-SiO₂ substrate, (b) detail of fabrication showing the patterned nanogap in the PMMA resist prior to RIE.

Status deliverables and milestones:

Milestones (all completed during Month 1-45)

MS16	Demonstration of decision on optimized structures for plasmonic amplifiers	4	UVEG	12	10/2012
MS17	Synthesis of nanoparticles with gain at 1550 nm	4	Ugent	12	10/2012
MS18	Demonstration of conductive QD layers with photoconductive properties	4	UVEG	15	01/2013
MS19	Demonstration of metal-(lithographic) polymer and QD metal-(lithographic) polymer nanocompo-sites	4	UVEG	15	01/2013
MS20	Demonstration and decision on photodetector operation: nano-gap (MIM) vs. Schottky / heterostructure	4	UVEG	18	04/2013
MS22	Demonstration of plasmonic amplifiers with optical pumping exhibiting 10dB gain	4	IMCV	21	07/2013
MS23	Operation of QD based photodetector with responsivity > 0.1 A/W	4	UVEG	24	10/2013
MS24	Demonstration of SPP amplifiers with electrical injection exhibiting 10dB/cm gain	4	UVEG IMEC	39	10/2014

Deliverables (all completed during Month 1-45):

D4.1	Designs of plasmonic amplifiers	4	UVEG	18	04/2013
D4.2	Report on optical properties of QDs layers and polymer nanocomposites	4	UVEG	18	04/2013
D4.3	Designs of plasmonic photodetectors	4	UVEG	24	07/2013
D4.4	Report on SPP amplifiers by using QDs	4	IMEC	30	10/2013
D4.5	Report on plasmonic photodetectors	4	UVEG	42	04/2015

Use of resources

Use of resources has been according to plan. The table below gives a review of each partners contribution. More efforts on person months are justified by the UVEG group without increase of costs (salary reductions in the last two years).

Partner	Person power	Main contribution
UVEG	22.2	Modelling, fabrication and characterization of polymer-QD plasmonic amplifiers, QD-based Schottky phodetectors / microgap photoconductors / plasmonic nanogap photoconductors
UGent	11	Synthesis of colloidal nanoparticles, fundamental particles properties characterization, study of electrical injection
IMEC	11.5	Fabrication and characterization of silicon hybrid plasmonic amplifier, study of electrical injection
AIT	4	Modelling of polymer plasmonic waveguides

Table WP4-1: Use of resources in work package 4.

3.2.5 Work Package 5: Optical and Electrical Interfaces

Work in WP5 was almost fully completed during the first half of the current reporting period, with the most important results already reported in the second and third intermediate reports. Hence for tasks 5.1, 5.3, 5.4 and 5.5 we restrict us to repeating the previously reported results. Only for task 5.2 we report some new results originating from D5.7

Task 5.1 Modelling and fabrication of coupling Si waveguide to plasmonic waveguide

Tapered Couplers: The tapered couplers for coupling light into the plasmonic modulators were numerically optimized, fabricated and tested. The mode converters have been fabricated as a part of plasmonic modulators. The modulators with various device lengths and with a slot size of 140 nm and 200 nm are fabricated on silicon on insulator (SOI) platform, where the silicon nanowire waveguides are used as access waveguides. The fabrication procedure is described in Milestone 11, “Fabrication of plasmonic modulator on a SOI platform” and Deliverable 3.4, “Report on fabrication of modulators”. Optical and scanning electron microscope images of the first generation device with device length of 34 μm and the slot size of 200 nm are given in Figure WP5-1(a) and Figure WP5-1(b), respectively.

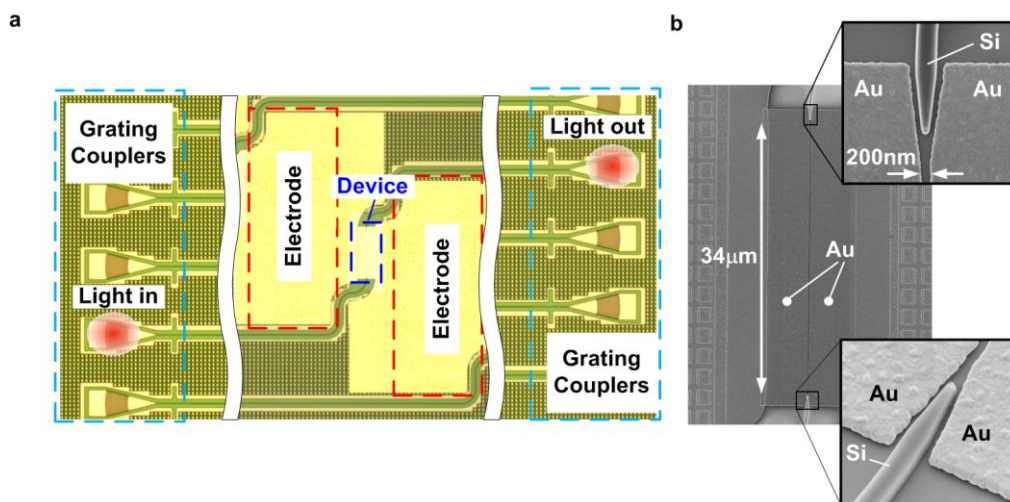


Figure WP5-1: Fabricated plasmonic phase modulator on silicon on insulator platform. (a) Optical microscope image of the device. Silicon nanowire waveguides are used as access waveguides for the plasmonic modulator. Light is launched in and out from the chip using grating couplers. (b) Scanning electron microscope image of the modulator with a length of 34 μm and a slot size of 200 nm. Metallic tapers are used for photonic to plasmonic mode conversion.

We used the experimental setup given in Figure WP5-2 for passive optical characterization. Light with from a tuneable laser source (TLS) is coupled into the device using a single mode fibers and a diffraction grating coupler. The transmitted optical power at the output of the device is measured with optical spectrum analyzer (OSA). We measured the optical loss of the modulator section by taking an equal-length of SOI strip waveguide as a reference. Example of the transmission spectrum of 34 μm long plasmonic modulator with a slot size of 200 nm is given in Figure WP5-2. The

average total loss is 12 dB (black solid line), close to the theoretically expected value (blue dashed horizontal line).

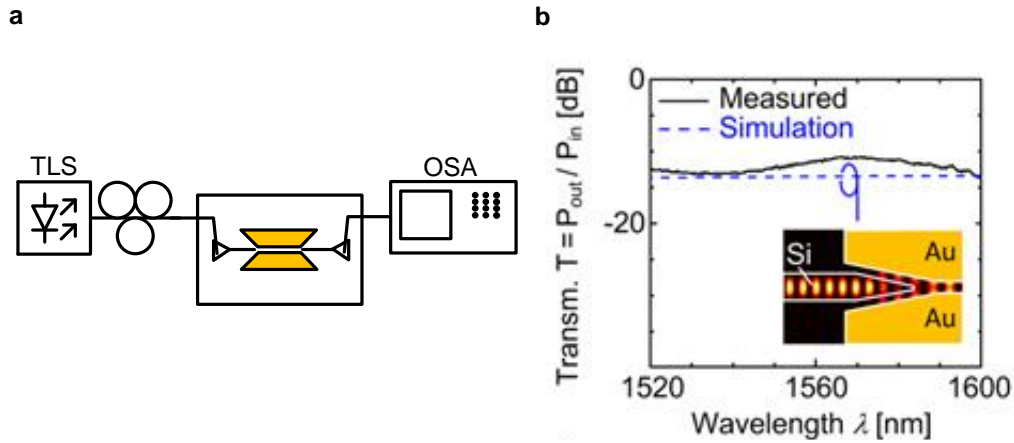


Figure WP5-2: The experimental setup used for passive optical characterization and the transmission spectrum of the plasmonic phase modulators. (a) The experimental setup used for measuring the optical losses of the device. Light from the tuneable laser source (TLS) is launched into the chip and the transmission spectrum is measured at the output using optical spectrum analyser (OSA). (b) The transmission spectrum of the 34 μm long device with a slot size of 200 nm, black solid line. The theoretically expected transmission spectrum is given in the blue dashed line.

We have performed an SPP coupling loss estimation on our second generation of plasmonic modulators with a slot size of 140 nm. A good alignment and a desired 140 nm slot size have been achieved for the modulators with a length of 1 μm , 29 μm and 44 μm . We used the measured losses at the wavelength of 1550 nm to derive the propagation loss and the coupling loss of our modulators. By fitting the total loss versus device length dependence with a linear function we could estimate that the coupling loss and the propagation loss at 1550 nm wavelength, see Figure WP5-3. The coupling loss in our second generation device is reduced below 1 dB. The propagation loss in the modulator with a slot size of 140 nm is 0.52dB / μm which is very close to theoretically expected value of 0.48dB / μm .

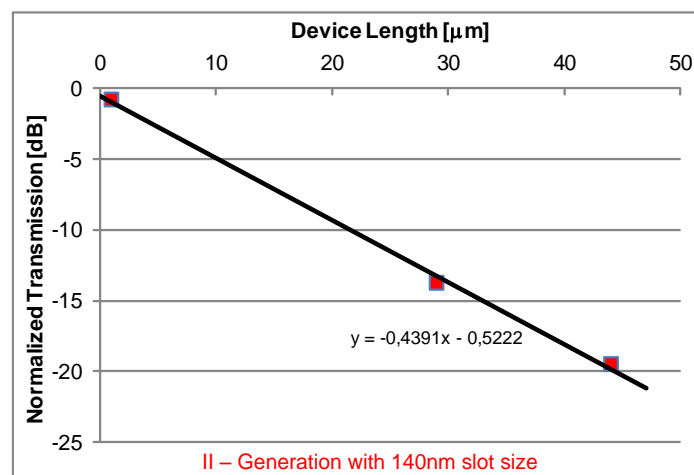


Figure WP5-3: Measured power transmission at the wavelength of 1550nm for plasmonic modulators with various lengths. Performing linear fit we can estimate the SPP coupling and propagation losses in the modulator.

Side Couplers: Horizontal metallic slot waveguide can be excited with a directional coupler configuration. In this coupling scheme, the photonic mode propagating through the silicon nanowire is phase matched with the SPP in a horizontal slot waveguide. SPP is then excited with the photonic mode propagating through the silicon nanowire similar to the conventional multimode interference couplers, see Figure WP5-2.

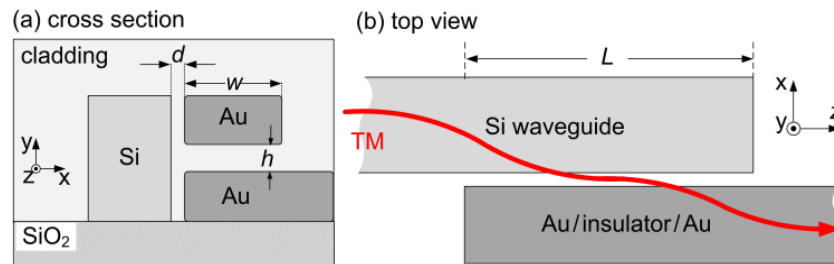


Figure WP5-4: (a) Cross section and (b) top view of the suggested coupler. The TM mode launched into the silicon nanowire couples to a plasmonic waveguide via a coupling section of length L .

We extended our previous study of this kind of plasmonic couplers and the results now have been reported in the Deliverable 5.5 “Report on plasmonic couplers”. In the Figure WP5-5, the conversion efficiency and the coupling length as a function of the distance d and the slot

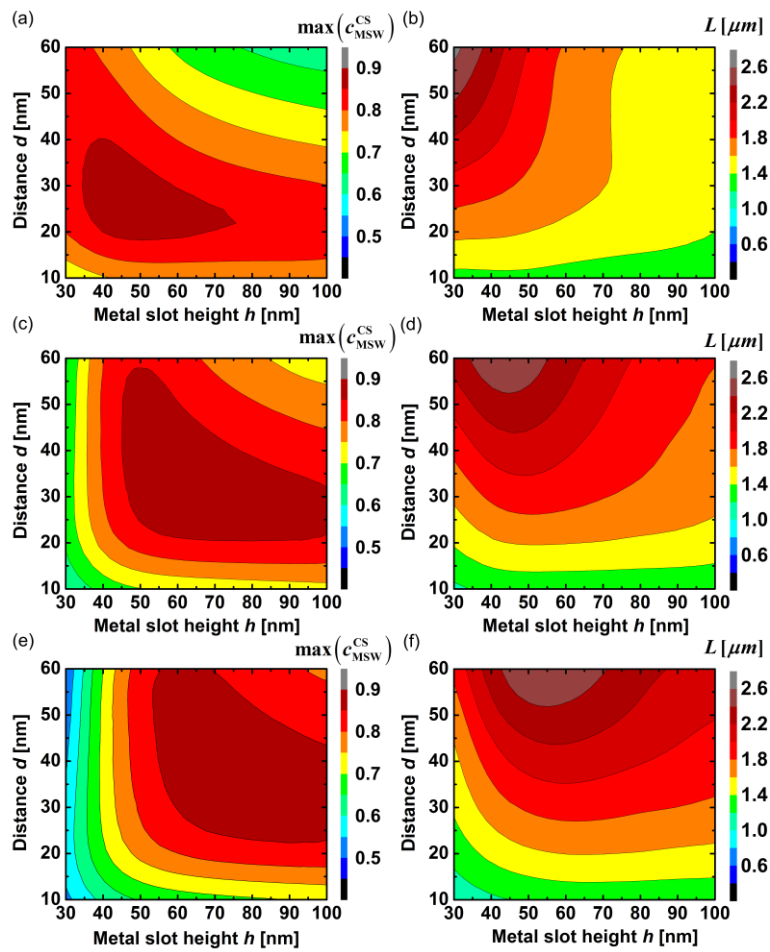


Figure WP5-5: Conversion efficiency (a), (c), (e) and optimum CS length L (b), (d), (f) for a MSW with a width w of 200 nm and for various cladding materials: (a) and (b) for Glass, (c) and (d) for organic materials with refractive indices of 1.6 and (e) and (f) for refractive index of 1.7.

are given for MSWs with a width w of 200 nm for various cladding materials. Glass with a refractive index of 1.44, see Figure WP5-5 (a), (b), and organic materials with refractive indices of 1.6, see Figure WP5-5 (c), (d), and 1.7, see Figure WP5-5 (e), (f), are considered as cladding materials. For all three types of cladding materials, conversion efficiencies exceeding 85 % can be achieved for MSWs with sub - 50nm slots. Moreover, by varying geometrical parameters e.g. the distance d , the conversion efficiency can be tuned. This might be needed e. g. in the case of plasmonic coupling scheme shows a great tolerance to fabrication errors in defining the length L .

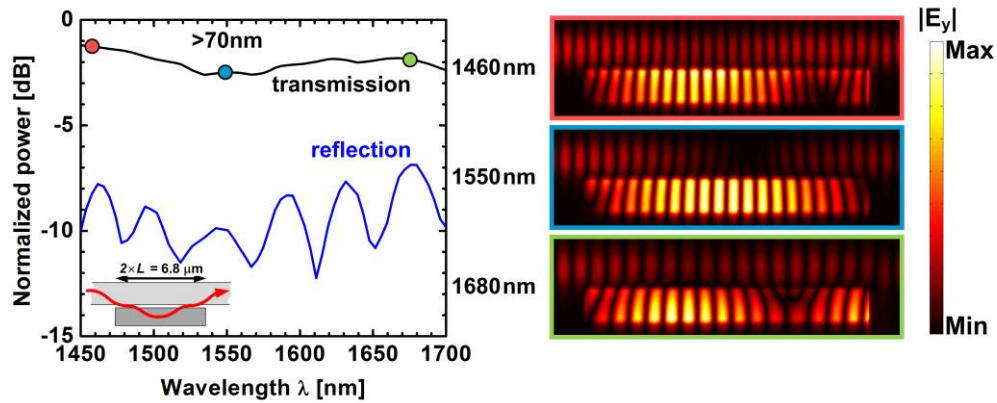


Figure WP5-6: Transmission and reflection spectra in the converter with a height h of 30 nm, a distance d of 60 nm and a cladding material with a refractive index of 1.44. The dip in the transmission shows the good photonic / plasmonic mode conversion, in which case the Ohmic losses are the highest. In addition, the electric field distributions for three different carrier wavelengths are given in the right side. It can be seen that the photonic mode is fully converted in a gap SPP in the case of 1550 nm wavelength.

To investigate how the performance of the proposed mode converter depends on the operating carrier wavelength, we investigate the mode conversion mechanism in a converter with a silicon dioxide cladding by finite difference time domain (FDTD) method simulations. In this particular simulation a metallic slot height h of 30 nm and a distance d of 60 nm have been chosen. A continuous silicon nanowire is used with a CS length of $2 \times L$ of $6.8 \mu\text{m}$, as plotted in the inset of Figure WP5-6. Transmission and reflection spectra are given in Figure WP5-6. The wavelength dependence of the optical properties of Au is taken into account by the Drude model. No strong resonance behaviour is seen in the optical response of the mode converter. The operating wavelength range of the proposed device is in the range of 50 nm, which is comparable to the one reported for metallic taper mode converters.

Task 5.2 Design and fabrication of Si beam shaper

In the first half of the project we focused on electrostatically moved grating couplers. This work was completed in the first reporting period. For the second period, the original plan was to focus on the design of grating couplers allowing to couple a transmitter and receiver chip through free space over distances from 0.1 to 1.0 mm. We started this work with a high level design study, estimating the distance that can be expected and the form factor of the grating that should be used. From this study it became clear the achievable improvement in coupling distance/minimum pitch when designing focussing grating couplers compared to standard grating couplers would be less than a factor two (Figure WP5-7). This, together with the fact that in the demonstrator foreseen this vertical coupling between two chips was no longer relevant and strong overlap with earlier published results from Oracle led to the decision to shift focus to work more linked to the colloidal quantum dot devices developed in WP4.

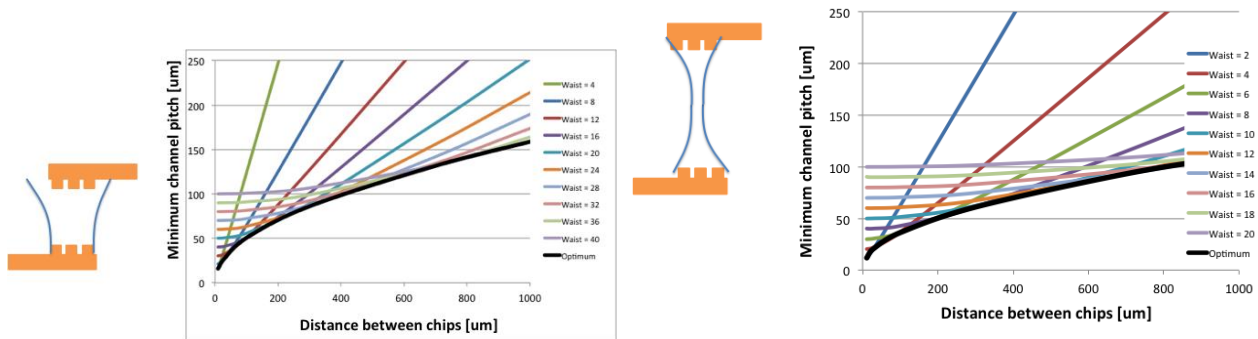


Figure WP5-7: Minimum channel pitch as function of distance between chips for different initial grating sizes, standard grating(left) and focusing gratings (right)

As described in WP4, imec together with UGent developed a platform whereby colloidal quantum dots are embedded in a SiN-stack. The possibility of using these quantum dots as single photon emitters is currently being investigated. In such applications it is important to efficiently couple the light from the SiN waveguide with embedded quantum dot to a microscope objective, for further analysis. Inspired by earlier work from the Vucovic group³ which demonstrated such a grating coupler for a III-V semiconductor material system, we studied the possibility of using a deeply etched, ultra compact grating as shown in Figure WP5-8 to realize this coupling. Compared to III-V semiconductor SiN has a considerable lower index contrast with air so it is not a priori trivial this is indeed possible. Therefore we carried out extensive simulations of the proposed device.

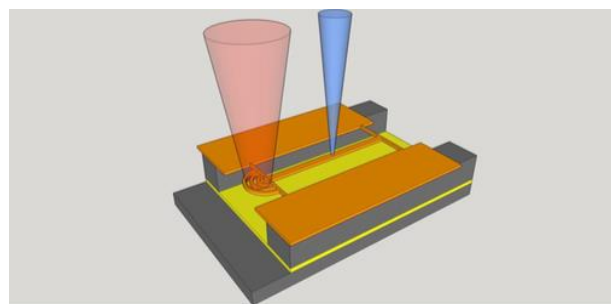


Figure WP5-8: Schematic view of proposed ultra-compact grating coupler. The «blue» beam excites a QD embedded in the SiN-waveguide. Light emitted by the QD is coupled in the waveguide and then coupled upwards to the microscope objective through the compact grating coupler (red beam).

Simulations were carried out using 2D and 3D FDTD. Figure WP5-9 shows some examples of the optimisation process. Both a 100nm thick (TE-polarization) and 220nm thick (TM-polarization) SiN layer were considered, because these maximise coupling of the QD “dipole emitter” to the waveguide. Initially no bottom substrate was considered. In this case coupling efficiencies of up to

³ Faraon, Andrei, et al. "Dipole induced transparency in waveguide coupled photonic crystal cavities." *Optics express* 16.16 (2008): 12154-12162.

50% can be reached (Figure WP5-9a). Next we added a high reflective bottom substrate. Optimising the distance between bottom substrate and grating coupler allows coupling efficiencies of up to 87%.

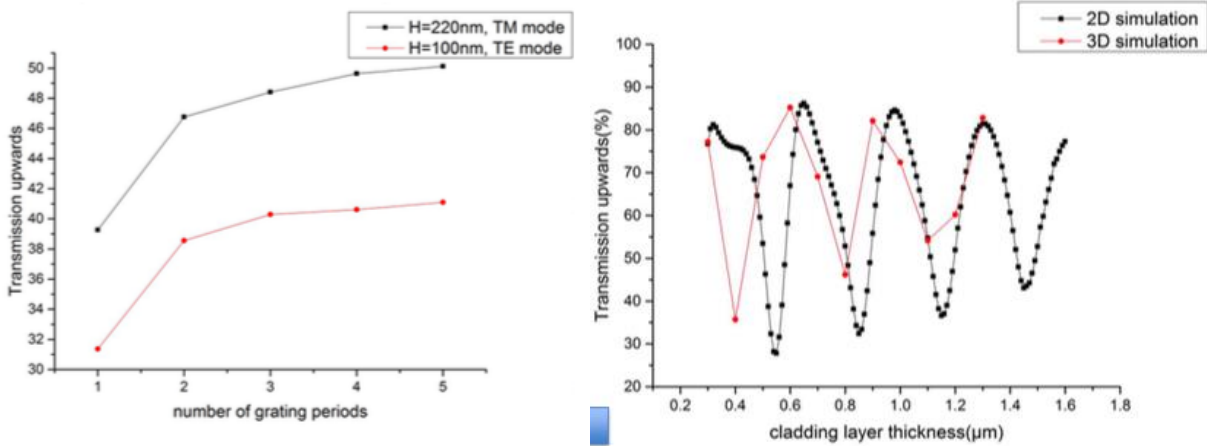


Figure WP5-9: Simulation of coupling efficiency for ultra-compact grating coupler. a) Coupling efficiency as function of number of grating periods. b) Coupling efficiency when including bottom mirror (as function of distance between bottom mirror and grating).

Some of the most promising designs were fabricated and characterised. An array of devices with constant input grating coupler and varying output coupler were realized. This allows measuring the relative coupling strength of these gratings. Good agreement with modelling was obtained. These results are described in more detail in D5.7.

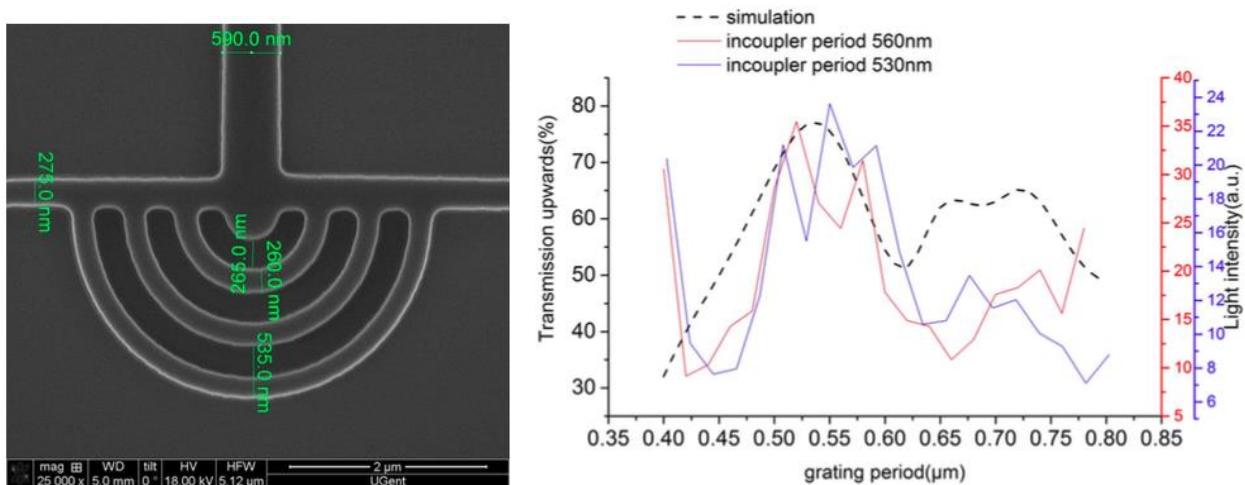


Figure WP5-10: SEM-picture of fabricated grating and measured transmission efficiency (relative) as function of grating period.

Task 5.3 Design and fabrication of passive ultra-compact components as filters

This task was finished during the first reporting period (see D5.3 for details)

Task 5.4 Signal generation module design

The **Dual Die Communication Module** (abbreviated **DDCM**) is the building-block responsible for the interconnection of different dice within a so called Network in Package (NiP), the communication system enabling inter dice data transmission in the context of Systems in Package (SiP) technology.

According to a widely used approach, the DDCM is seen composed of two main building blocks:

- the DDCM **controller**, responsible for managing incoming/outgoing STNoC/SBus/AMBA-AXI traffic, generating IDN segments through encapsulation and preparing them to be sent to the PHY transmitter, as well as collecting them from the PHY receiver;
- the DDCM **PHY**, responsible for transmitting output phyts across the physical link and collecting inputs phyts from the physical link.

As shown in , the DDCM top level in each die consists of a transmitter (DDCM Tx) and a receiver (DDCM Rx).

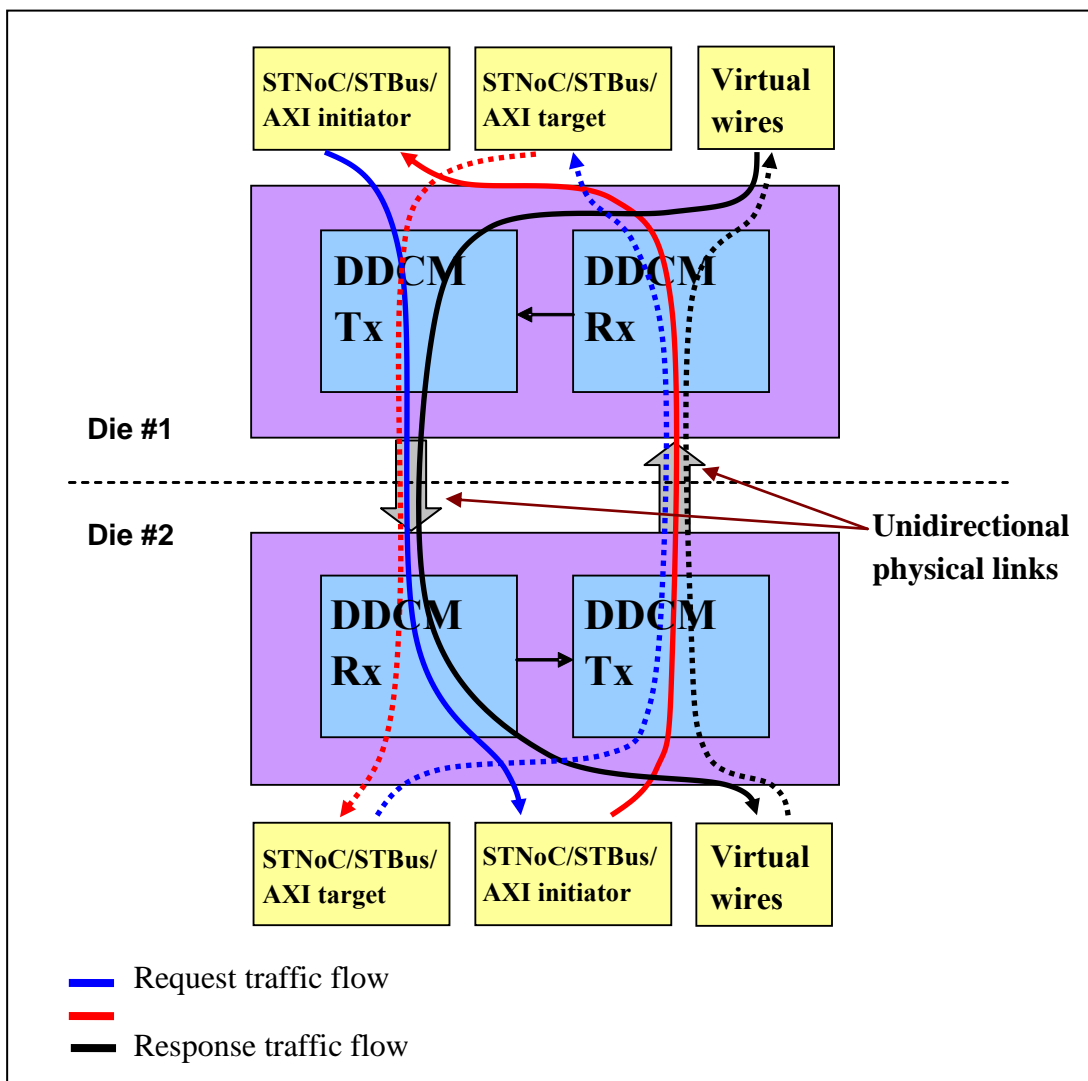


Figure WP5-11 DDCM top level architecture and information flow

In such a figure it's possible to see the two information flows supported by a complete DDCM architecture, i.e.

- requests from STNoC/STBus/AMBA-AXI initiators in chip 1 to STNoC/STBus/AMBA-AXI targets in chip 2, responses from STNoC/STBus/AMBA-AXI targets in chip 2 to STNoC/STBus/AMBA-AXI initiators in chip 1, virtual wires from chip 1 to chip 2 (continuous lines);
- requests from STNoC/STBus/AMBA-AXI initiators in chip 2 to STNoC/STBus/AMBA-AXI targets in chip 1, responses from STNoC/STBus/AMBA-AXI targets in chip 1 to STNoC/STBus/AMBA-AXI initiators in chip 2, virtual wires from chip 2 to chip 1 (dotted lines).

The DDCM is a **parametric** design that, depending on the SoC where it is used, can be configured properly in order to meet system requirements and needs in terms of interfaces, FIFOs sizes, clock domains synchronization and functionality.

So as for the DDCM with electrical PHY, a VHDL model of the plasmonics-based PHY has been developed in order to be co-simulated with the digital parts of the DDCM described as synthesizable VHDL

The DDCM data base is located in the ST Interconnect System Group server design area under the directory **ddcm_lib** identifying the design library.

The **ddcm_lib** directory contains the following two subdirectories:

- **dev** (development) containing the generic design and the generic verification environment;
- **run** containing the simulation area for a set of specific configurations of the design.

The directory **dev** contains the following subdirectories:

- **doc** containing the functional specification of the block (deliverable D5.4 in NAVOLCHI project context);
- **rtl_vhdl** containing the VHDL files representing the rtl description of the DDCM top level and all its building-blocks;
- **model** containing the VHDL files representing the rtl behavioural description of the analog building-blocks and the plasmonic devices implementing the plasmonics-based PHY;
- **corekit** containing the generic view of the DDCM;
- **verif_env** containing the generic verification environment, i.e. testbench and stimuli sources;
- **verif_run** containing the tests to verify the different functionality of the DDCM;
- **synth** containing the area for the logic synthesis of the DDCM.

The design environment consists of the directory **rtl_vhdl** and **corekit**.

In the `rtl_vhdl` directory there are the files describing VHDL entity and architecture of the DDCM top level and all its building-blocks (i.e. transmitter, receiver, FIFOs, etc.)

All these blocks are described following a parametric approach, so that after setting a proper set of parameters to the required values, the generic design gets configured accordingly and becomes specific for a well defined application. As described in the DDCM functional specification (deliverable D5.4) the design parameters allow to characterize the DDCM in terms of interfaces size, FIFO depth, traffic management policy, clock frequencies, etc.).

The VHDL description is *technology independent*, that is to say the VHDL files describe the structure and the functionality of the DDCM, with no links with the CMOS technology with which the DDCM itself will be implemented.

In the `model` directory there are the files describing the VHDL behavioural models of the analog electronic parts (modulator driver, TIA, comparator) and the plasmonic devices (emitter, modulator, waveguide, detector) to be co-simulated with the digital parts of the DDCM.

The `corekit` directory contains a set of scripts allowing to build the so called *corekit*, a file containing all the information about the generic design and allowing by means of a GUI (Graphic User Interface) the user to assign the required values to the design parameters and getting a specific configuration of the DDCM, moving from the generic description.

The verification environment, strongly based on the one developed for the DDCM with electrical PHY, consists of the directories **verif_env** and **verif_run**.

The `verif_env` directory in turn contains the following main subdirectories:

- **rtl_tb** containing the VHDL testbench, i.e. the structure instantiating the DDCM and the plasmonics-based PHY behavioural model, considered the **DUT** (Device Under Test) and the traffic generators for stimulating the design and verify its behaviour accordingly;
- **e** containing the functional description of the traffic generators in *e* language, an object oriented high level language specific for verification suites;
- **config_files** containing a variety of files with different set of design parameters so to configure the DDCM in different ways in order to verify as many different specific implementations as possible;
- **tests** containing the description of different tests, aiming at stimulating the different DDCM functionalities.

The `verif_env` directory contains generic descriptions of all the structures described in it (testbench, stimuli generators, tests); the `verif_run` directory contains a replication of the `verif_env` subdirectories but configured according to the design parameters, and the specific for a well defined application or product employing the DDCM.

Task 5.5 Signal Generation Module implementation via FPGA

The FPGA mapping activity was impacted by some HW failures and some problems with SW licenses. It started actually in January 2014, and in order to speed up the process at first a simplified system, composed of only a PHY adapter transmitter and a PHY adapter receiver connected back to back will be implemented. This in any case is sufficient to effectively test the off-chip plasmonic interconnect. In a second phase, if enough time is available, the whole system including two complete DDCM modules will be implemented.

Because of an objective difficulty in moving ST FPGA equipment from Catania (it's embedded within a server shared with other ST groups requiring to work with it) it has been agreed that the synthesized rtl, after all the verifications have been run, will be sent to another partner responsible for mapping it onto an own FPGA that will be easily interfaced with the board where the plasmonic interconnect components will be integrated.

After digital design and functional verification phases, the developed rtl code has been synthesized in order to get a gate level netlist, representing the Front-End view (schematic) of the DDCM.

The synthesis environment consists of the directory **synth**.

This in turn contains the following subdirectories:

- **input** containing the configured VHDL code for a specific DDCM implementation;
- **scripts** containing the commands for the synthesis tool;
- **run**, the directory where the synthesis tool is invoked and log files are recorded;
- **reports** containing the characterization of the synthesized design in terms of area, timing (speed) and power consumption
- **output** containing the synthesized DDCM design in terms of Front-End netlist.

The generic DDCM synthesis environment is fully based on **Synopsys** tools, i.e. **Design Compiler** as synthesis engine and **Design Vision** as interactive GUI.

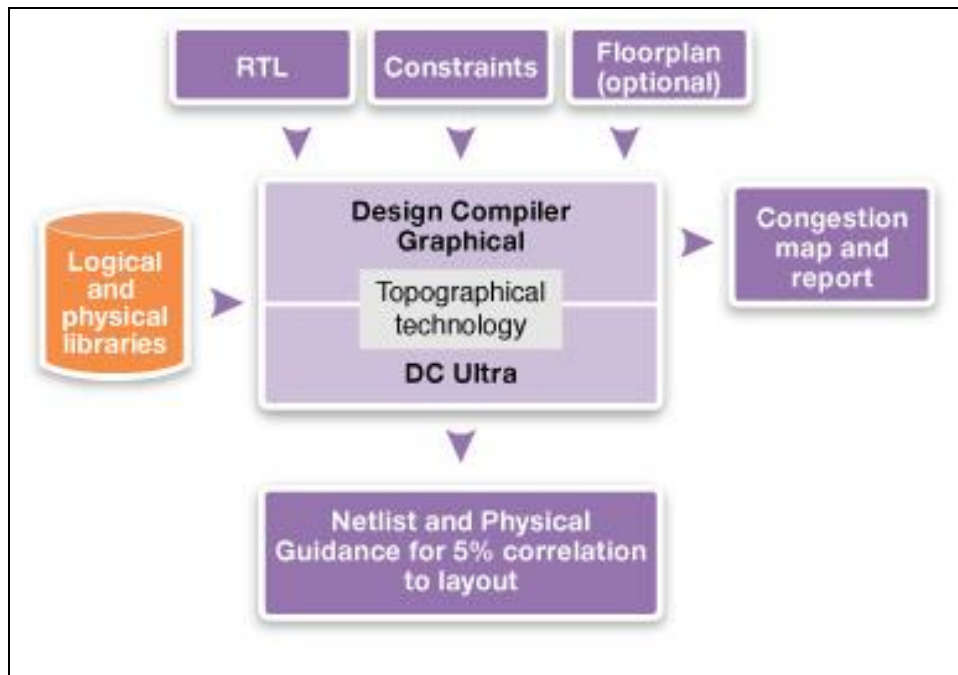


Figure WP5-12 Synthesis flow based on Synopsys Design Compiler

The synthesis design phase is strongly technology dependent, since the results of the synthesis process, i.e. the gate level netlist, is an assembly of technological standard cells implementing the structure and the functionality of the DDCM in the required technology.

Also the version the DDCM supporting a plasmonics-based PHY has been synthesized using 65nm and 40nm CMOS technologies. Of course no synthesis activities have been carried out for the analog parts and for the plasmonic devices composing the plasmonics-based PHY, since a specific full custom design is required for them.

Based on the Synthesis environment, a flow for the characterization of the digital parts of the DDCM in terms of power consumption has been developed, as shown in Fig. 5-3.

According to this flow a specific configuration of the DDCM is simulated many times, and for each simulation the switching activity at each node and across each wire of the design is recorded; then this switching activity is back-annotated on the netlist in Design Compiler environment, and the power analysis tool is invoked so to calculate the power consumed by the DDCM block taking into account the switching activity determined by the traffic injected in different scenarios.

Relying on the obtained data, average and peak power consumption was determined. However the contribution of the digital parts to the power consumption of the overall system is negligible, since the highest contribution is expected to come from the plasmonic components.

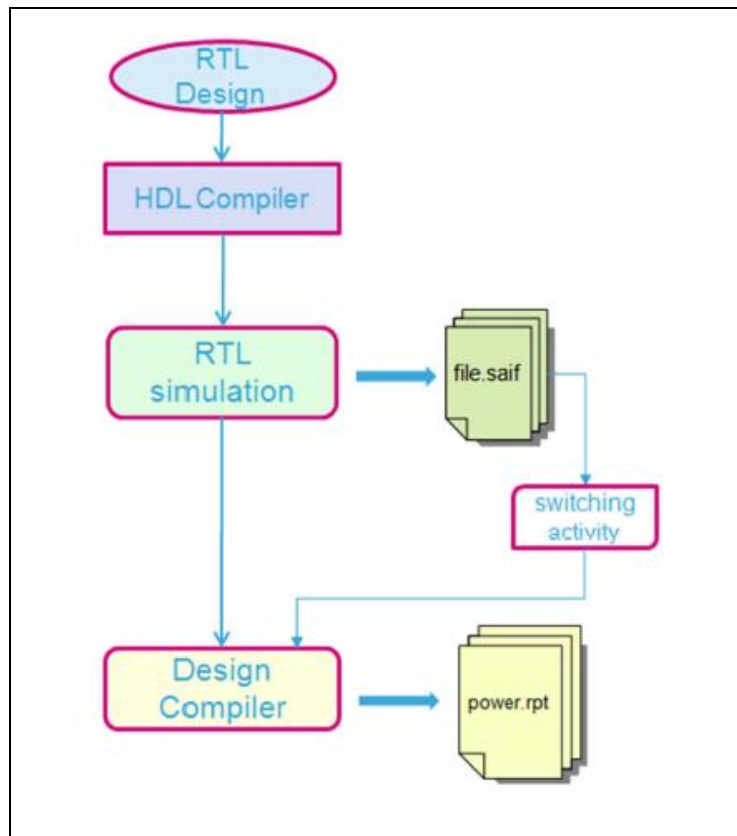


Figure WP5-13: Power consumption characterization flow

After synthesis and characterization flows have been carried out, the DDCM rtl code has been synthesized for FPGA mapping, exploiting ZeBu equipment and related environment. The synthesis flow for FPGA is fundamentally the same as the one already described; the main difference is in the synthesis engine, that instead of translating the rtl design into a set of standard cells exploiting technology libraries, translates the rtl design into a set of logic structures that can be mapped into the hardware basic logic structures available in the ZeBu FPGA chip. The mapped FPGA has then been stimulated and functionally validated with a verification environment very similar to the one used for rtl functional verification, the main difference being in the DUT; not an rtl code anymore, but an FPGA chip connected to the PC via a parallel interface, across which stimuli go from verification environment to FPGA, and FPGA reactions go back to verification environment.

Status deliverables and milestones

WP5 Deliverables

D5.1	DDCM specification document	5	ST	6
------	-----------------------------	---	----	---

D5.2	DDCM with electrical PHY design and verification data base	5	ST	12
D5.3	Compact optical filters (2nm bandwidth, >30nm FSR) and first generation beam shapers	5	IMEC	21
D5.4	Generic DDCM compatible with plasmonic-based PHY specification document	5	ST	24
D5.5	Report on plasmonic waveguide couplers	5	KIT	24
D5.6	Generic DDCM compatible with plasmonic-based PHY design and verification data base	5	ST	39
D5.7	Second generation beam shapers (distance 1mm, with bandwidth > 10nm and efficiency > 3dB)	5	IMEC	42

WP5 Milestones

MS25	Decision on optimized plasmonic waveguide couplers	5	KIT	6	04/2012
MS26	Fabrication of plasmonic waveguide couplers with less than 3 dB coupling loss	5	KIT	12	10/2012
MS27	Design of first generation beam shapers and compact optical filters	5	IMEC	12	10/2012
MS28	DDCM with electrical PHY design and verification	5	ST	12	10/2012
MS29	Data codecs for power consumption reduction	5	ST	15	01/2013
MS30	Decision on plasmonic waveguide couplers with less than 3 dB coupling loss	5	KIT	15	01/2013
MS31	Fabrication of compact optical filters and first generation beam shapers	5	IMEC	18	04/2013
MS32	Data codecs for error detection and correction	5	ST	18	04/2013
MS33	Design of second generation beam shapers	5	IMEC	24	10/2013
MS34	Generic DDCM compatible with plasmonic-based PHY	5	ST	24	10/2013
MS35	Fabrication of compact optical filters and first generation beam shapers	5	IMEC	39	01/2015
MS36	DDCM evolution for NiP solutions	5	ST	39	01/2015

Use of resources (second reporting period)

The table below gives a review of each partner contribution.

Partner	Person power	Main contribution
IMEC	5	Design and fabrication of grating couplers
KIT	18	Plasmonic couplers: fabrication and characterisation
ST	3.6	DDCM design and verification activities completed Study of DDCM evolution for NiP application not carried out because of ST interest change

3.2.6 Work Package 6: Integration, Characterising and Testing

In this section we summarize the work of WP6. D6.1 and 6.2 were already reported in the 3rd intermediate report which is why we focus on D6.3 and D6.4.

Task 6.3 Chip to chip interconnect characterization

This task contains the implementation and characterization of a prototype of the plasmonic interconnect, built by integrating an array of the plasmonic Mach-Zehnder modulator. A transmitter operating at 4×36 Gbit/s is shown on a footprint that is only limited by the size of the high-speed contact pads, see Figure WP6-1 and Figure WP6-2. The array is contacted through a multicore fiber with a channel spacing of $50 \mu\text{m}$ (D6.2). The array has been characterized for optical interchannel crosstalk which was found to be below -31 dB. No electrical crosstalk was observed. The MZMs showed no bandwidth limitation up to 70 GHz. The individual MZMs comprise plasmonic phase modulator sections that are as short as $12.5 \mu\text{m}$. This allows for a dense arrangement of the MZMs that is only limited by the size of the contact pads needed for addressing the devices with electrical probes. The devices are able to operate over a broad spectral range of >100 nm.

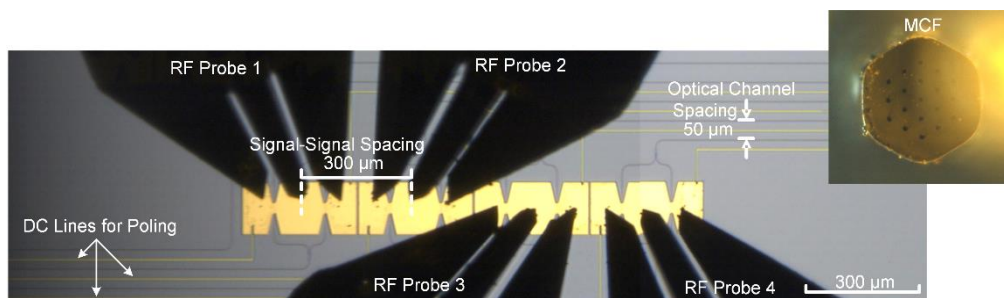


Figure WP6-1 Optical microscope image of the fabricated four-channel MZM array contacted by RF probes. The plasmonic phase modulators are $12.5 \mu\text{m}$ long with slot widths of 75 nm .

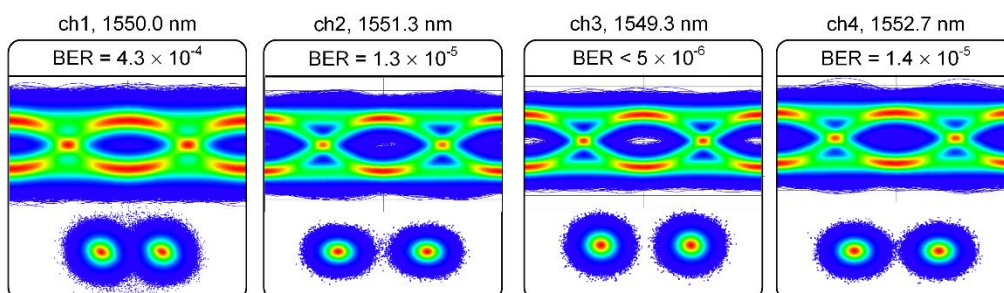


Figure WP6-2 Optical eye and constellation diagrams with bit error ratios (BER) of the data experiments (BPSK) at data rates of 36 Gbit/s. All four channels have a BER below the FEC limit of 2×10^{-3} .

Task 6.4 Plasmonic system-in-package interconnect prototype testing and evaluation

In this task, a simple but complete SiP for a chip-to-chip interconnect is demonstrated. Light from an external laser is fed to an array of four plasmonic modulators. All four modulators are driven with electrical signals after amplification on an electrical board. On the receiver side, IMEC's conventional Si-Ge photodiodes are used to make the optical to electrical signal conversion. The electrical signals after the photodiodes are amplified with the transimpedance amplifiers. The optical link between transmitter and receiver is realized through multicore fibers. Each component was tested independently before assembly.

Before integrating the driving electronics with the plasmonic modulators, the amplifiers were tested using RF probes at the output. Data experiments were carried out at 10 Gbit/s and 20 Gbit/s (PRBS 15, 500 mV_{pp} input signal) showing open eye diagrams for all amplifiers, see Figure WP6-3.

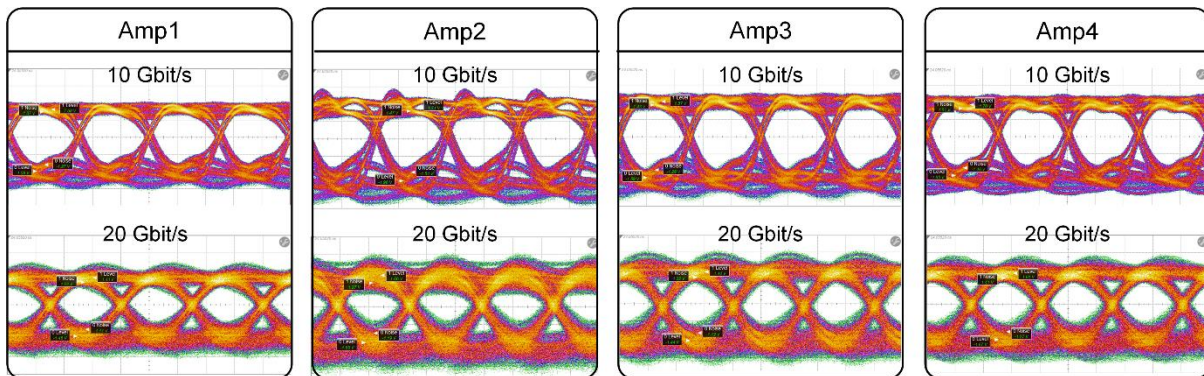


Figure WP6-3 Eye diagrams at 10 Gbit/s and 20 Gbit/s for the four amplifiers on the PCB before bonding to the plasmonic modulators.

In a next step, the plasmonic modulators were integrated with their driving electronics in a single package as shown in Figure WP6-4. The applicability plasmonic transmitter in communication systems was verified by data modulation experiments. Figure WP6-5 depicts the measured optical eye diagrams and constellation diagrams for all four channels at 10 Gbit/s. All channels have bit error ratios (BERs) below the FEC limit of 2×10^{-3} (7 % overhead); no error was detected within the 10 million recorded bits for channel 1 and 3.

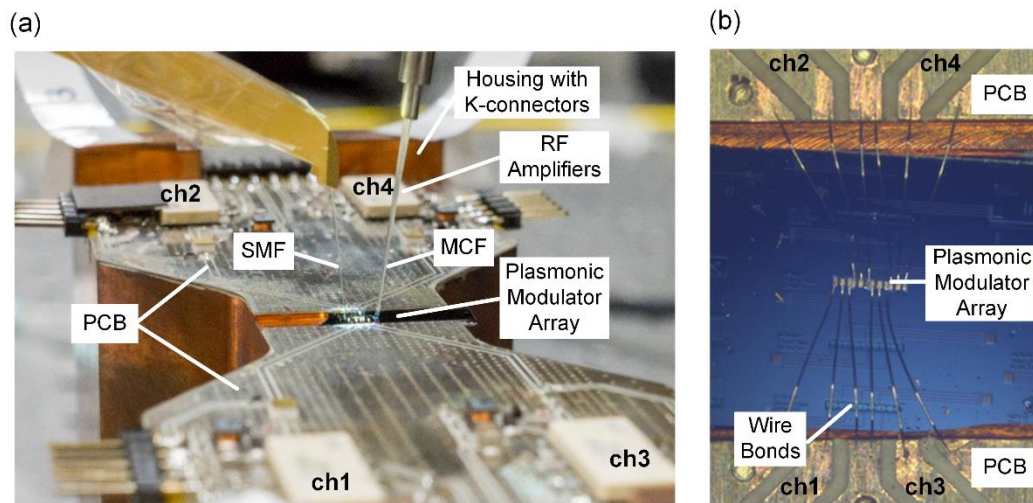


Figure WP6-4 Transmitter. (a) Customized package with plasmonic modulator array and PCB containing driving electronics. (b) Plasmonic modulators wirebonded to the PCB.

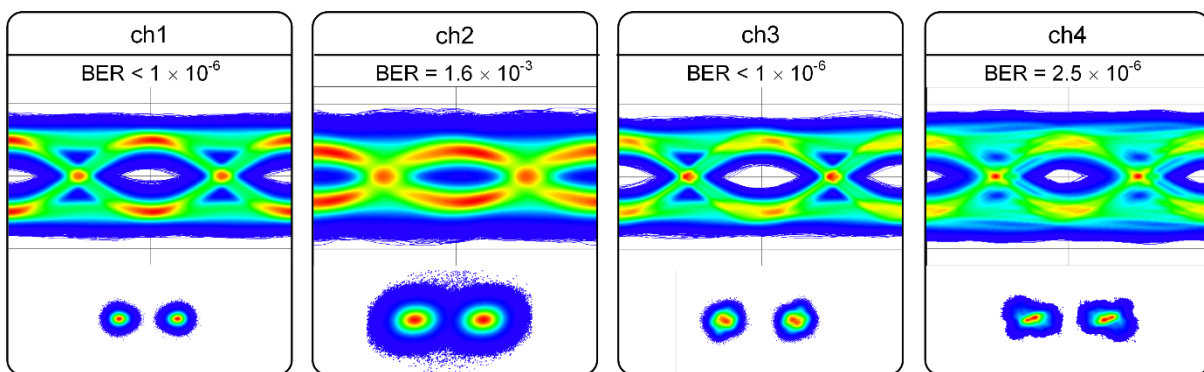


Figure WP6-5 Optical eye and constellation diagrams with bit error ratios (BER) of the data experiments (BPSK) at data rates of 10 Gbit/s. All four channels have a BER below the FEC limit of 2×10^{-3} .

On the receiver side, IMEC's Si-Ge photodiodes (PD) were used and wire bonded to a 4 channel 28 Gb/s transimpedance limiting amplifier (TIA) array, see Figure WP6-6. The receiver was tested in data experiments as shown in Figure WP6-7. While channel 2 could not be bonded (Figure WP6-6), open eye diagrams are shown for Channel 1,3,4.

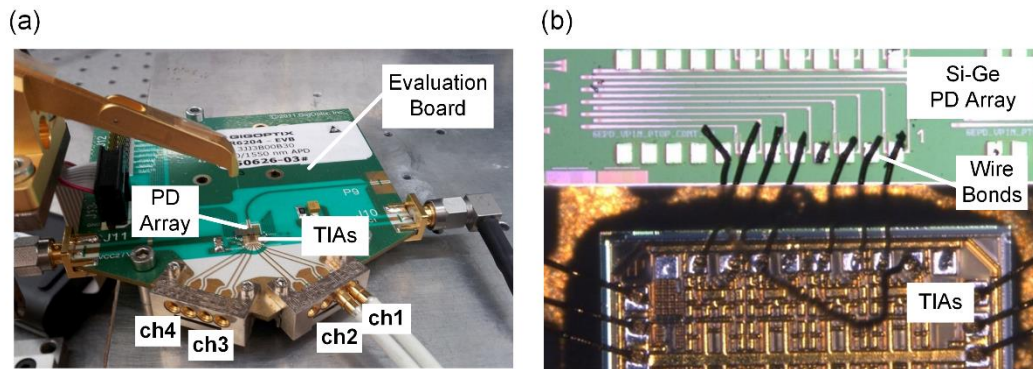


Figure WP6-6 Receiver (a) Evaluation board with Si-Ge photodiode array and PCB containing electronics. (b) Photodiodes wirebonded to the PCB. Channel 2 could not be bonded, since the arrangement of the anode and cathode contact pads on the optical and the electronic chip did not perfectly match.

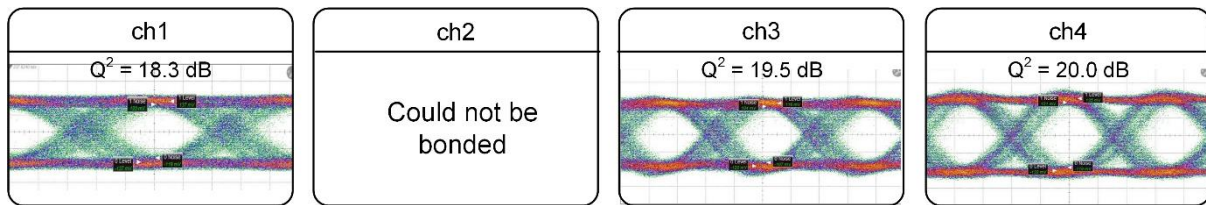


Figure WP6-7 Optical eye diagrams with quality factor (Q^2) of the data experiments (NRZ, rectangular) at data rates of 28 Gbit/s. Channel 2 could not be bonded, so no data experiment was carried out. Channel 2,3,4 show open eye diagrams.

In a final step, transmitter and receiver were tested as a full chip-to-chip interconnect, see Figure WP6-8. Since time at the end of the project was very limited, only one channel is shown here as an example. The chip-to-chip interconnect successfully operated at 20 Gbit/s with a BER of 7.9×10^{-5} .

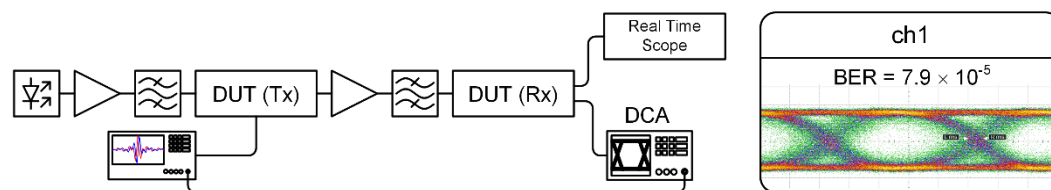


Figure WP6-8 Experimental setup for data modulation experiments of the full chip-to-chip interconnect. Laser light at 1547.8 nm was coupled to the transmitter. Electrical data streams were generated by an arbitrary waveform generator (AWG) and sent to the channel under test of the transmitter. The modulated signal was amplified and sent to the receiver. At the receiver output, eye diagrams were measured with a digital communication analyser (DCA), while the bit error ratios were obtained with a real time scope. (b) Optical eye diagram of the data experiment (NRZ, rectangular, DBBS 15) at data rates of 20 Gbit/s for Channel 1 as an example.

WP6 Deliverables

	Name of Deliverable	Responsible Partner	Delivery Month
D6.1	Report on characterization results of all plasmonic devices	TU/e	27
D6.2	Report on characterization results of all optical interface plasmonic passive components	KIT	27
D6.3	Report on chip to chip interconnect characterization	ST/ETH	45
D6.4	Report on plasmonic system-in-package interconnect prototype testing and evaluation	AIT/ETH	45

WP6 Milestones

	Name of Milestone	Responsible Partner	Delivery Month
MS39	Concept for system integration developed	AIT	40
MS40	Individual plasmonic devices characterization, testing and evaluation	TU/e	39
MS41	Chip to chip interconnect characterization	ST/ETH	42
MS42	Plasmonic components integration to demonstrate chip-to-chip interconnect	AIT/ETH	42
MS43	Plasmonic chip to chip interconnect prototype testing and evaluation	ST/ETH	45

The table below gives a review of each partner contribution. AIT shifted 5 PM to ETH Zurich.

Partner	Person power	Main contribution
KIT	7.00	Plasmonic modulators characterisation
IMEC	2.00	Plasmonic photodetector characterization
TU/e	3.00	Plasmonic laser characterization
AIT	1	Definition of testing procedures

ETH Zürich	25.1	Assembly and packaging, characterization of the individual components, analysis on the developed chip to chip interconnect
---------------	------	---

3.2.7 Work Package 7: Exploitation and Dissemination

General Status

During the whole period of NAVOLCHI all tasks (Task 7.1 (Dissemination) and Task 7.2 (Exploitation) and Task 7.3 (Promotion)) have been active. NAVOLCHI partners have contributed several publications to high-quality scientific journals, magazines and conferences disseminating project results. Communication has been established with another plasmonics-related EU-funded project (PLATON).

Task 7.1 Dissemination

Dissemination of ideas and results is of high importance in the NAVOLCHI project. The partners of NAVOLCHI are top research organizations with proven track records in their field and are very active in disseminating research results in a worldwide range to scientists, industry, and the public.

NAVOLCHI partners have been very active disseminating and promoting the activities and results of the project. The following list summarizes the related activities of the project.

- 37 journals to highly ranked journals
- 74 conference publications disseminating the project have been published by NAVOLCHI partners,
- in addition, a cover article on plasmonic communications has been published in the May 2013 issue of *Optics & Photonics News*.
- a white paper on the innovation potential of plasmonic interconnects has been published online,
- a NAVOLCHI workshop on plasmonics-based components has been organized at the ICTON 2012 conference at Warwick (UK), attracting more than 50 attendees. Another NAVOLCHI workshop has been scheduled for ICTON 2013 (June 2013, Cartagena, Spain).
- communication has been established with plasmonics-related EU-funded project PLATON (<http://www.ict-platon.eu>),
- the project website is up and running with useful information on the project,
- a brochure on NAVOLCHI activities and goals has been issued.

Journals

1. Melikyan, A.; Koehnle, K.; Lauermaun, M.; Palmer, R.; Koeber, S.; Muehlbrandt, S.; Schindler, P. C.; Elder, D. L.; Wolf, S.; Heni, W.; Haffner, C.; Fedoryshyn, Y.; Hillerkuss, D.; Sommer, M.; Dalton, L. R.; Thourhout, D. V.; Freude, W.; Kohl, M.; Leuthold, J.; Koos, C. Plasmonic-organic hybrid (POH) modulators for OOK and BPSK signaling at 40 Gbit/s *Opt. Express* 23, 9938--9946 (2015)
2. Melikyan, A.; Alloatti, L.; Muslija, A.; Hillerkuss, D.; Schindler, P. C.; Li, J.; Palmer, R.; Korn, D.; Muehlbrandt, S.; Thourhout, D. V.; Chen, B.; Dinu, R.; Sommer, M.; Koos, C.;

- Kohl, M.; Freude, W.; Leuthold, J. High-speed plasmonic phase modulators *Nature Photonics* 8, 229--233 (2014)
3. Melikyan, A.; Kohl, M.; Sommer, M.; Koos, C.; Freude, W.; Leuthold, J. Photonic-to-plasmonic mode converter *Opt. Lett.* 39, 3488--3491 (2014)
 4. Leuthold, J.; Hoessbacher, C.; Muehlbrandt, S.; Melikyan, A.; Kohl, M.; Koos, C.; Freude, W.; Dolores-Calzadilla, V.; Smit, M.; Suarez, I.; Martinez-Pastor, J. P.; Fitrakis, E. P.; Tomkos, I. Plasmonic Communications: Light on a Wire *Opt. Photon. News* 24, 28--35 (2013)
 5. H. Gordillo, I. Suárez, R. Abargues, P. Rodríguez-Cantó and J.P. Martínez-Pastor, Color tuning and white light by dispersing CdSe, CdTe and CdS in PMMA nanocomposite waveguides, *IEEE Photon. J.* 5, 2201412 (12 pgs) (2013).
 6. H. Gordillo, I. Suárez, R. Abargues, P. Rodríguez-Cantó, G. Almuneau and J. P. Martínez-Pastor, Quantum-dot double layer polymer waveguides by evanescent light coupling, *IEEE/OSA J. of Lightwave Technol.* 31, 2515-2525 (2013).
 7. Suárez, H. Gordillo, R. Abargues, P. Rodríguez-Cantó, S. Albert and J.P. Martínez-Pastor, Dielectric and plasmonic waveguides based on quantum dots embedded in polymers, *Opt. Pura Apl.* 46, 303-308 (2013).
 8. Suárez, A. Larrue, P.J. Rodríguez-Cantó, G. Almuneau, R. Abargues, V. S. Chirvony and J.P. Martínez-Pastor, Efficient excitation of photoluminescence in a two-dimensional waveguide consisting of a QD-polymer heterostructure, *Optics Letters* 39, 4692-4695 (2014).
 9. P. Rodríguez-Cantó, R. Abargues, H. Gordillo, I. Suarez, V. Chirvony, S. Albert, J. Martínez-Pastor, UV-patternable nanocomposite containing CdSe and PbS as minituarized luminiscent chemo-sensors, *RSC Advances* 5, 19874-19883 (2015), DOI: 10.1039/C4RA02812K.
 10. J. Hervás, I. Suárez, J. Pérez, P. J. Rodríguez Cantó, R. Abargues, J. P. Martínez-Pastor, S. Sales and J. Capmany, MWP phase shifters integrated in PbS-SU8 waveguides, *Optics Express* 23, 14351-14359 (2015).
 11. W. Xie, Y. Zhu, Tangi Aubert, S. Verstuyft, Zeger Hens, D. Van Thourhout, Low-Loss Silicon Nitride Waveguide Hybridly Integrated With Colloidal Quantum Dots, *Optics Express*, 23(9), United States, p.12152-12160 (2015)
 12. P. Geiregat, A.J. Houtepen, F.C. Grozema, D. Van Thourhout, Z. Hens, Picosecond All-Optical Wavelength Conversion using Hot Carrier Intraband Absorption in Colloidal PbS Nanocrystals , (under review).
 13. A. Omari, W. Xie, P. Geiregat, D. Van Thourhout, Z. Hens, Modeling the optical properties of low-cost colloidal quantum dot functionalized strip SOI waveguides, *Journal of Selected Topics in Quantum Electronics*, 99, (2013)
 14. P. Geiregat, Y. Justo, S. Flamee, S. Abe, Z. Hens, Giant and Broadband Absorption Enhancement in Colloidal Quantum Dot Monolayers through Dipolar Coupling, *ACS Nano*, 7(2), p.987-993 (2012)

15. A. Omari, P. Geiregat, D. Van Thourhout, Z. Hens, Light absorption in hybrid silicon-on-insulator/quantum dot waveguides, *Optics Express*, 21(20), p.23272-23285 (2013)
16. De Geyter, B.; Houtepen, A. J.; Carrillo, S.; Geiregat, P.; Gao, Y.; ten Cate, S.; Schins, J. M.; Van Thourhout, D.; Delerue, C.; Siebbeles, L. D. A.; Hens, Z., Broadband and Picosecond Intraband Absorption in Lead-Based Colloidal Quantum Dots. *Acs Nano* 2012, 6, 6067-6074.
17. B. De Geyter, K. Komorowska, E. Brainis, P. Emplit, P. Geiregat, A. Hassinen, Z. Hens, D. Van Thourhout, From fabrication to mode mapping in silicon nitride microdisk with embedded colloidal quantum dots, *Applied Physics Letters*, 101(16), p.161101~4 (2012)
18. Yolanda Justo, Bart Goris, John Sundar Kamal, Pieter Geiregat, Sara Bals, and Zeger Hens, "Multiple Dot-in-Rod PbS/CdS Heterostructures with High Photoluminescence Quantum Yield in the Near-Infrared", *Journal of the American Chemical Society* 2012, 134, 5484-5487
19. J. Leuthold, C. Hoessbacher, S. Muehlbrandt, A. Melikyan, M. Kohl, C. Koos, W. Freude, V. Dolores-Calzadilla, M. Smit, I. Suarez, J. Martínez-Pastor, E.P. Fitrakis, and I. Tomkos, "Plasmonic Communications: Light on a Wire", *Optics & Photonics News* 24, 24-35 (2013). Cover article.
20. Henry Gordillo, Isaac Suarez, Rafael Abargues, Pedro Rodriguez-Cantó, Sandra Albert Juan Martinez-Pastor, "Polymer/QDs nanocomposites for wave-guiding applications", *Journal of nanomaterials*, 2012, 960201 (2012).
21. A. Bueno, I. Suárez, R. Abargues, S. Sales and J. Martínez-Pastor, "Temperature sensor based on colloidal Quantum Dots-PMMA nanocomposite waveguides", *IEEE sensors*, 12, 3069-3074 (2012).
22. R. Abargues, P. J. Rodríguez-Cantó, R. García-Calzada and J. Martínez-Pastor, "Patterning of conducting polymers using UV lithography: the in-situ polymerization approach," *Journal of Physical Chemistry C*, 116 17547-17553 (2012).
23. I. Suárez, H. Gordillo, R. Abargues, P. Rodríguez-Cantó and J.P. Martínez-Pastor, "Color tuning and white light by dispersing CdSe, CdTe and CdS in PMMA nanocomposite waveguides", *IEEE Photon. J.* 5, 2201412 (12 pgs) (2013).
24. H. Gordillo, I. Suárez, R. Abargues, P.J. Rodríguez-Cantó, and J.P. Martínez-Pastor, "Color tuning and white light by dispersing CdSe, CdTe and CdS in PMMA nanocomposite waveguides", *IEEE Photonics J.*
25. P. J. Rodríguez-Cantó; M. L. Martínez-Marco; R. Abargues ; V. Latorre-Garrido and J. P. Martínez-Pastor, *Novel patternable and conducting metal-polymer nanocomposites: a step towards advanced multifunctional materials*, *Proc. SPIE* 8682, Advances in Resist Materials and Processing Technology XXX, (9 pgs) (2013); <http://dx.doi.org/10.1117/12.2011716>
26. R. Abargues, M. L. Martínez-Marco, P. J. Rodriguez-Cantó, J. Marques-Hueso, and J. P. Martínez-Pastor, *Metal-polymer nanocomposite resist: a step towards in-situ nanopatterns metallization*, *Proc. SPIE* 8682, Advances in Resist Materials and Processing Technology XXX, 86820X (8 pgs) (2013); <http://dx.doi.org/10.1117/12.2011555>.

27. Pieter Geiregat, Yolanda Justo, Sofie Abe, Stijn Flamee, Zeger Hens, "Giant and Broadband absorption enhancement in colloidal quantum dot monolayers through dipolar coupling", *ACS Nano*, 7(2),987-993.
28. Yolanda Justo, Bart Goris, John Sundar Kamal, Pieter Geiregat, Sara Bals, and Zeger Hens, "Multiple Dot-in-Rod PbS/CdS Heterostructures with High Photoluminescence Quantum Yield in the Near-Infrared", *Journal of the American Chemical Society* 2012, 134, 5484–5487.
29. B. De Geyter, Houtepen, Arjan J., Carrillo, Sergio, P. Geiregat, Gao, Yunan, Ten Cate, Sybren, Schins, Juleon M., D. Van Thourhout, Delerue, Christophe, Siebbeles, Laurens D.A., Hens, Zeger, "Broadband and Picosecond Intraband Relaxation in Lead-Based Colloidal Quantum Dots", accepted for *ACS Nano* 2012 July, 24;6(7):6067-74,
30. B. De Geyter, K. Komorowska, E. Brainis, P. Emplit, P. Geiregat, A. Hassinen, Z. Hens, D. Van Thourhout, "From fabrication to mode mapping in silicon nitride microdisk with embedded colloidal quantum dots", *Applied Physics Letters*, 101(16), p.161101~4 (2012).
31. Abdoulghafar Omari, Pieter Geiregat, Dries Van Thourhout and Zeger Hens, "Light Absorption in Hybrid Silicon-On-Insulator/Quantum Dot Waveguides", *Phys Rev*.
32. Yolanda Justo, Bart Goris, John Sundar Kamal, Pieter Geiregat, Sara Bals, and Zeger Hens, "Multiple Dot-in-Rod PbS/CdS Heterostructures with High Photoluminescence Quantum Yield in the Near-Infrared", *Journal of the American Chemical Society* 2012, 134, 5484–5487.
33. C. Hoessbacher, Y. Fedoryshyn, A. Emboras, A. Melikyan, M. Kohl, D. Hillerkuss, C. Hafner, and J. Leuthold, "The plasmonic memristor: a latching optical switch," *Optica* 1, 198-202 (2014).
34. W. Heni, C. Haffner, B. Baeuerle, Y. Fedoryshyn, A. Josten, D. Hillerkuss, J. Niegemann, A. Melikyan, M. Kohl, D. Elder, L. Dalton, C. Hafner, and J. Leuthold, "108 Gbit/s Plasmonic Mach-Zehnder Modulator with > 70 GHz Electrical Bandwidth," *J. Lightwave Technol.*, submitted for publication (2015).
35. HaffnerC, HeniW, FedoryshynY, NiegemannJ, MelikyanA, D. L. Elder, BaeuerleB, SalaminY, JostenA, KochU, HoessbacherC, DucryF, JuchliL, EmborasA, HillerkussD, KohlM, L. R. Dalton, HafnerC, and LeutholdJ, "All-plasmonic Mach-Zehnder modulator enabling optical high-speed communication at the microscale," *Nat Photon* 9, 525-528 (2015).
36. D. Hillerkuss, and J. Leuthold, "Software-Defined Transceivers in Dynamic Access Networks," *J. Lightwave Technol.*, submitted for publication (2015).
37. I. Suárez, E. J. Juárez-Pérez, I. Mora-Seró, J. Bisquert and J. P. Martínez-Pastor, *Polymer/perovskite amplifying waveguides for active hybrid silicon photonics*, *Advanced Materials*, DOI: 10.1002/adma.201503245, published online 31 august (2015).
38. M. Signoretto, I. Suárez, V.S. Chirvony, R. Abargues, P.J. Rodríguez-Cantó and J. Martínez-Pastor, *Optical waveguide couplers based on metal nanoparticle-polymer nanocomposites*, *Nanotechnology*, in press.

Conferences

1. Muehlbrandt, S.; Melikyan, A.; Koehnle, K.; Harter, T.; Muslija, A.; Vincze, P.; Wolf, S.; Jakobs, P. -J.; Fedoryshyn, Y.; Freude, W.; Leuthold, J.; Koos, C.; Kohl, M.
Plasmonic Internal Photoemission Detectors with Responsivities above 0.12 A/W
Conf. on Lasers and Electro-Optics (CLEO'15), San Jose (CA), USA, May 10–15, paper FTh3E. *Optical Society of America (OSA)* (2015)
2. Melikyan, A.; Koehnle, K.; Lauermann, M.; Palmer, R.; Koeber, S.; Muehlbrandt, S.; Schindler, P. C.; Elder, D. L.; Wolf, S.; Heni, W.; Haffner, C.; Fedoryshyn, Y.; Hillerkuss, D.; Sommer, M.; Dalton, L. R.; Van Thourhout, D.; Freude, W.; Kohl, M.; Leuthold, J.; Koos, C.
Plasmonic-organic hybrid (POH) modulators for OOK and BPSK signaling at 40 Gbit/s
Conf. on Lasers and Electro-Optics (CLEO'15), San Jose (CA), USA, May 10–15, paper SM11.1. *Optical Society of America (OSA)* (2015)
3. Leuthold, J.; Melikyan, A.; Alloatti, L.; Korn, D.; Palmer, R.; Hillerkuss, D.; Lauermann, M.; Schindler, P. C.; Chen, B.; Dinu, R.; Elder, D. L.; Dalton, L. R.; Koos, C.; Kohl, M.; Freude, W.; Hafner, C.
From silicon-organic hybrid to plasmonic modulation
Optical Communication (ECOC), 2014 European Conference on, 1-3, Cannes, France, September 21–25 (2014), (invited)
4. Muehlbrandt, S.; Muslija, A.; Koehnle, K.; Melikyan, A.; Leuthold, J.; Kohl, M.
Fabrication of Ultra-Compact Plasmonic Waveguide Photo Diodes
Micro and Nano Engineering (MNE'2014), Lausanne, Switzerland, paper 8274 (2014)
5. Melikyan, A.; Alloatti, L.; Muslija, A.; Hillerkuss, D.; Schindler, P. C.; Li, J.; Palmer, R.; Korn, D.; Lindenmann, N.; Muehlbrandt, S.; Walheim, S.; Vincze, P.; Leufke, P. M.; Ulrich, S.; Ye, J.; Thourhout, D. V.; Chen, B.; Dinu, R.; Sommer, M.; Hahn, H.; Schimmel, T.; Koos, C.; Kohl, M.; Freude, W.; Leuthold, J.
High-speed Plasmonic Modulators
Integrated Photonics Research, Silicon and Nanophotonics (IPR'14), San Diego, California United States, July 13-17, paper IT2A.6 *Optical Society of America (OSA)* (2014)
6. Melikyan, A.; Alloatti, L.; Muslija, A.; Hillerkuss, D.; Schindler, P. C.; Li, J.; Palmer, R.; Korn, D.; Muehlbrandt, S.; Thourhout, D. V.; Chen, B.; Dinu, R.; Sommer, M.; Koos, C.; Kohl, M.; Freude, W.; Leuthold, J.
Surface Plasmon Polariton High-Speed Modulator
Conf. on Lasers and Electro-Optics (CLEO'13), San Jose (CA), USA, June 9–14, paper CTh5D.2 *Optical Society of America* (2013) (postdeadline)
7. R. Abargues, M. L. Martínez-Marco, P. J. Rodríguez-Cantó, J. Marques-Hueso, and J. P. Martínez-Pastor, Metal-polymer nanocomposite resist: a step towards in-situ nanopatterns metallization, Proc. SPIE 8682, Advances in Resist Materials and Processing Technology XXX, 86820X (8 pgs) (2013); SPIE Advanced Lithography Conference, San José, USA, 25-28 February 2013.
8. P. J. Rodríguez-Cantó; M. L. Martínez-Marco; R. Abargues ; V. Latorre-Garrido and J. P. Martínez-Pastor, Novel patternable and conducting metal-polymer nanocomposites: a step towards advanced multifunctional materials, Proc. SPIE 8682, Advances in Resist Materials

- and Processing Technology XXX, (9 pgs) (2013); SPIE Advanced Lithography Conference, San José, USA, 25-28 February 2013.
9. Suárez, E.P. Fitrakis, P. Geiregat, H. Gordillo, Y. Justo, P.J. Rodríguez-Cantó, Z. Hens, R. Abargues, D. Van Thourhout, I. Tomkos and J.P. Martínez-Pastor, International Conference on Surface Plasmon Photonics, SPP6, 2013, Ottawa, Canada, oral.
 10. Suárez, E. P. Fitrakis, H. Gordillo, P. Rodríguez-Cantó, R. Abargues, I. Tomkos and J. Martínez-Pastor, Light Coupling from Active Polymer Layers to Hybrid Dielectric-Plasmonic Waveguides, 15th International Conference on Transparent Optical Networks (ICTON 2013), 23-27 June 2013, Cartagena, Spain, Oral (invited). PUBLISHED IN Proceedings of the 15th International Conference on Transparent Optical Networks (ICTON 2013), IEEE Conf. Pubs., ISBN 978-1-4799-0682-6, pp. We.D6.3 - 1/4 (2013).
 11. Suárez, E. P. Fitrakis, R. Abargues, P. Rodriguez-Cantó, I. Tomkos and J. Martinez-Pastor, Photon plasmon coupling in nanocomposite plasmonic waveguides, 16th International Conference on Transparent Optical Networks (ICTON 2014) July 2014, Graz, Austria, oral (invited). PUBLISHED IN Proceedings of the 16th International Conference on Transparent Optical Networks (ICTON 2014), IEEE Conf. Pubs., ISBN 978-1-4799-5600-5, DOI: 10.1109/ICTON.2014.6876431 pp. 1-4 (2014).
 12. A. Maulu, P. J. Rodríguez-Cantó and J. P. Martínez-Pastor, Colloidal QD-solid photodetectors produced by doctor-blading based on two configurations: nano-gap (MIM) vs Schottky/heterostructure, 8th International Conference on Quantum Dots, 11-16 May 2014, Pisa (Italy), Oral.
 13. A. Maulu, P.J. Rodríguez-Cantó, I. Suarez, R. Abargues, J.P. Martinez-Pastor, Fabrication of solution-processed QD-solids by doctor blading technique and their application for photodetection, 4th International Colloids Conference, 15-18 June 2014, Madrid (Spain), Poster.
 14. A. Maulu, P. J. Rodríguez-Cantó, J. P. Martínez Pastor, Efficient photodetectors at telecom wavelengths based on thin films of lead sulfide quantum dots, Nanomeeting 2015, 26-29 May 2015, Minsk (Belarus), oral contribution. PUBLISHED IN “Physics, Chemistry and Application of Nanostructures (Proceedings of International Conference Nanomeeting – 2015)”, World Scientific Pub. Co., ISBN 978-981-4696-51-7, pp. 556-559, 2015.
 15. A. Maulu, P. Javier Rodríguez Cantó, J. Navarro Arenas, R. Abargues and J. Martínez Pastor, Photodetectors at 1.3-1.7 μm Based on Thin Films of PbS Quantum Dots. Poster. IX Reunión Española de Optoelectrónica (IX Spanish Meeting of Optoelectronics), OPTOEL2015, Salamanca (Spain), 13-15 July 2015.
 16. Suárez, J. Marques Hueso, R. Abargues, P. Rodríguez-Cantó and J. Martínez-Pastor, QD-PMMA nanocomposite plasmonic waveguides. Poster. IX Reunión Española de Optoelectrónica (IX Spanish Meeting of Optoelectronics), OPTOEL2015, Salamanca (Spain), 13-15 July 2015.
 17. M. Signoretto, I. Suárez, R. Abargues, P. Rodríguez-Cantó, M. L. Martínez, V. Chirvony and J. Martínez-Pastor, Integration of metal nanoparticles in organic waveguides. Poster. IX Reunión Española de Optoelectrónica (IX Spanish Meeting of Optoelectronics), OPTOEL2015, Salamanca (Spain), 13-15 July 2015.

18. Suárez, E. P. Fitrakis, P. Rodriguez-Cantó, R. Abargues, H. Gordillo, I. Tomkos and J. Martinez-Pastor, Colloidal QDs/PMMA nanocomposites as a material to provide gain in surface plasmon polaritons, CEN2012, October 2012, Carmona, Spain, oral. (NO PUBLICATION)
19. Suárez, E. P. Fitrakis, P. Rodriguez-Cantó, R. Abargues, I. Tomkos and J. Martinez-Pastor, Surface plasmon-polariton amplifiers, 14th International Conference on Transparent Optical Networks (ICTON 2013), June 2013, Coventry, UK, Oral (invited). PUBLISHED IN Proceedings of the 14th International Conference on Transparent Optical Networks (ICTON 2012), IEEE Conf. Pubs., ISBN 978-1-4673-2228-7, pp. Th.A5.2-1/5 (2012).
20. W. Xie, Y. Zhu, Tangi Aubert, Zeger Hens, Edouard Brainis, D. Van Thourhout, On-chip Hybrid Integration of Silicon Nitride Microdisk With Colloidal Quantum Dots, submitted for publication in 12th International Conference on Group IV Photonics, (accepted).
21. P. Geiregat, A.J. Houtepen, F.C. Grozema, D. Van Thourhout, Z. Hens, Picosecond All-Optical Wavelength Conversion using Hot Carrier Intraband Absorption in Colloidal PbS Nanocrystals , MRS Spring Meeting - WW4.04, United States, (2015)
22. W. Xie, D. Van Thourhout, Fabrication of high-Q silicon nitride microdisk resonator coupled with on-chip waveguide, Proceedings of the 19th Annual Symposium of the IEEE Photonics Society Benelux Chapter, Netherlands, p.145-148 (2014)
23. P. Geiregat, A. Houtepen, L.K. Sagar, C. Delerue, G. Allan, D. Van Thourhout, Z. Hens, Thresholdless Optical Gain using Colloidal HgTe Nanocrystals, CLEO, United States, p.paper FtH4C4 (2014)
24. W. Xie, D. Van Thourhout, High-Q Free-standing Silicon Nitride Microdisk Vertically Coupled with On-chip Waveguide, CLEO 2014, United States, (2014)
25. Y. Zhu, W. Xie, S. Verstuyft, Tangi Aubert, Zeger Hens, D. Van Thourhout, Colloidal quantum dot silicon nitride platform, Proceedings of the 2013 Annual Symposium of the IEEE Photonics Society Belenux Chapter, Netherlands, p.175-178 (2013).
26. P. Geiregat, B. De Geyter, S. Carillo, A. Houtepen, Y. Gao, S. Ten Cate, J. Schins, D. Van Thourhout, C. Delerue, L. Siebbeles, Z. Hens, "Broadband and Picosecond Intraband Relaxation in Lead Chalcogenide Nanocrystals", International Quantum Dot Conference 2012, (2012).
27. P. Geiregat, Y. Justo, H. Zeger, "Giant Absorption Enhancement in Colloidal Quantum Dot Supercrystals", International Quantum Dot Conference 2012, United States, (2012).
28. Dries Van Thourhout, "Collodial quantum dots for silicon photonics", invited presentation at NaNaX 5, Fuengirola (Spain)
29. Yolanda Justo, Bart Goris, John Sundar Kamal, Pieter Geiregat, Sara Bals and Zeger Hens, "PbS/CdS core/shell nanorods, highly luminescent anisotropic near infrared nanomaterials by cationic exchange", NaNaX 5, Fuengirola (Spain), 2012.
30. Pieter Geiregat, Yolanda Justo, Zeger Hens, "Absorption enhancement in colloidal quantum dot monolayers through coherent dipolar coupling", NaNaX 5, Fuengirola (Spain), 2012.

31. Bram De Geyter, Pieter Geiregat, Yunan Gao, Sybren ten Cate, Arjan J. Houtepen, Juleon M. Schins, Dries Van Thourhout, Laurens D.A. Siebbeles, Zeger Hens, "Broadband and Ultrafast Intraband Absorption in Lead based Colloidal Quantum Dots", *NaNaX 5*, Fuengirola (Spain), 2012.
32. B. De Geyter, P. Geiregat, A. J. Houtepen, D. Van Thourhout, L. Siebbeles, Z. Hens, "Ultrafast Photoinduced Intraband Absorption in PbS, PbSe and PbSe/CdSe Core/Shell Nanocrystals for near-Infrared to Mid-Infrared All-Optical Signal Processing", *MRS Fall Meeting 2011*, United States, (2011).
33. Pieter Geiregat, Yolanda Justo and Zeger Hens, "Giant Absorption Enhancement in Close Packed Monolayers of Colloidal Quantum Dots through Dipolar Coupling Effects", *MRS Fall Meeting*, Boston (US), 2011.
34. A. Melikyan, C. Gaertner, K. Köhnle, A. Muslija, M. Sommer, M. Kohl, C. Koos, W. Freude, and J. Leuthold, "Integrated Wire Grid Polarizer and Plasmonic Polarization Beam Splitter", in *Optical Fiber Communication Conference*, OSA Technical Digest (Optical Society of America, 2012), paper OW1E.3
35. Melikyan A, Sommer M, Muslija A, et al., "Chip-to-Chip Plasmonic Interconnects and the Activities of EU Project NAVOLCHI", *ICTON 2012*, Warwick (GB); 2012:14-16.
36. J. Leuthold, "Ultracompact CMOS-compatible Modulators," in *Frontiers in Optics 2012/Laser Science XXVIII*, OSA Technical Digest (online) (Optical Society of America, 2012), paper FTu4A.1.
37. I. Suarez et al., "Surface plasmon-polariton amplifiers", *ICTON 2012* (UK).
38. V. Dolores-Calzadilla, A. Fiore, M. K. Smit, "Towards plasmonic lasers for optical interconnects", *IEEE Proceedings of the 14th International Conference on Optical Transparent Networks*, 2012.
39. V. Dolores-Calzadilla, D. Heiss, A. Fiore, M. K. Smit, "Metallo-dielectric nanolaser coupled to an InP-membrane waveguide", *Proceeding of the Proceedings of the 17th Annual Symposium of the IEEE Photonics Society Benelux Chapter*, 2012.
40. D. Heiss, V. Dolores-Calzadilla, A. Fiore, M. Smit, "Design of a waveguide-coupled nanolaser for photonic integration", *Integrated Photonics Research, Silicon and Nano-Photonics*, 2013.
41. V. Dolores-Calzadilla, D. Heiss, A. Fiore, M. K. Smit, "Waveguide-coupled nanolasers in III-V membranes on silicon", *IEEE Proceedings of the 15th International Conference on Optical Transparent Networks*, 2013.
42. V. Dolores-Calzadilla, D. Heiss, A. Fiore, M. K. Smit, "Nanometallic lasers for optical interconnects", *The 18th OptoElectronics and Communications Conference/Photonics in Switching*, 2013.
43. Poster contribution at the ITC (Lisboa, Portugal) 01/2012. P. Rodríguez-Cantó, Rafael Abargues, Raúl García-Calzada, and Juan P. Martínez- Pastor, "In-situ synthesis of conducting polymers into patternable polymer matrices".
44. Poster contribution at the European Conference of Integrated Optics ECIO (Barcelona, Spain) 04/2012. I. Suárez, H. Gordillo, P. Rodríguez-Cantó, R. Abargues, S. Albert and J.

- Martínez-Pastor, “Multicolor wave-guiding in polymer/quantum dot nanocomposite waveguides”.
45. Poster contribution at Conference on Laser Ablation and Nanoparticle Generation in
 46. Liquids Taormina ANGEL2012 (Sicilia, Italy) 05/2012. R. García-Calzada, P. Rodríguez-Cantó, V. Chirvony, R. Abargues, J. Martínez-Pastor, "Gold nanoparticles obtained by pulsed laser ablation in liquids: formation of monolayers on chemically functionalized patterns/substrates".
 47. Talk at the International Conference of Transparent Optical Networks ICTON (Warwick, England) 06/2012. I. Suárez, E. P. Fitrakis, P. Rodriguez-Cantó, R. Abargues, I. Tomkos and J. Martinez-Pastor, “Surface plasmon-polariton amplifiers”.
 48. Poster contribution at the Spanish Conference of Nanophotonics CEN2012 (Carmona, Spain) 09/2012.
 49. H. Gordillo, I. Suárez, P. Rodríguez-Cantó, R. Abargues, S. Albert and J. Martínez- Pastor, “Waveguides based on Colloidal QDs embedded in PMMA and SU8”.
 50. Talk contribution at the Spanish Conference on Nanophotonics CEN2012 (Carmona, Spain) 09/2012. I. Suárez, E. P. Fitrakis, P. Rodriguez-Cantó, R. Abargues, H. Gordillo, I. Tomkos and J.
 51. Martinez-Pastor, “Colloidal QDs/PMMA nanocomposites as a material to provide gain in surface plasmon polaritons”. · Poster contribution at the Spanish Conference on Nanophotonics CEN2012 (Carmona, Spain) 09/2012.
 52. M. L. Martinez-Marco, P. J. Rodriguez-Canto, R. Abargues, V. Latorre-Garrido and J. P. Martinez-Pastor, "In - situ synthesis of conducting polymers and gold nanoparticles into PMMA".
 53. Talk at the SPIE advanced lithography (California, EEUU) 02/2013. R. Abargues, M. Martínez-Marco, P. J. Rodríguez-Cantó, J. Marqués-Hueso, J. Martínez-Pastor, “Metal-polymer nanocomposite resists: a step toward in situ nanopatterns metallization”.
 54. Talk at the SPIE advanced lithography (California, EEUU) 02/2013. J. Rodríguez-Cantó, M. Martínez-Marco, R. Abargues, V. Latorre-Garrido, J. P. Martínez-Pastor, “Novel patternable and conducting metal-polymer nanocomposite: a step toward advanced multifunctional materials”.
 55. P. Geiregat, B. De Geyter, S. Carillo, A. Houtepen, Y. Gao, S. Ten Cate, J. Schins, D. Van Thourhout, C. Delerue, L. Siebbeles, Z. Hens, “Broadband and Picosecond Intraband Relaxation in Lead Chalcogenide Nanocrystals”, International Quantum Dot Conference 2012, (2012).
 56. B. De Geyter, P. Geiregat, A. J. Houtepen, D. Van Thourhout, L. Siebbeles, Z. Hens, “Ultrafast Photoinduced Intraband Absorption in PbS, PbSe and PbSe/CdSe Core/Shell Nanocrystals for near-Infrared to Mid-Infrared All-Optical Signal Processing”, MRS Fall Meeting 2011, United States, (2011).
 57. Pieter Geiregat, Yolanda Justo and Zeger Hens; “Giant Absorption Enhancement in Close Packed Monolayers of Colloidal Quantum Dots through Dipolar Coupling Effects”, MRS Fall Meeting, Boston (US), 2011.

58. Q. Lu, P. Geiregat, D. Van Thourhout, Zeger Hens, "Design of Nanocrystal Light Source for Silicon Photonics", IEEE Photonics Annual Meeting 2011, WP4, United States, p.527-528 (2011).
59. P. Geiregat, Y. Justo, Z. Hens, "Giant Absorption Enhancement in Colloidal Quantum Dot Supercrystals", International Quantum Dot Conference 2012, United States, (2012).
60. Pieter Geiregat, Floris Tallieu, Philippe Smet, Kilian Devloo – Casier, Sreeparvathi Warriar, Dries Van Thourhout and Zeger Hens, "Integrated light source for silicon photonics using colloidal nanocrystal light emitters under AC field excitation", ELOPTO 2012.
61. Bram De Geyter, Pieter Geiregat Yunan Gao, Sybren ten Cate, Arjan J. Houtepen, Juleon M. Schins, Dries Van Thourhout³ Laurens D.A. Siebbele , Zeger Hens, "Broadband and Ultrafast Intraband Absorption in Lead based Colloidal Quantum Dots", NaNaX 5, Fuengirola (Spain), 2012.
62. Bram De Geyter, Pieter Geiregat, Arjan Houtepen, Dries Van Thourhout and Zeger Hens, "Ultrafast Photoinduced Intraband Absorption in PbS, PbSe and PbSe/CdSe Core/shell Nanocrystals for Near-infrared to Mid-infrared All-optical Signal Processing", ICTON, Warwick (UK), 2012.
63. Dries Van Thourhout, "Silicon Photonics: short course (3 hours)", CLEO Europe 2013, May 2013, Munich.
64. B. De Geyter, P. Geiregat, K. Komorowska, A. Hassinen, E. Brainis, D. Van Thourhout, Z. Hens, "Embedding Colloidal Nanocrystals in Silicon Nitride Micro-Disk Resonators: From mode-mapping to single dot spectroscopy", E-MRS Spring Meeting (2013).
65. P. Geiregat, Y. Justo, A. Omari, S. Abe, S. Flamee, Z. Hens, D. Van Thourhout, "Giant And Broadband Absorption Enhancement in colloidal nanocrystal monolayers through dipolar coupling", E-MRS Spring Meeting (2013).
66. C. Kachris, Optical Interconnects in Data Center Networks, HiPEAC Computing System Week, Ghent, 2012, presentation
67. P. Geiregat, Y. Justo, A. Omari, S. Abe, S. Flamee, Z. Hens, D. Van Thourhout, "Absorption Enhancement in 2D Nanocrystal Superlattices through Near-Field Dipolar Coupling: A Novel Optical Phenomenon at the Nanoscale", CLEO (USA), (2013)
68. Pieter Geiregat, Yolanda Justo and Zeger Hens, "Giant Absorption Enhancement in Close Packed Monolayers of Colloidal Quantum Dots through Dipolar Coupling Effects", MRS Fall Meeting, Boston (US), 2011.
69. C. Hoessbacher, Y. Fedoryshyn, A. Emboras, D. Hillerkuss, A. Melikyan, M. Kohl, M. Sommer, C. Hafner, and J. Leuthold, "Latching Plasmonic Switch with High Extinction Ratio," in CLEO: 2014(Optical Society of America, San Jose, California, 2014), p. FTu3K.6.
70. C. Haffner, W. Heni, Y. Fedoryshyn, D. L. Elder, A. Melikyan, B. Baeuerle, J. Niegemann, A. Emboras, A. Josten, F. Ducry, M. Kohl, L. R. Dalton, D. Hillerkuss, C. Hafner, and J. Leuthold, "High-speed plasmonic Mach-Zehnder modulator in a waveguide," in Optical Communication (ECOC), 2014 European Conference on(2014), pp. 1-3.
71. W. Heni, A. Melikyan, C. Haffner, Y. Fedoryshyn, B. Baeuerle, A. Josten, J. Niegemann, D. Hillerkuss, M. Kohl, D. Elder, L. Dalton, C. Hafner, and J. Leuthold, "Plasmonic Mach-Zehnder Modulator with >70 GHz Electrical Bandwidth Demonstrating 90 Gbit/s 4-ASK,"

- in Optical Fiber Communication Conference(Optical Society of America, Los Angeles, California, 2015), p. Tu2A.2.
72. D. Hillerkuss, and J. Leuthold, "Software-Defined Transceivers for Dynamic Access Networks," in Optical Fiber Communication Conference(Optical Society of America, Los Angeles, California, 2015), p. Tu2E.4.
 73. C. Hoessbacher, W. Heni, A. Melikyan, Y. Fedoryshyn, C. Haffner, B. Baeuerle, A. Josten, D. Hillerkuss, Y. Salamin, M. Kohl, D. Elder, L. Dalton, C. Hafner, and J. Leuthold, "Dense Plasmonic Mach-Zehnder Modulator Array for High-Speed Optical Interconnects," in Advanced Photonics 2015(Optical Society of America, Boston, Massachusetts, 2015), p. IM2B.1.

Ph.D. Thesis

1. Henry Gordillo Millán, Defended 15th July 2013, "Guías ópticas activas de polímero con puntos cuánticos coloidales" (Active optical waveguides based on polymers with colloidal quantum dots). Co-supervisors: Drs. Juan Martínez Pastor and Isaac Suárez.
2. Alberto Maulu, He is developing his PhD research work on "Photodetector devices based on PbS quantum dots" since 15th June 2013.
3. Pieter Geiregat, "Colloidal Quantum Dots for Integrated Photonics: From Optical Gain to Ultrafast Modulation, 2/2015" (PhD Thesis)
4. Bram De Geyter, "Colloidal Quantum Dots as Light Emitters for Silicon Photonics", 11/2012
5. Argishti Melikyan, "Active and Passive Plasmonic Devices for Optical Communications" KIT, 2014

Master Thesis

1. Víctor Latorre Garrido, December 2012: "Propiedades Eléctricas y Ópticas del PMMA 3T- Au" (Electrical and optical properties of PMMA 3T-Au).
2. Juan Navarro Arenas, September 2015: "Fabrication and Characterization of Photodetectors based on PbS and AgSe₂ quantum dots".

Task 7.2 Exploitation

The main objective of this task was to explore the research outcomes of the NAVOLCHI project and promote market penetration of the end products. Due to the early stage of plasmonic technology, it is difficult to prepare for commercial products within or shortly after the timeframe of the project. At the same time, this early stage also means that project partners have the opportunity to lead the way in the technological advancement in their respective fields. In NAVOLCHI, this is mainly expressed through patent opportunities and innovative research through theses at the Master's and PhD level of participating institutions.

For a detailed list of exploitation activities, see D7.2. The main points are also summarized below.

- (UVEG) Patent: “Method to obtain metallic structures of nano- and micro-metric size from lithographic resists based on nanocomposites,, (P201201282).
 (“Método de obtención de estructuras metálicas de tamaño nano y micrométrico a partir de resinas litográficas basadas en nanocomposites)
- V. M. Dolores-Calzadilla, A. Higuera Rodriguez, D. Heiss, (2014). “Metal grating coupler for membrane-based integrated photonics”, USA Provisional Patent Application filed, application number: 61/979, 2014.

Task 7.3 Promotion

The promotion activities of the NAVOLCHI project have been mainly focused on the dissemination of the results to highly ranked conferences (OFC, ECOC, etc.) and highly ranked journal papers in the domain of optical communications (i.e. 2 nature photonics papers, 1 cover story at Optics and Photonics news, Optics Express, etc.). The dissemination of the results to highly ranked journals have resulted to high number of citations and has helped significantly in the promotion and awareness of the NAVOLCHI project.

ETHZ also participated in the “Scientifica” event (<http://www.scientifica.ch/scientifica-2015>) in which they had a booth at this outreach event in Zurich and they had the chance to present their activities in NAVOLCHI to over 25 000 visitors (general public).



Figure WP7- 1: Visit of Minister Dr. Jet Bussemaker to NanoLab@TU/e cleanroom facilities.

Finally, we also presented our research on nanolasers funded by NAVOLCHI to Dr. Jet Bussemaker, Minister of Education, Culture and Science of The Netherlands, during her visit to the Technical University of Eindhoven.

3.3 Project Management (Work Package 1)

3.3.1 Request for Amendment

As already explained in the intermediate report 2, the consortium requested for an amendment to the General Agreement to master the challenges raised by

- STs reduced engagement in work package 6, and
- Difficulties in the current tasks and with respect to STs reduced engagement.

Mainly, the amendment contained

- Adding ETH Zürich as a new partner to replace ST, and
- Extension of the project by 9 months.

Aside with topics of minor relevance, the amendment was granted by the EC at September 16th 2014. Major effects of this decision are discussed in 3.3.2 and 3.3.5. An updated Annex I to the General Agreement has been submitted to the EC by July 25th 2014.

3.3.2 Administrative Boards and Decisions

One consequence of the amendment is that Prof. Jürg Leuthold (ETH Zürich) becomes a member of the General Assembly instead of Alberto Scandurra (ST) and that he becomes work package leader of WP6.

General Assembly:

Karlsruhe Institute of Technology, Germany	KIT	Manfred Kohl
Interuniversity Microelectronics Centre VZW-IMEC, Belgium	IMEC	Dries Van Thourhout
Eindhoven University of Technology, Netherlands	TU/e	Meint Smit
Research and education laboratory in information technologies, Greece	AIT	Ioannis Tomkos
University of Valencia, Institute of Materials Science, Spain	UVEG	Juan Martinez Pastor

Eidgenössische Technische Hochschule Zürich, Switzerland	ETH	Jürg Leuthold
Ghent University, Belgium	Ugent	Zeger Hens

Table WP1- 1: General Assembly.

Technical Project Manager and Project Management Committee:

In June 2013, Prof. Jürg Leuthold (KIT/ETH Zurich) and Prof. Manfred Kohl (KIT) switched their positions in the Project Management Committee. Prof. Jürg Leuthold became Technical Project Manager, Prof. Manfred Kohl became Coordinator.

Technical Project Manager (Chair)	Jürg Leuthold
Coordinator	Manfred Kohl

+

WP1 Leader	KIT	Manfred Kohl
WP2 Leader	AIT	Ioannis Tomkos
WP3 Leader	TU/e	Meint Smit
WP4 Leader	UVEG	Juan Martinez Pastor
WP5 Leader	IMEC	Dries Van Thourhout
WP6 Leader	ETH	Jürg Leuthold
WP7 Leader	AIT	Ioannis Tomkos

Table WP1-2: Project Management Committee.

3.3.3 Management Deliverables

Deliverables covered by work package 1 with delivery dates are:

D1.1	Project web site with .eu domain (M01) and continuous update	11/2011
D1.2	Project reference online manual	01/2012
D1.3	Project quality assurance manual	04/2012
D1.4	Intermediate Progress Report 1	07/2012
D1.5	Intermediate Progress Report 2	04/2014

All have been prepared in time, for access to the WEB-site and the manuals please follow the links.

3.3.4 Communication: Meetings and Phone Conferences

Up to now, seven meetings and 30 phone conferences have been held:

Meetings:

- 1) Kick-Off meeting in Karlsruhe, Germany, February 3rd 2012.
- 2) Intermediate Meeting in Warwick, Great Britain, July 6th 2012.
- 3) Meeting in Ghent, Belgium, November 26th 2012.
- 4) Project Review Meeting 1 in Brussels, Belgium, November 27th 2012.
- 5) Midterm Meeting in Karlsruhe, Germany, April 26th 2013.
- 6) Project Review Meeting 2 in Brussels, Belgium, July 10th 2013.
- 7) Meeting in Eindhoven, Belgium, January 28th 2014.
- 8) Meeting in Brussels, Belgium, November 3rd 2014.

To provide a short reaction time on possible problems, it was decided that phone conferences will be held every month if applicable, typically on the first Monday of every month.

Phone Conferences:

1) November 16 th , 2011	13) February 4 th , 2013	25) April 7 th , 2014
2) December 12 th , 2011	14) March 4 th , 2013	26) May 5 th , 2014
3) March 12 th , 2012	15) April 8 th , 2013	27) May 26 th , 2014
4) April 2 nd , 2012	16) May 13 th , 2013	28) July 25 th , 2014
5) May 7 th , 2012	17) June, 13 th , 2013	29) September 1 st , 2014
6) June 4 th , 2012	18) July 1 st , 2013	30) October 6 th , 2014
7) September 3 rd , 2012	19) September 23 th , 2013	31) March 2 nd , 2015
8) October 8 th , 2012	20) October 14 th , 2013	32) April 13 th , 2015
9) November 5 th , 2012	21) November 4 th , 2013	33) May 4 th , 2015
10) November 16 th , 2012	22) December 4 th , 2013	34) June 8 th , 2015
11) December 17 th , 2012	23) January 13 th , 2014	35)
12) January 14 th , 2013	24) March 3 rd , 2014	36)

Detailed documentation of partner presentations, results obtained and decisions made during the meetings and phone conferences can be found in the minutes-files available on our [WEB-site](#) (please follow the link).

3.3.5 New Delivery Dates for Deliverables and Milestones

Deliverables and milestones with new delivery dates are listed below. A complete list can be found in the next subchapter.

D3.3	m24 → m33
D4.5	m33 → m42
D5.6	m30 → m39
D5.7	m33 → m42
D6.3, D6.4	m36 → m45
D7.5 - D7.7	m36 → m45

MS35, MS36, MS40	m30 → m39
MS41, MS42	m33 → m42
MS43, MS48, MS49	m36 → m45

3.3.6 Legal Status

No changes.

3.3.7 WEB-site

Since project start in November 2011, the WEB-site is available under www.navolchi.eu and is updated periodically. The WEB-Site is located at the Steinbuch Center for Computing (SCC), the IT- organization of the KIT, Karlsruhe.

3.3.8 Management Summary

As stated in the work package reports, all deliverables and milestones have been accomplished successfully.

The severe problems caused by the retreat of ST have been solved by gaining ETH as a new partner and the project extension by nine months.

3.4 Deliverables and Milestones Tables

3.4.1 Deliverables

Status levels: finished in progress due critical

Deliverable		WP	Partner	Type	Diss	Delivery	
Nr.	Title					Mnth	Date
 D1.1	Project web site with .eu domain (M01) and continuous update	1	KIT	O	PU	1	11/2011
 D1.2	Project reference online manual	1	KIT	O	RE	3	01/2012
 D2.1	Definition of chip-to-chip interconnection system environment and specification	2	ST	R	RE	3	01/2012
 D1.3	Project quality assurance manual	1	KIT	O	RE	6	04/2012
 D5.1	DDCM specification document	5	ST	R	CO	6	04/2012
 D1.4	Intermediate progress report (1)	1	KIT	R	PU	9	07/2012
 D2.2	Definition of plasmonic devices	2	AIT	R	RE	12	10/2012
 D3.1	Report on studies of optimized structure for metallic / plasmonic nano-laser and its coupling to Si WG	3	TU/e	R	CO	12	10/2012
 D3.2	Report on modelling of the modulator structure	3	KIT	R	CO	12	10/2012
 D5.2	DDCM with electrical PHY design and verification data base	5	ST	R	CO	12	10/2012
 D4.1	Designs of plasmonic amplifiers	4	AIT	R	CO	18	04/2013
 D4.2	Report on optical properties of QDs layers and polymer nanocomposites	4	AIT	R	PU	18	04/2013
 D7.1	First report on NAVOLCHI dissemination and promotion activities	7	ST	R	RE	18	04/2013
 D7.2	First report on NAVOLCHI exploitation activities	7	AIT	R	RE	18	04/2013
 D7.3	Mirror Deliverable of D7.1, which will be available to the public on the website.	7	TU/e	R	PU	18	04/2013
 D7.4	Intermediate report on recent achievements.	7	AIT	R	PU	18	04/2013



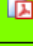







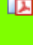




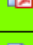











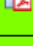









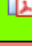









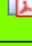
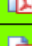

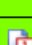
 D5.3	Compact optical filters (2nm bandwidth, >30nm FSR) and first generation beam shapers	5	IMEC	R	CO	21	07/2013
 D2.3	Investigation of chip-to-chip interconnectionlevel specifications employing new plasmonic devices	2	AIT	R	RE	24	10/2013
 D2.4	Interface and plasmonic interconnect models and reports	2	ST	R	RE	24	10/2013
 D3.4	Report on fabrication of modulators	3	KIT	R	CO	24	10/2013
 D4.3	Designs of plasmonic photodetectors	4	AIT	R	CO	24	10/2013
 D5.4	Generic DDCM compatible with plasmonic-based PHY specification document	5	ST	R	PU	24	10/2013
 D5.5	Report on plasmonic waveguide couplers	5	KIT	R	CO	24	10/2013
 D1.5	Intermediate progress report (2)	1	KIT	R	RE	27	01/2014
 D6.1	Report on characterization results of all plasmonic devices	6	TU/e	R	RE	27	01/2014
 D6.2	Report on characterization results of all optical interface plasmonic passive components	6	KIT	R	RE	27	01/2014
 D4.4	Report on SPP amplifiers by using QDs	4	IMEC	R	PU	30	04/2014
 D3.3	Fabrication of plasmonic laser device	3	TU/e	R	CO	33	07/2014
 D5.6	Generic DDCM compatible with plasmonic-based PHY design and verification data base	5	ST	R	CO	39	01/2015
 D4.5	Report on plasmonic photodetectors	4	UVEG	R	PU	42	04/2015
 D5.7	Second generation beam shapers (distance 1mm, with bandwidth > 10nm and efficiency > 3dB)	5	IMEC	P	CO	42	04/2015
 D2.5	Technoeconomical evaluation with respect to the cost efficiency and green aspects	2	AIT	R	PU	45	07/2015
 D2.6	Report on new applications and their opportunities	2	AIT	R	PU	45	07/2015
 D6.3	Report on chip to chip interconnect characterization	6	ST/ETH	R	PU	45	07/2015
 D6.4	Report on plasmonic chip-to-chip interconnect prototype testing and evaluation	6	AIT	R	PU	45	07/2015
 D7.5	Reports on the impact and outcome of the organized promotion events.	7	AIT	R	PU	45	07/2015
D7.6	Final report on NAVOLCHI dissemination and promotion activities	7	AIT	R	RE	45	07/2015
D7.7	Dissemination kit	7	AIT	O	PU	45	07/2015














Table WP1-3: Deliverables of the NAVOLCHI project, ordered by delivery date.

3.4.2 Milestones

Status levels: finished in progress due critical

Milestone		WP	Partner	Delivery	
Nr.	Title			Mnth	Date
 MS44	Dissemination of activities in the project's web site and continuous update	7	KIT	1	11/2011
 MS45	Press release on start of project to the public distributed	7	AIT	2	12/2011
 MS1	Definition of chip-to-chip interconnection system environment and specification	2	AIT	3	01/2012
 MS2	Definition of plasmonic devices and material properties for chip-to-chip interconnection	2	AIT	6	04/2012
 MS8	Decision on an optimized structure for metallic/plasmonic nano-laser and its coupling to Si waveguide	3	TU/e	6	04/2012
 MS9	Decision on an optimized structure for plasmonic modulator	3	KIT	6	04/2012
 MS25	Decision on optimized plasmonic waveguide couplers	5	KIT	6	04/2012
 MS10	Grown wafer structure for plasmonic lasers	3	IMEC	12	10/2012
 MS16	Decision on optimized structures for plasmonic amplifiers	4	UVEG	12	10/2012
 MS17	Synthesis of nanoparticles with gain at 1550nm	4	Ugent	12	10/2012
 MS26	Fabrication of plasmonic waveguide couplers with less than 3 dB coupling loss	5	KIT	12	10/2012
 MS27	Design of first generation beam shapers and compact optical filters	5	IMEC	12	10/2012
 MS28	DDCM with electrical PHY design and verification	5	ST	12	10/2012
 MS37	Plasmonic active device characterization results	6	KIT	12	10/2012
 MS11	Fabrication of plasmonic modulator on a SOI platform	3	KIT	15	01/2013
 MS18	Demonstration of conductive QD layers with photoconductive properties	4	UVEG	15	01/2013
 MS19	Demonstration of metal-(lithographic) polymer and QD metal-(lithographic) polymer nanocompo-sites	4	UVEG	15	01/2013

 MS29	Data codecs for power consumption reduction	5	ST	15	01/2013
 MS30	Decision on plasmonic waveguide couplers with less than 3 dB coupling loss	5	KIT	15	01/2013
 MS46	Identification of possible contributions to the industrial partners for commercialization	7	ST	15	01/2013
 MS3	Development of a system and device simulation platform	2	AIT	18	04/2013
 MS4	Definition of the interconnection level specification employing developed plasmonic photonic devices	2	ST	18	04/2013
 MS12	Decision on an optimized structure for plasmonic modulator with a maximum loss of 20dB	3	KIT	18	04/2013
MS13*	Initial characterization of unbonded plasmonic lasers	3	TU/e	18	04/2013
 MS20	Demonstration and decision on photodetector operation: nano-gap (MIM) vs. Schottky / heterostructure	4	UVEG	18	04/2013
 MS21	Electroluminescence from QD stack embedded within conductive oxides (>1 μ W)	4	IMEC	18	04/2013
 MS31	Fabrication of compact optical filters and first generation beam shapers	5	IMEC	18	04/2013
 MS32	Data codecs for error detection and correction	5	ST	18	04/2013
 MS5	Digital domain to plasmonic domain interface specification and VHDL modelling	2	ST	21	07/2013
 MS14	Initial testing and characterization of plasmonic modulators	3	KIT	21	07/2013
 MS22	Demonstration of plasmonic amplifiers with optical pumping exhibiting 10dB gain  Appendix A	4	IMEC	21	07/2013
 MS6	Plasmonic interconnect VHDL modeling	2	ST	24	10/2013
 MS15	Initial testing of bonded plasmonic lasers	3	TU/e	24	10/2013
 MS23	Operation of QD based photodetector with responsivity > 0.1A/W	4	UVEG	24	10/2013
 MS33	Design of second generation beam shapers	5	IMEC	24	10/2013
 MS34	Generic DDCM compatible with plasmonic-based PHY	5	ST	24	10/2013
 MS38	Plasmonic passive components characterization results with a 1dB coupling loss	6	KIT	24	10/2013

 MS47	Organization of workshop on silicon photonics interface for chip-to-chip communication	7	TU/e	34	08/2014
 MS35	Fabrication of compact optical filters and first generation beam shapers	5	IMEC	39	01/2015
MS36**	DDCM evolution for NiP solutions	5	ST	39	01/2015
 MS40	Individual plasmonic devices characterization, testing and evaluation	6	TU/e	39	01/2015
 MS39	Concept for system integration developed	6	AIT	40	02/2015
 MS50	Final planning of system demonstrator	6	AIT/ETH	41	03/2015
 MS51	Report on enhanced metal grating couplers	7	TU/e	41	03/2015
 MS41	Chip to chip interconnect characterization	6	ST/ETH	42	04/2015
 MS42	Plasmonic components integration to demonstrate chip-to-chip interconnect	6	AIT	42	04/2015
 MS7	Investigation of the cost and power consumption efficiency of the developed plasmonic devices	2	AIT	45	07/2015
 MS24	Demonstration of SPP amplifiers with electrical injection exhibiting 10dB/cm gain	4	UVEG	45	07/2015
 MS43	Plasmonic chip to chip interconnect prototype testing and evaluation	6	ST/ETH	45	07/2015
 MS48	Public web site for NAVOLCHI prepared to stay open for at least another year	7	KIT	45	07/2015
 MS49	Press release distributed comprising key results with a public target audience	7	AIT	45	07/2015

*: MS13 has been identified as inappropriate to the course of the project and was skipped in agreement with EC

** : MS36 has been skipped after the retreat of ST

Table WP1-4: Milestones of the NAVOLCHI project, ordered by delivery date.

3.5 Explanation of the Use of the Resources and Financial Statements

3.5.1 Manpower

The table below (Table WP1-5) compares the spent man-months for both reporting periods 1 and 2 with the planned values. Major deviations can be seen with KIT and TUE. The underspending of ST is by reason of the shift of work to ETH.

	WP1		WP2		WP3		WP4		WP5		WP6		WP7		Total	
	Real	Plan	Real	Plan	Real	Plan	Real	Plan	Real	Plan	Real	Plan	Real	Plan	Real	Plan
KIT	20.1	16.0	4.3	2.0	52.7	26.0	4.8	3.0	22.9	12.0	8.4	4.0	4.8	3.0	118.0	66.0
IMEC	-	1.0	-	1.0	2.8	3.0	20.5	11.0	11.5	14.0	2.0	3.0	1.2	1.0	38.0	34.0
TUe	1.0	1.0	6.0	6.0	46.4	29.0	-	-	-	-	3.0	3.0	1.0	1.0	57.4	40.0
AIT	2.3	2.0	19.4	18.0	-	-	13.0	9.0	-	-	3.2	10.0	10.3	8.0	48.2	47.0
UVEG	2.3	2.0	1.0	2.0	-	-	42.8	32.0	-	4.0	-	2.0	1.9	1.0	48.0	43.0
ST	0.9	2.0	4.5	12.0	-	1.0	0.2	1.0	28.1	30.0	2.5	4.5	1.7	10.0	37.9	60.5
UGent	-	-	-	-	-	-	26.5	24.0	-	-	-	-	-	-	26.5	24.0
ETHZ	0.5	0.5	-	-	-	-	-	-	-	-	25.1	17.0	-	-	25.6	17.5
Total	27.1	24.5	35.2	41.0	101.9	59.0	107.8	80.0	62.5	60.0	44.2	43.5	20.9	24.0	399.6	332.0

Table WP1-5: Total Person-Month Status Table. Real: Actual state for months 1-45; Plan: Total for months 1-36.

3.5.2 Finances

In Table WP1-6 the total amount of planned funding is compared with the requested amount as claimed by the FormCs of the project partners. Detailed explanations of the deviations are given in the text below from KIT, TUE, AIT and ETH.

Beneficiary	Funding			
	Plan Total	Requested P1	Requested P2	Requested Total
KIT	495.615	334.069	619.026	953.095
IMEC	386.013	163.050	226.189	389.239
TUE	362.224	138.620	307.086	445.706
AIT	304.988	88.302	142.716	231.018
UVEG	311.540	143.772	196.335	340.107
ST	288.500	191.622	26.046	217.668
UGent	127.920	74.206	52.621	126.827
ETH	123.200	-	266.256	266.256
Sum	2.400.000	1.133.641	1.836.275	2.969.916

Table WP1-6: Costs claimed in the reporting periods and totally versus the total costs planned. Values in €.

KIT has spent almost double of the planned effort in WPs 3 and 5, because the development and characterization of the different variants of modulators took several iterations more than expected in order to find the best concept and to develop and evaluate the different coupling principles proposed originally. Due to limited resources of AIT, KIT spent two additional MMs in WP 6.1 for characterization of plasmonic modulators. Finally, the unexpected retreat of ST caused additional management effort to reorganize the project, rewrite the DoW and extend the project.

TUE: The reasons for the additional PMs that TUE charged to the project are:

- The extension of the project as a result of which Victor Calzadilla has spent more PMs on the development of the metallo-dielectric laser.
- To help solving a number of unforeseen problems we have had a technician working on the project for 11 months, more than originally foreseen.

AIT's under-spending is due to the following reasons:

1. Lower actual PM rate (3793€), compared to the originally planned one (4500€)
2. Lower actual overhead rate (60.5 % mean average overhead rate; per year was: 2011: 66%, 2012: 61%, 2013 – 2015: 60%), compared to the originally planned one (70%)
3. Reduced effort (measured in PMs or budget) at WP6 (due to lack of available human resources): originally we planned for 10PMs and we finally allocated 3.2PMs
4. Reduced spending in the "other costs" category (for travel, equipment, etc) of only 9.597€ actual, compared to the 42.000€ original estimation (which relates with our reduction of effort in WP6)

ETH was joining the NAVOLCHI consortium only after ST decided to reduce the efforts on the project. ETH was then assigned the two ST tasks and inherited the MMs on these tasks. The tasks assigned to ETH were

- Tasks 6.3 (will carry out an analysis on the developed chip to chip interconnect) and
- Task 6.4 (will assemble all the building-blocks coming from previous tasks and generate a system top level that will be simulated and characterized, and then passed to WP2 for benchmarking.).

For performing the final demonstrator, ETH got the receiver arrays from IMEC and the FPGA coding from ST. ETH then first had to fabricate the modulator arrays (Task 3.4) and characterize it. Further, ETH packaged the fiber modulator array and packaged the detector arrays (Task 6.2). Task 6.2 was particularly expensive, because all the high-speed electronics and rf amplifiers had to be purchased for this project and RF packaging had to be done.

Also, for the testing, ETH got the FPGA code from ST for the signal regeneration modules. Even though this helped a lot, ETH had to adapt the FPGA code and make it compatible with the demonstrator.

Finally, ETH took helped AIT in handing in the missing milestones and deliverables that AIT could not cover due to a lack of human resources. ETH wrote both the MS4.2 and deliverble 6.4 that were assigned to AIT. The AIT efforts will be covered by a of 21 k€ transferred from AIT to ETH.

In summary, ETH had overspending, because tasks 3.4, 5.5 and 6.1 had to be redone by ETH for the demonstrator. Beyond ETH performed the work of task 6.2 and some of the WP6 assignments of AIT. All of which have not been foreseen to be done with the ST MMs.

Summary Financial report - Collaborative project																				
Project acronym		NAVOLCHI			Project nr		288869		Reporting period from		01/11/2011		to		30/04/2013		Page		1/1	
Funding scheme		CP		Type of activity								Total								
Benef. nr	If 3rd Party, linked to benef.	Adjustment (Yes/No)	Organisation Short Name	RTD (A)		Demonstration (B)		Management (C)		Other (D)		Total (A+B+C+D)		Req. EC Contrib.	Receipts	Interest				
				Total	Max EC Contrib.	Total	Max EC Contrib.	Total	Max EC Contrib.	Total	Max EC Contrib.	Total	Max EC Contrib.							
1		No	KIT	297,270	222,952	0	0	111,117	111,117	0	0	408,387	334,099	334,099	0	3,674				
2		No	IMEC	217,400	163,050	0	0	0	0	0	0	217,400	163,050	163,050	0					
3		No	TU/e	172,100	129,075	0	0	9,545	9,545	0	0	181,645	138,620	138,620	0					
4		No	AIT	108,490	81,367	0	0	6,935	6,935	0	0	115,425	88,302	88,302	0					
5		No	UVEG	177,886	133,414	0	0	10,358	10,358	0	0	188,244	143,772	143,772	0					
6		No	ST	370,370	185,185	0	0	6,437	6,437	0	0	376,807	191,622	191,622	0					
7		No	Ugent	98,942	74,206	0	0	0	0	0	0	98,942	74,206	74,206	0					
Total				1,442,458	989,249	0	0	144,392	144,392	0	0	1,586,850	1,133,641	1,133,641	0					

Summary Financial report - Collaborative project																				
Project acronym		NAVOLCHI			Project nr		288869		Reporting period from		01/05/2013		to		31/07/2015		Page		1/1	
Funding scheme		CP		Type of activity								Total								
Benef. nr	If 3rd Party, linked to benef.	Adjustment (Yes/No)	Organisation Short Name	RTD (A)		Demonstration (B)		Management (C)		Other (D)		Total (A+B+C+D)		Req. EC Contrib.	Receipts	Interest				
				Total	Max EC Contrib.	Total	Max EC Contrib.	Total	Max EC Contrib.	Total	Max EC Contrib.	Total	Max EC Contrib.							
1		No	KIT	631,660	473,745	0	0	142,318	142,318	0	0	773,978	616,063	616,063	0	0				
1		Yes (1)	KIT	2,312	1,734	0	0	1,229	1,229	0	0	3,541	2,963	2,963	0	0				
2		No	IMEC	296,167	222,125	0	0	3,500	3,500	0	0	299,667	225,625	225,625	0					
2		Yes (1)	IMEC	752	564	0	0	0	0	0	0	752	564	564	0					
3		No	TU/e	392,234	294,175	0	0	11,473	11,473	0	0	403,707	305,648	305,648	0					
3		Yes (1)	TU/e	1,830	1,372	0	0	66	66	0	0	1,896	1,438	1,438	0					
4		No	AIT	177,789	133,341	0	0	9,590	9,590	0	0	187,379	142,931	142,931	0					
4		Yes (1)	AIT	-229	-171	0	0	-13	-13	0	0	-242	-184	-184	0					
5		No	UVEG	240,147	180,110	0	0	14,030	14,030	0	0	254,177	194,140	194,140	0					
5		Yes (1)	UVEG	2,044	1,533	0	0	662	662	0	0	2,706	2,195	2,195	0					
6		No	ST	42,333	21,166	0	0	4,880	4,880	0	0	47,213	26,046	26,046	0					
7		No	Ugent	72,848	54,636	0	0	0	0	0	0	72,848	54,636	54,636	0					
7		Yes (1)	Ugent	-2,686	-2,014	0	0	0	0	0	0	-2,686	-2,014	-2,014	0					
8		No	ETH Zürich	344,091	258,068	0	0	8,188	8,188	0	0	352,279	266,256	266,256	0					
Total				2,201,292	1,640,384	0	0	195,923	195,923	0	0	2,397,215	1,836,307	1,836,306	0					

Table WP1-7: Detailed cost claim overviews for period 1 (above) and period 2 (below). Values in €

4 Attachments

As determined in the projects “Description of Work”, the milestones (refer to chapter 3.4.2) achieved so far are delivered with this report. To avoid redundant lengthening of this document, the milestones are delivered as separate files. Additionally, you can find them on our web site www.navolchi.eu.

4.1 Detailed Explanation of the Use of the Resources and Financial Statements

The tables and forms presented at the following pages are taken from the NEF database provided by the EC.

- The adjustment of the use of resources for period 1
- The use of resources for period 2
- The FormCs for period 2

Use of Resources

Period 1 (1 - 18)
 (01-11-2011 - 30-04-2013)

Project Number	288869	Project Acronym	NAVOLCHI
----------------	--------	-----------------	----------

Table 3.1 Personnel, subcontracting and other Major cost items for beneficiary 1 for the period.				
KARLSRUHER INSTITUT FUER TECHNOLOGIE				
Work Package	Item description	Amount in €	Explanation	Free Text
WP 3	Other direct cost	152 €	Travelling	Additional costs to the travel of 1 person to ANAHEIM 16.03.2013-23.03.2013 WP3 Oral Conference contribution.
	Personnel costs	2,160 €	Personnel costs	Recalculation of actual personnel costs after the end of the calendar year.
	Personnel costs	1,229 €	Personnel Costs	Recalculation of actual personnel costs after the end of the calendar year.
	Indirect costs	0 €		
TOTAL COSTS		3,541 €		

Table 3.1 Personnel, subcontracting and other Major cost items for beneficiary 2 for the period.				
INTERUNIVERSITAIR MICRO-ELECTRONICA CENTRUM VZW				
Work Package	Item description	Amount in €	Explanation	Free Text
	Other direct cost	176 €	travel	27/11/12 Brussel, review meeting (1 person) 30/11/12 Mons, IEEE conference (1 person) 06/12/12 Lyon, meeting at EC Lyon (1 person) 13/12/12 Leuven, project meeting (1 person) 22/01/13 Leuven, project meeting (1 person) 14/02/13 Diavolezza, ITN cQOM workshop (1 person) 25-26/04/13 Karlsruhe, project meeting (1 person)
	Indirect costs	576 €		
TOTAL COSTS		752 €		

Table 3.1 Personnel, subcontracting and other Major cost items for beneficiary 3 for the period.				
TECHNISCHE UNIVERSITEIT EINDHOVEN				
Work Package	Item description	Amount in €	Explanation	Free Text
WP 2 WP 3 WP 6 WP 7	Personnel costs	-93 €	Personnel Direct Costs RTD	Annually the TU/e recalculates the percentages regarding reduced pay & other personnel costs which affects the previous used tariff.
WP 2 WP 3 WP 6 WP 7	Other direct cost	-55 €	Other Direct Costs	Small correction on P1 Materials
WP 1	Personnel costs	5 €	Personnel Direct Costs MAN	Annually the TU/e recalculates the percentages regarding reduced pay & other personnel costs which affects the previous used tariff.
	Indirect costs	2,039 €		
TOTAL COSTS		1,896 €		

Table 3.1 Personnel, subcontracting and other Major cost items for beneficiary 4 for the period.				
RESEARCH AND EDUCATION LABORATORY IN INFORMATION TECHNOLOGIES				
Work Package	Item description	Amount in €	Explanation	Free Text
WP 2 WP 4 WP 6 WP 7	Personnel costs	1,586 €	Adjustment due to recalculaion of personnel rates	The adjustment in the indirect costs corresponds to the overheads amount claimed in period 1 upon finalization of the overhead factor for year 2012 to 0.61 & year 2013 to 0.60
WP 1	Personnel costs	90 €	adjustment due to recalculation of personnel rates	The adjustment in the indirect costs corresponds to the overheads amount claimed in period 1 upon finalization of the overhead factor for year 2012 to 0.61 & year 2013 to 0.60
	Indirect costs	-1,918 €		
TOTAL COSTS		-242 €		

Table 3.1 Personnel, subcontracting and other Major cost items for beneficiary 5 for the period.				
UNIVERSITAT DE VALENCIA				
Work Package	Item description	Amount in €	Explanation	Free Text

Table 3.1 Personnel, subcontracting and other Major cost items for beneficiary 5 for the period.				
UNIVERSITAT DE VALENCIA				
Work Package	Item description	Amount in €	Explanation	Free Text
WP 2 WP 4 WP 7	Personnel costs	1,402 €	Personnel costs	Adjustment due to a recalculation of the hourly rate on a yearly basis: Juan Martinez (+1.632,63 €), Juan F. Sanchez (-230,30 €).
	Other direct cost	-124 €	Consumable costs. WP 2,4,7	Adjustment to remove VAT unduly claimed on period 1.
	Personnel costs	414 €	Personnel costs	Adjustment due to a recalculation of the hourly rate on a yearly basis (Juan Martinez (413,95 €).
	Indirect costs	1,014 €		
TOTAL COSTS		2,706 €		

Table 3.1 Personnel, subcontracting and other Major cost items for beneficiary 6 for the period.				
STMICROELECTRONICS SRL				
Work Package	Item description	Amount in €	Explanation	Free Text
	Indirect costs	0 €		
TOTAL COSTS		0 €		

Table 3.1 Personnel, subcontracting and other Major cost items for beneficiary 7 for the period.				
UNIVERSITEIT GENT				
Work Package	Item description	Amount in €	Explanation	Free Text
	Other direct cost	-668 €	general consumables, not specifically for NAVOLCHI	consumables
WP 4	Personnel costs	-1,011 €	adjustment salary period 1 Yolanda Justo Zarraquinos	
	Indirect costs	-1,007 €		
TOTAL COSTS		-2,686 €		

Table 3.1 Personnel, subcontracting and other Major cost items for beneficiary 8 for the period.				
EIDGENOESSISCHE TECHNISCHE HOCHSCHULE ZURICH				
Work Package	Item description	Amount in €	Explanation	Free Text
	Indirect costs	0 €		
TOTAL COSTS		0 €		

Adjusted Form C for period 1 from KIT

Form C - Financial Statement (to be filled in by each beneficiary)			
Project Number	288869	Funding scheme	Collaborative project
Project Acronym	NAVOLCHI		
Period from	01/05/2013	Is this an adjustment to a previous statement ?	Yes
To	31/07/2015	Adjustment relates to Period :	1
Legal Name	KARLSRUHER INSTITUT FUER TECHNOLOGIE	Participant Identity Code	990797674
Organisation Short Name	KIT	Beneficiary nr	1
Funding % for RTD activities (A)	75.0	If flat rate for indirect costs, specify %	N/A

1. Declaration of eligible costs/lump sum/flat-rate/scale of unit (in €)

	Type of Activity				Total (A+B+C+D)
	RTD (A)	Demonstration (B)	Management (C)	Other (D)	
Personnel costs	2,160	0	1,229	0	3,389
Subcontracting	0	0	0	0	0
Other direct costs	152	0	0	0	152
Indirect costs	0	0	0	0	0
Total costs	2,312	0	1,229	0	3,541
Maximum EU contribution	1,734	0	1,229	0	2,963
Requested EU contribution					2,963

2. Declaration of receipts

Did you receive any financial transfers or contributions in kind, free of charge from third parties or did the project generate any income which could be considered a receipt according to Art.II. 17 of the grant agreement ?
If yes, please mention the amount (in €)

No

3. Declaration of interest yielded by the pre-financing (to be completed only by the coordinator)

Did the pre-financing you received generate any interest according to Art.II.19 ?
If yes, please mention the amount (in €)

No

4. Certificate on the methodology

Do you declare average personnel costs according to Art.II.14.1 ?

No

Is there a certificate on the methodology provided by an independent auditor and accepted by the Commission according to Art.II.4.4 ?

No

Name of the auditor		Cost of the certificate (in €), if charged under this project	
---------------------	--	---	--

5. Certificate on the financial statements

Is there a certificate on the financial statements provided by an independent auditor attached to this financial statement according to Art.II.4.4 ?

Yes

Name of the auditor	PKF Riedel Appel Hornig GmbH, Heidelberg	Cost of the certificate (in €)	1,125
---------------------	--	--------------------------------	-------

6. Beneficiary's declaration on its honour

We declare on our honour that:

- the costs declared above are directly related to the resources used to attain the objectives of the project and fall within the definition of eligible costs specified in Articles II.14 and II.15 of the grant agreement, and, if relevant, Annex III and Article 7 (special clauses) of the grant agreement;
- the receipts declared above are the only financial transfers or contributions in kind, free of charge, from third parties and the only income generated by the project which could be considered as receipts according to Art.II.17 of the grant agreement;
- the interest declared above is the only interest yielded by the pre-financing which falls within the definition of Art.II.19 of the grant agreement;
- there is full supporting documentation to justify the information hereby declared. It will be made available at the request of the Commission and in the event of an audit by the Commission and/or by the Court of Auditors and/or their authorised representatives.

Beneficiary's Stamp	Name of the Person(s) Authorised to sign this Financial Statement
	Prof. Dr. Kohl / Dasselaar
	Date & signature

Adjusted Form C for period 1 from IMEC

Form C - Financial Statement (to be filled in by each beneficiary)			
Project Number	288869	Funding scheme	Collaborative project
Project Acronym	NAVOLCHI		
Period from	01/05/2013	Is this an adjustment to a previous statement ?	Yes
To	31/07/2015	Adjustment relates to Period :	1
Legal Name	INTERUNIVERSITAIR MICRO-ELECTRONICA CENTRUM VZW	Participant Identity Code	999981149
Organisation Short Name	IMEC	Beneficiary nr	2
Funding % for RTD activities (A)	75.0	If flat rate for indirect costs, specify %	N/A

1. Declaration of eligible costs/lump sum/flat-rate/scale of unit (in €)

	Type of Activity				Total (A+B+C+D)
	RTD (A)	Demonstration (B)	Management (C)	Other (D)	
Personnel costs	0	0	0	0	0
Subcontracting	0	0	0	0	0
Other direct costs	176	0	0	0	176
Indirect costs	576	0	0	0	576
Total costs	752	0	0	0	752
Maximum EU contribution	564	0	0	0	564
Requested EU contribution					564

2. Declaration of receipts

Did you receive any financial transfers or contributions in kind, free of charge from third parties or did the project generate any income which could be considered a receipt according to Art.II. 17 of the grant agreement ?
If yes, please mention the amount (in €)

No

4. Certificate on the methodology

Do you declare average personnel costs according to Art.II.14.1 ?

No

Is there a certificate on the methodology provided by an independent auditor and accepted by the Commission according to Art.II.4.4 ?

No

Name of the auditor	Cost of the certificate (in €), if charged under this project
---------------------	---

5. Certificate on the financial statements

Is there a certificate on the financial statements provided by an independent auditor attached to this financial statement according to Art.II.4.4 ?

Yes

Name of the auditor	KPMG Bedrijfsrevisoren	Cost of the certificate (in €)	3,500
---------------------	------------------------	--------------------------------	-------

6. Beneficiary's declaration on its honour

We declare on our honour that:

- the costs declared above are directly related to the resources used to attain the objectives of the project and fall within the definition of eligible costs specified in Articles II.14 and II.15 of the grant agreement, and, if relevant, Annex III and Article 7 (special clauses) of the grant agreement;
- the receipts declared above are the only financial transfers or contributions in kind, free of charge, from third parties and the only income generated by the project which could be considered as receipts according to Art.II.17 of the grant agreement;
- the interest declared above is the only interest yielded by the pre-financing which falls within the definition of Art.II.19 of the grant agreement;
- there is full supporting documentation to justify the information hereby declared. It will be made available at the request of the Commission and in the event of an audit by the Commission and/or by the Court of Auditors and/or their authorised representatives.

Beneficiary's Stamp	Name of the Person(s) Authorised to sign this Financial Statement
	Hannelore Marain
	Date & signature

Adjusted Form C for period 1 from TUE

Form C - Financial Statement (to be filled in by each beneficiary)			
Project Number	288869	Funding scheme	Collaborative project
Project Acronym	NAVOLCHI		
Period from	01/05/2013	Is this an adjustment to a previous statement ?	Yes
To	31/07/2015	Adjustment relates to Period :	1
Legal Name	TECHNISCHE UNIVERSITEIT EINDHOVEN	Participant Identity Code	999977269
Organisation Short Name	TU/e	Beneficiary nr	3
Funding % for RTD activities (A)	75.0	If flat rate for indirect costs, specify %	N/A

1. Declaration of eligible costs/lump sum/flat-rate/scale of unit (in €)

	Type of Activity				Total (A+B+C+D)
	RTD (A)	Demonstration (B)	Management (C)	Other (D)	
Personnel costs	-93	0	5	0	-88
Subcontracting	0	0	0	0	0
Other direct costs	-55	0	0	0	-55
Indirect costs	1,978	0	61	0	2,039
Total costs	1,830	0	66	0	1,896
Maximum EU contribution	1,372	0	66	0	1,438
Requested EU contribution					1,438

2. Declaration of receipts

Did you receive any financial transfers or contributions in kind, free of charge from third parties or did the project generate any income which could be considered a receipt according to Art.II. 17 of the grant agreement ?
If yes, please mention the amount (in €)

No

4. Certificate on the methodology

Do you declare average personnel costs according to Art.II.14.1 ?

No

Is there a certificate on the methodology provided by an independent auditor and accepted by the Commission according to Art.II.4.4 ?

No

Name of the auditor	Cost of the certificate (in €), if charged under this project
---------------------	---

5. Certificate on the financial statements

Is there a certificate on the financial statements provided by an independent auditor attached to this financial statement according to Art.II.4.4 ?

Yes

Name of the auditor	L.A.M. Ververs RA	Cost of the certificate (in €)	1,500
---------------------	-------------------	--------------------------------	-------

6. Beneficiary's declaration on its honour

We declare on our honour that:

- the costs declared above are directly related to the resources used to attain the objectives of the project and fall within the definition of eligible costs specified in Articles II.14 and II.15 of the grant agreement, and, if relevant, Annex III and Article 7 (special clauses) of the grant agreement;
- the receipts declared above are the only financial transfers or contributions in kind, free of charge, from third parties and the only income generated by the project which could be considered as receipts according to Art.II.17 of the grant agreement;
- the interest declared above is the only interest yielded by the pre-financing which falls within the definition of Art.II.19 of the grant agreement;
- there is full supporting documentation to justify the information hereby declared. It will be made available at the request of the Commission and in the event of an audit by the Commission and/or by the Court of Auditors and/or their authorised representatives.

Beneficiary's Stamp	Name of the Person(s) Authorised to sign this Financial Statement
	drs. J.C. Boot-Van Wevelingen
	Date & signature

Adjusted Form C for period 1 from AIT

Form C - Financial Statement (to be filled in by each beneficiary)			
Project Number	288869	Funding scheme	Collaborative project
Project Acronym	NAVOLCHI		
Period from	01/05/2013	Is this an adjustment to a previous statement ?	Yes
To	31/07/2015	Adjustment relates to Period :	1
Legal Name	RESEARCH AND EDUCATION LABORATORY IN INFORMATION TECHNOLOGIES	Participant Identity Code	999582382
Organisation Short Name	AIT	Beneficiary nr	4
Funding % for RTD activities (A)	75.0	If flat rate for indirect costs, specify %	N/A

1. Declaration of eligible costs/lump sum/flat-rate/scale of unit (in €)

	Type of Activity				Total (A+B+C+D)
	RTD (A)	Demonstration (B)	Management (C)	Other (D)	
Personnel costs	1,588	0	80	0	1,678
Subcontracting	0	0	0	0	0
Other direct costs	0	0	0	0	0
Indirect costs	-1,815	0	-103	0	-1,918
Total costs	-229	0	-13	0	-242
Maximum EU contribution	-171	0	-13	0	-184
Requested EU contribution					-184

2. Declaration of receipts

Did you receive any financial transfers or contributions in kind, free of charge from third parties or did the project generate any income which could be considered a receipt according to Art.II. 17 of the grant agreement ?
If yes, please mention the amount (in €)

No

4. Certificate on the methodology

Do you declare average personnel costs according to Art.II.14.1 ?

No

Is there a certificate on the methodology provided by an independent auditor and accepted by the Commission according to Art.II.4.4 ?

No

Name of the auditor	Cost of the certificate (in €), if charged under this project
---------------------	---

5. Certificate on the financial statements

Is there a certificate on the financial statements provided by an independent auditor attached to this financial statement according to Art.II.4.4 ?

No

Name of the auditor	Cost of the certificate (in €)
---------------------	--------------------------------

6. Beneficiary's declaration on its honour

We declare on our honour that:

- the costs declared above are directly related to the resources used to attain the objectives of the project and fall within the definition of eligible costs specified in Articles II.14 and II.15 of the grant agreement, and, if relevant, Annex III and Article 7 (special clauses) of the grant agreement;
- the receipts declared above are the only financial transfers or contributions in kind, free of charge, from third parties and the only income generated by the project which could be considered as receipts according to Art.II.17 of the grant agreement;
- the interest declared above is the only interest yielded by the pre-financing which falls within the definition of Art.II.19 of the grant agreement;
- there is full supporting documentation to justify the information hereby declared. It will be made available at the request of the Commission and in the event of an audit by the Commission and/or by the Court of Auditors and/or their authorised representatives.

Beneficiary's Stamp	Name of the Person(s) Authorised to sign this Financial Statement
	SPYRIDOULA PREVEDOUROU
	Date & signature

Adjusted Form C for period 1 from UVEG

Form C - Financial Statement (to be filled in by each beneficiary)			
Project Number	288869	Funding scheme	Collaborative project
Project Acronym	NAVOLCHI		
Period from	01/05/2013	Is this an adjustment to a previous statement ?	Yes
To	31/07/2015	Adjustment relates to Period :	1
Legal Name	UNIVERSITAT DE VALENCIA	Participant Identity Code	999953019
Organisation Short Name	UVEG	Beneficiary nr	5
Funding % for RTD activities (A)	75.0	If flat rate for indirect costs, specify %	60

1. Declaration of eligible costs/lump sum/flat-rate/scale of unit (in €)

	Type of Activity				Total (A+B+C+D)
	RTD (A)	Demonstration (B)	Management (C)	Other (D)	
Personnel costs	1,402	0	414	0	1,816
Subcontracting	0	0	0	0	0
Other direct costs	-124	0	0	0	-124
Indirect costs	768	0	248	0	1,014
Total costs	2,044	0	662	0	2,706
Maximum EU contribution	1,533	0	662	0	2,195
Requested EU contribution					2,195

2. Declaration of receipts

Did you receive any financial transfers or contributions in kind, free of charge from third parties or did the project generate any income which could be considered a receipt according to Art.II. 17 of the grant agreement ?
 If yes, please mention the amount (in €)

No

4. Certificate on the methodology

Do you declare average personnel costs according to Art.II.14.1 ?

No

Is there a certificate on the methodology provided by an independent auditor and accepted by the Commission according to Art.II.4.4 ?

No

Name of the auditor	Cost of the certificate (in €), if charged under this project
---------------------	---

5. Certificate on the financial statements

Is there a certificate on the financial statements provided by an independent auditor attached to this financial statement according to Art.II.4.4 ?

No

Name of the auditor	Cost of the certificate (in €)
---------------------	--------------------------------

6. Beneficiary's declaration on its honour

We declare on our honour that:

- the costs declared above are directly related to the resources used to attain the objectives of the project and fall within the definition of eligible costs specified in Articles II.14 and II.15 of the grant agreement, and, if relevant, Annex III and Article 7 (special clauses) of the grant agreement;
- the receipts declared above are the only financial transfers or contributions in kind, free of charge, from third parties and the only income generated by the project which could be considered as receipts according to Art.II.17 of the grant agreement;
- the interest declared above is the only interest yielded by the pre-financing which falls within the definition of Art.II.19 of the grant agreement;
- there is full supporting documentation to justify the information hereby declared. It will be made available at the request of the Commission and in the event of an audit by the Commission and/or by the Court of Auditors and/or their authorised representatives.

Beneficiary's Stamp	Name of the Person(s) Authorised to sign this Financial Statement
	Inmaculada Santaemilia Alcacer
	Date & signature

Adjusted Form C for period 1 from UGent

Form C - Financial Statement (to be filled in by each beneficiary)			
Project Number	288869	Funding scheme	Collaborative project
Project Acronym	NAVOLCHI		
Period from	01/05/2013	Is this an adjustment to a previous statement ?	Yes
To	31/07/2015	Adjustment relates to Period :	1
Legal Name	UNIVERSITEIT GENT	Participant Identity Code	999986096
Organisation Short Name	Ugent	Beneficiary nr	7
Funding % for RTD activities (A)	75.0	If flat rate for indirect costs, specify %	60

1. Declaration of eligible costs/lump sum/flat-rate/scale of unit (in €)

	Type of Activity				Total (A+B+C+D)
	RTD (A)	Demonstration (B)	Management (C)	Other (D)	
Personnel costs	-1,011	0	0	0	-1,011
Subcontracting	0	0	0	0	0
Other direct costs	-668	0	0	0	-668
Indirect costs	-1,007	0	0	0	-1,007
Total costs	-2,686	0	0	0	-2,686
Maximum EU contribution	-2,014	0	0	0	-2,014
Requested EU contribution					-2,014

2. Declaration of receipts

Did you receive any financial transfers or contributions in kind, free of charge from third parties or did the project generate any income which could be considered a receipt according to Art.II. 17 of the grant agreement ?
If yes, please mention the amount (in €)

No

4. Certificate on the methodology

Do you declare average personnel costs according to Art.II.14.1 ?

No

Is there a certificate on the methodology provided by an independent auditor and accepted by the Commission according to Art.II.4.4 ?

No

Name of the auditor	Cost of the certificate (in €), if charged under this project
---------------------	---

5. Certificate on the financial statements

Is there a certificate on the financial statements provided by an independent auditor attached to this financial statement according to Art.II.4.4 ?

No

Name of the auditor	Cost of the certificate (in €)
---------------------	--------------------------------

6. Beneficiary's declaration on its honour

We declare on our honour that:

- the costs declared above are directly related to the resources used to attain the objectives of the project and fall within the definition of eligible costs specified in Articles II.14 and II.15 of the grant agreement, and, if relevant, Annex III and Article 7 (special clauses) of the grant agreement;
- the receipts declared above are the only financial transfers or contributions in kind, free of charge, from third parties and the only income generated by the project which could be considered as receipts according to Art.II.17 of the grant agreement;
- the interest declared above is the only interest yielded by the pre-financing which falls within the definition of Art.II.19 of the grant agreement;
- there is full supporting documentation to justify the information hereby declared. It will be made available at the request of the Commission and in the event of an audit by the Commission and/or by the Court of Auditors and/or their authorised representatives.

Beneficiary's Stamp	Name of the Person(s) Authorised to sign this Financial Statement
	Geert Van de Gucht
	Date & signature

Use of Resources

Period 2 (19 - 45)
 (01-05-2013 - 31-07-2015)

Project Number	288869	Project Acronym	NAVOLCHI
----------------	--------	-----------------	----------

Table 3.1 Personnel, subcontracting and other Major cost items for beneficiary 1 for the period.				
KARLSRUHER INSTITUT FUER TECHNOLOGIE				
Work Package	Item description	Amount in €	Explanation	Free Text
WP 7	Other direct cost	1,850 €	Travelling	1 Person SAN JOSE 08.05.-15.05.2013 WP7 Oral conference contribution.
WP 7	Other direct cost	2,672 €	Travelling	1 Person SAN FRANCISCO 09.05.-16.05.2015 WP7 Oral conference contribution.
WP 2 WP 3 WP 4 WP 5 WP 6 WP 7	Personnel costs	304,681 €	Personnel Costs	Total 61,8 PM: WP2: 1PM postdoc; 2 PM PhD student/ WP3: 11,3 PM engineer; 10 PM PhD student; 6 PM postdoc/ WP4: 2 PM engineer; 1 PM PhD student/ WP5: 10 PM PhD student; 8 PM engineer/ WP6: 7 PM PhD student/ WP7: 1,5 PM postdoc; 2 PM PhD student.
WP 3	Other direct cost	41 €	Other Costs	WP3: Sample transport.
WP 7	Other direct cost	1,614 €	Other Costs	WP7: Publication fees.
WP 7	Other direct cost	1,351 €	Other Costs	WP7: Publication fees.
WP 3 WP 4	Other direct cost	663 €	Other Costs	WP3+4: Contact porbe servicing.
WP 3	Other direct cost	715 €	Other Costs	Preparation of samples.
WP 7	Other direct cost	2,489 €	Travelling	1 Person SAN DIEGO 12.07.-18.07.2014 WP7 Oral conference contribution.
WP 7	Other direct cost	1,665 €	Travelling	1 Person LAUSANNE 22.09.-27.09.2014

Table 3.1 Personnel, subcontracting and other Major cost items for beneficiary 1 for the period.				
KARLSRUHER INSTITUT FUER TECHNOLOGIE				
Work Package	Item description	Amount in €	Explanation	Free Text
				WP7 Oral conference contribution.
WP 7	Other direct cost	171 €	Travelling	1 Person FRANKFURT 26.06.2014 WP7 Visa for travelling to San Diego.
WP 3	Other direct cost	7,628 €	Consumables	WP3: SOI Wafer purchase for fabrication.
WP 3	Other direct cost	41 €	Consumables	WP3: Lab supplies.
WP 7	Other direct cost	1,947 €	Travelling	1 Person SAN JOSE 11.05.-17.05.2015 WP7 Oral conference contribution.
WP 1	Other direct cost	1,364 €	Travelling	3 Persons BRÜSSEL 09.07.-10.07.2013 WP1 Project Meeting.
WP 1	Other direct cost	613 €	Travelling	2 Persons EINDHOVEN 27.01.-28.01.2014 WP1 Project Meeting.
WP 1	Other direct cost	1,501 €	Travelling	2 Persons BRÜSSEL 03.11.-05.11.2014 WP1 Project Meeting.
WP 1	Other direct cost	899 €	Other Costs	WP1: Meeting room rent / Brussels.
WP 1	Other direct cost	379 €	Other Costs	WP1: Transport fo project members to meeting.
WP 1	Other direct cost	36 €	Other Costs	WP1: Catering.
WP 1	Subcontracting	1,125 €	Subcontracting	CFS for Period 1+2 (01.11.2011-31.07.2015).
WP 1	Personnel costs	67,715 €	Personnel Costs	WP1 total 10,3 PM: 6,8 PM senior researcher; 3,5 PM post-doc.
	Indirect costs	372,818 €		
TOTAL COSTS		773,978 €		

Table 3.1 Personnel, subcontracting and other Major cost items for beneficiary 2 for the period.				
INTERUNIVERSITAIR MICRO-ELECTRONICA CENTRUM VZW				
Work Package	Item description	Amount in €	Explanation	Free Text
WP 4 WP 5 WP 6 WP 7	Personnel costs	122,467 €	personnel cost for a senior technician (2 MM) and 5 engineers (19 MM)	WP 4 : 13 MM - WP 5 : 5 MM - WP 6 : 2 MM - WP 7 : 1 MM
WP 4 WP 5 WP 6 WP 7	Other direct cost	858 €	travel	12-14/05/13 Munich, CLEO EUROPE presentation (1 person)
WP 4 WP 5 WP 6 WP 7	Other direct cost	5,500 €	consumables	post processing and coupler
WP 1	Subcontracting	3,500 €	Audit certificate	
	Indirect costs	167,342 €		
TOTAL COSTS		299,667 €		

Table 3.1 Personnel, subcontracting and other Major cost items for beneficiary 3 for the period.				
TECHNISCHE UNIVERSITEIT EINDHOVEN				
Work Package	Item description	Amount in €	Explanation	Free Text
WP 2 WP 3 WP 6 WP 7	Personnel costs	180,532 €	Personnel Direct Costs RTD	Salaries of V.M. Dolores Calzadilla (Doctoral Candidate), E.J. Geluk (Technician) and M.K. Smit (Professor)
WP 2 WP 3 WP 6 WP 7	Other direct cost	10,639 €	Travelling	Travel to Karlsruhe, Gent, Mons, Oostduinkerke, Brussel, Cartagena, London and San Diego
WP 2 WP 3 WP 6 WP 7	Other direct cost	45,500 €	Consumables	Including Cleanroom costs (42k€)
WP 1	Personnel costs	7,641 €	Personnel Direct Costs MAN	Salary of M.K. Smit (Professor)
WP 1	Other direct cost	1,500 €	Other Direct Costs	Audit Costs (CFS)
	Indirect costs	157,895 €		
TOTAL COSTS		403,707 €		

Table 3.1 Personnel, subcontracting and other Major cost items for beneficiary 4 for the period.				
RESEARCH AND EDUCATION LABORATORY IN INFORMATION TECHNOLOGIES				
Work Package	Item description	Amount in €	Explanation	Free Text
WP 2 WP 4 WP 6 WP 7	Personnel costs	110,662 €	Cost of 26.90 PMs performed by 9 persons	

Table 3.1 Personnel, subcontracting and other Major cost items for beneficiary 4 for the period.				
RESEARCH AND EDUCATION LABORATORY IN INFORMATION TECHNOLOGIES				
Work Package	Item description	Amount in €	Explanation	Free Text
WP 2 WP 4 WP 6 WP 7	Other direct cost	730 €	KACHRIS 27-29/01/2014 NETHERLANDS- EIDHOVEN PROJECT MEETING	
WP 1	Personnel costs	4,937 €	Cost of 1.20 PMs performed by 3 persons	
WP 1	Other direct cost	829 €	FITRAKIS EMM. 08-10/07/2013 BELGIUM- BRUSSELS REVIEW MEETING	
WP 1	Other direct cost	615 €	KACHRIS 04-05/11/2014 BELGIUM- BRUSSELS REVIEW MEETING	
WP 1	Other direct cost	247 €	TOMKOS 04-06/10/2015 BELGIUM- BRUSSELS FINAL REVIEW MEETING, AIR TICKET COST ONLY	
	Indirect costs	69,359 €		
TOTAL COSTS		187,379 €		

Table 3.1 Personnel, subcontracting and other Major cost items for beneficiary 5 for the period.				
UNIVERSITAT DE VALENCIA				
Work Package	Item description	Amount in €	Explanation	Free Text
WP 2 WP 7 WP 4	Personnel costs	117,665 €	Personnel costs	Part of the salary for the hours devoted to project by researchers as follows: Juan Martinez (9,02 PM; 58.327,70 €. Juan F. Sanchez (3,21 PM; 12.975,41 €). Isaac Suarez (7,27 PM; 29.004,96 €). Pedro Rodriguez (4,14 PM; 17.356,61 €)
WP 4	Other direct cost	2,281 €	Durable costs	Part of the equipment depretiation corresponding to period for the purchase of: LASER Nd: Yag PULSED;

Table 3.1 Personnel, subcontracting and other Major cost items for beneficiary 5 for the period.				
UNIVERSITAT DE VALENCIA				
Work Package	Item description	Amount in €	Explanation	Free Text
				SRS DELAY GENERATOR (STANFORD RESEARCH) MOD. DG535/01; LASER LDH-P 780; INFRARED CAMERA CHILLED; System and software of lithography assisted by UV
WP 4	Other direct cost	22,233 €	Consumable costs	* Optics/ Optomechanics, Chemical, substrates, labware: 11.660,12 €. * Delivery of different nanomaterials: quantum dots (CdSe, CdTe, CdS and PbS) in polymers and resists, conducting polymers and PbS quantum dots): 10.573,12 €.
WP 4 WP 7	Other direct cost	5,383 €	Travel costs	1) Attendance to project meeting. Karlsruhe (Germany). Isaac Suarez. 25-24/04/13. WP4. 628,61 €. 2) Attendance to ICON Congress. Cartagena8 Spain). Isaac Suarez. 23-27/06/13. WP7. 590.63 €. 3) Attendance to project meeting. Eindhoven (Holland). Isaac Suarez. 25-29/01/14. WP4. 624,62 €. 4) Attendance to ICTON 2014 Congress. Graz (Austria). Isaac Alvarez. 3-5/11/14. WP7. 944,19 €. 5) Attendance to 8th AQUANTUM DOTS Congress. Pisa (Italy). Javier Rodriguez. 11-16/05/15. WP7. 1.622,97 €. 6) Attendance to

Table 3.1 Personnel, subcontracting and other Major cost items for beneficiary 5 for the period.				
UNIVERSITAT DE VALENCIA				
Work Package	Item description	Amount in €	Explanation	Free Text
				8th AQUANTUM DOTS Congress. Pisa (Italy). Alberto Maulu. 11-16/05/15. WP7. 971,96 €.
WP 4	Other direct cost	2,530 €	Other costs	Courier costs (163,23 €). Microscopy costs (589,84 €). Printing costs (42,80 €). Registration costs (1.734,55 €)
WP 1	Other direct cost	1,930 €	Travel costs	1) Attendance to project meeting. Brussels (Belgium). Juan Martinez. 9-10/07/13. WP1. 1.009,86 €. 2) Attendance to project meeting. Brussels (Belgium). Juan Martinez. 3-5/11/14. 919,84 €.
WP 1	Personnel costs	6,839 €	Personnel costs	Part of the salary for the hours devoted to project by researchers as follows: Juan Martinez (1,30PM; 6.839,09 €).
	Indirect costs	95,316 €		
TOTAL COSTS		254,177 €		

Table 3.1 Personnel, subcontracting and other Major cost items for beneficiary 6 for the period.				
STMICROELECTRONICS SRL				
Work Package	Item description	Amount in €	Explanation	Free Text
WP 5	Personnel costs	19,049 €	Salaries of 1 project manager for a total of 3,56 pm	
WP 1	Personnel costs	2,195 €	Salaries of 1 project manager, for a total 0,41 pm	
	Indirect costs	25,969 €		
TOTAL COSTS		47,213 €		

Table 3.1 Personnel, subcontracting and other Major cost items for beneficiary 7 for the period.				
UNIVERSITEIT GENT				
Work Package	Item description	Amount in €	Explanation	Free Text
WP 4	Personnel costs	32,945 €		

Table 3.1 Personnel, subcontracting and other Major cost items for beneficiary 7 for the period.				
UNIVERSITEIT GENT				
Work Package	Item description	Amount in €	Explanation	Free Text
			Laxmi Kishore Sagar, PhD, 01/05/2013 - 31/03/2014, 11 PM	
WP 4	Other direct cost	7,803 €	Specific Lab consumables for Synthesis of Colloidal Nano Crystals as foreseen within work package 4 of the project.	consumables
WP 4	Other direct cost	3,513 €	Spitfire ACE, depreciation (10540 euro/60 months) * 20 months	equipment
WP 4	Other direct cost	1,075 €	use HRTEM (3rd quarter 2014)	other
WP 4	Other direct cost	194 €	Laxmi Kishore Sagar, ChemCYS 2014, Blankenberge (Belgium), 27-28/02/2014 (€ 113.87) --- Zeger Hens, meeting NAVOLCHI, Brussels (Belgium), 09/07/2013 (€ 9.60) --- Zeger Hens, meeting NAVOLCHI, Lille (France), 7/10/2013 (€ 70.90)	travel
	Indirect costs	27,318 €		
TOTAL COSTS		72,848 €		

Table 3.1 Personnel, subcontracting and other Major cost items for beneficiary 8 for the period.				
EIDGENOESSISCHE TECHNISCHE HOCHSCHULE ZURICH				
Work Package	Item description	Amount in €	Explanation	Free Text
WP 6	Personnel costs	67,446 €	Personnel	Postdoc, 7.25 PM
WP 6	Other direct cost	1,819 €	Travel	1 staff, Boston, 27.06.-01.07.2015, conference
WP 6	Personnel costs	54,991 €	Personnel	PhD, 8.6 PM
WP 6	Personnel costs	32,933 €	Personnel	PhD, 5.25 PM
WP 6	Personnel costs	24,521 €	Personnel	PhD, 4 PM
WP 6	Other direct cost	846 €	Travel	1 staff, Brussels, 03.-05.11.2014, meeting
WP 6	Other direct cost	107 €	Travel	

Table 3.1 Personnel, subcontracting and other Major cost items for beneficiary 8 for the period.				
EIDGENOESSISCHE TECHNISCHE HOCHSCHULE ZURICH				
Work Package	Item description	Amount in €	Explanation	Free Text
				1 staff, Brussels, 03.-05.11.2014, meeting
WP 6	Other direct cost	498 €	Consumables	
WP 6	Other direct cost	597 €	Consumables	
WP 6	Other direct cost	617 €	Consumables	
WP 6	Other direct cost	747 €	Consumables	
WP 6	Other direct cost	874 €	Consumables	
WP 6	Other direct cost	1,095 €	Consumables	
WP 6	Other direct cost	3,495 €	Consumables	Stage, characterization setup
WP 6	Other direct cost	3,504 €	Consumables	Stage, characterization setup
WP 6	Other direct cost	3,504 €	Consumables	Stage, characterization setup
WP 6	Other direct cost	3,660 €	Consumables	Stage, characterization setup
WP 6	Other direct cost	3,153 €	Consumables	fiber array, transmitter optical characterization
WP 6	Other direct cost	3,312 €	Consumables	fiber array, receiver optical characterization
WP 6	Other direct cost	4,393 €	Consumables	RF probe, device characterization
WP 6	Other direct cost	19 €	Consumables	
WP 6	Other direct cost	19 €	Consumables	
WP 6	Other direct cost	21 €	Consumables	
WP 6	Other direct cost	85 €	Consumables	
WP 6	Other direct cost	193 €	Consumables	
WP 6	Other direct cost	1,304 €	Equipment	12.11.2014, 10124€, 5 years, 100%, 3D manipulator
WP 6	Other direct cost	1,304 €	Equipment	12.11.2014, 10124€, 5 years, 100%, 3D manipulator
WP 1	Personnel costs	5,118 €	Personnel	PhD, 0.5 PM
	Indirect costs	132,104 €		
TOTAL COSTS		352,279 €		

Form C for period 2 from KIT

Form C - Financial Statement (to be filled in by each beneficiary)			
Project Number	288869	Funding scheme	Collaborative project
Project Acronym	NAVOLCHI		
Period from	01/05/2013	Is this an adjustment to a previous statement ?	No
To	31/07/2015		
Legal Name	KARLSRUHER INSTITUT FUER TECHNOLOGIE	Participant Identity Code	990797874
Organisation Short Name	KIT	Beneficiary nr	1
Funding % for RTD activities (A)	75.0	If flat rate for indirect costs, specify %	N/A

1. Declaration of eligible costs/lump sum/flat-rate/scale of unit (in €)

	Type of Activity				Total (A+B+C+D)
	RTD (A)	Demonstration (B)	Management (C)	Other (D)	
Personnel costs	304,681	0	67,715	0	372,396
Subcontracting	0	0	1,125	0	1,125
Other direct costs	22,847	0	4,792	0	27,639
Indirect costs	304,132	0	68,686	0	372,818
Total costs	631,660	0	142,318	0	773,978
Maximum EU contribution	473,745	0	142,318	0	616,063
Requested EU contribution					616,063

2. Declaration of receipts

Did you receive any financial transfers or contributions in kind, free of charge from third parties or did the project generate any income which could be considered a receipt according to Art.II. 17 of the grant agreement ?
If yes, please mention the amount (in €)

No

3. Declaration of interest yielded by the pre-financing (to be completed only by the coordinator)

Did the pre-financing you received generate any interest according to Art.II.19 ?
If yes, please mention the amount (in €)

No

4. Certificate on the methodology

Do you declare average personnel costs according to Art.II.14.1 ?

No

Is there a certificate on the methodology provided by an independent auditor and accepted by the Commission according to Art.II.4.4 ?

No

Name of the auditor		Cost of the certificate (in €), if charged under this project	
---------------------	--	---	--

5. Certificate on the financial statements

Is there a certificate on the financial statements provided by an independent auditor attached to this financial statement according to Art.II.4.4 ?

Yes

Name of the auditor	PKF Riedel Appel Hornig GmbH, Heidelberg	Cost of the certificate (in €)	1,125
---------------------	--	--------------------------------	-------

6. Beneficiary's declaration on its honour

We declare on our honour that:

- the costs declared above are directly related to the resources used to attain the objectives of the project and fall within the definition of eligible costs specified in Articles II.14 and II.15 of the grant agreement, and, if relevant, Annex III and Article 7 (special clauses) of the grant agreement;
- the receipts declared above are the only financial transfers or contributions in kind, free of charge, from third parties and the only income generated by the project which could be considered as receipts according to Art.II.17 of the grant agreement;
- the interest declared above is the only interest yielded by the pre-financing which falls within the definition of Art.II.19 of the grant agreement;
- there is full supporting documentation to justify the information hereby declared. It will be made available at the request of the Commission and in the event of an audit by the Commission and/or by the Court of Auditors and/or their authorised representatives.

Beneficiary's Stamp	Name of the Person(s) Authorised to sign this Financial Statement
	Prof. Dr. Kohl / Dasselaar
	Date & signature

Form C for period 2 from IMEC

Form C - Financial Statement (to be filled in by each beneficiary)			
Project Number	288869	Funding scheme	Collaborative project
Project Acronym	NAVOLCHI		
Period from	01/05/2013	Is this an adjustment to a previous statement ?	No
To	31/07/2015		
Legal Name	INTERUNIVERSITAIR MICRO-ELECTRONICA CENTRUM VZW	Participant Identity Code	999981149
Organisation Short Name	IMEC	Beneficiary nr	2
Funding % for RTD activities (A)	75.0	If flat rate for indirect costs, specify %	N/A

1. Declaration of eligible costs/lump sum/flat-rate/scale of unit (in €)

	Type of Activity				Total (A+B+C+D)
	RTD (A)	Demonstration (B)	Management (C)	Other (D)	
Personnel costs	122,487	0	0	0	122,487
Subcontracting	0	0	3,500	0	3,500
Other direct costs	6,358	0	0	0	6,358
Indirect costs	167,342	0	0	0	167,342
Total costs	296,187	0	3,500	0	299,687
Maximum EU contribution	222,125	0	3,500	0	225,625
Requested EU contribution					225,625

2. Declaration of receipts

Did you receive any financial transfers or contributions in kind, free of charge from third parties or did the project generate any income which could be considered a receipt according to Art.II. 17 of the grant agreement ?
If yes, please mention the amount (in €)

No

4. Certificate on the methodology

Do you declare average personnel costs according to Art.II.14.1 ?

No

Is there a certificate on the methodology provided by an independent auditor and accepted by the Commission according to Art.II.4.4 ?

No

Name of the auditor

Cost of the certificate (in €), if charged under this project

5. Certificate on the financial statements

Is there a certificate on the financial statements provided by an independent auditor attached to this financial statement according to Art.II.4.4 ?

Yes

Name of the auditor

KPMG Bedrijfsrevisoren

Cost of the certificate (in €)

3,500

6. Beneficiary's declaration on its honour

We declare on our honour that:

- the costs declared above are directly related to the resources used to attain the objectives of the project and fall within the definition of eligible costs specified in Articles II.14 and II.15 of the grant agreement, and, if relevant, Annex III and Article 7 (special clauses) of the grant agreement;
- the receipts declared above are the only financial transfers or contributions in kind, free of charge, from third parties and the only income generated by the project which could be considered as receipts according to Art.II.17 of the grant agreement;
- the interest declared above is the only interest yielded by the pre-financing which falls within the definition of Art.II.19 of the grant agreement;
- there is full supporting documentation to justify the information hereby declared. It will be made available at the request of the Commission and in the event of an audit by the Commission and/or by the Court of Auditors and/or their authorised representatives.

Beneficiary's Stamp	Name of the Person(s) Authorised to sign this Financial Statement
	Hannelore Marain
	Date & signature

Form C for period 2 from TUE

Form C - Financial Statement (to be filled in by each beneficiary)			
Project Number	288869	Funding scheme	Collaborative project
Project Acronym	NAVOLCHI		
Period from	01/05/2013	Is this an adjustment to a previous statement ?	No
To	31/07/2015		
Legal Name	TECHNISCHE UNIVERSITEIT EINDHOVEN	Participant Identity Code	999977269
Organisation Short Name	TU/e	Beneficiary nr	3
Funding % for RTD activities (A)	75.0	If flat rate for indirect costs, specify %	N/A

1. Declaration of eligible costs/lump sum/flat-rate/scale of unit (in €)

	Type of Activity				Total (A+B+C+D)
	RTD (A)	Demonstration (B)	Management (C)	Other (D)	
Personnel costs	180,532	0	7,641	0	188,173
Subcontracting	0	0	0	0	0
Other direct costs	56,139	0	1,500	0	57,639
Indirect costs	155,563	0	2,332	0	157,895
Total costs	392,234	0	11,473	0	403,707
Maximum EU contribution	294,175	0	11,473	0	305,648
Requested EU contribution					305,648

2. Declaration of receipts

Did you receive any financial transfers or contributions in kind, free of charge from third parties or did the project generate any income which could be considered a receipt according to Art.II. 17 of the grant agreement ?
If yes, please mention the amount (in €)

No

4. Certificate on the methodology

Do you declare average personnel costs according to Art.II.14.1 ?

No

Is there a certificate on the methodology provided by an independent auditor and accepted by the Commission according to Art.II.4.4 ?

No

Name of the auditor		Cost of the certificate (in €), if charged under this project	
---------------------	--	---	--

5. Certificate on the financial statements

Is there a certificate on the financial statements provided by an independent auditor attached to this financial statement according to Art.II.4.4 ?

Yes

Name of the auditor	L.A.M. Ververs RA	Cost of the certificate (in €)	1,500
---------------------	-------------------	--------------------------------	-------

6. Beneficiary's declaration on its honour

We declare on our honour that:

- the costs declared above are directly related to the resources used to attain the objectives of the project and fall within the definition of eligible costs specified in Articles II.14 and II.15 of the grant agreement, and, if relevant, Annex III and Article 7 (special clauses) of the grant agreement;
- the receipts declared above are the only financial transfers or contributions in kind, free of charge, from third parties and the only income generated by the project which could be considered as receipts according to Art.II.17 of the grant agreement;
- the interest declared above is the only interest yielded by the pre-financing which falls within the definition of Art.II.19 of the grant agreement;
- there is full supporting documentation to justify the information hereby declared. It will be made available at the request of the Commission and in the event of an audit by the Commission and/or by the Court of Auditors and/or their authorised representatives.

Beneficiary's Stamp	Name of the Person(s) Authorised to sign this Financial Statement
	drs. J.C. Boot-Van Wevelingen
	Date & signature

Form C for period 2 from AIT

Form C - Financial Statement (to be filled in by each beneficiary)			
Project Number	288869	Funding scheme	Collaborative project
Project Acronym	NAVOLCHI		
Period from	01/05/2013	Is this an adjustment to a previous statement ?	No
To	31/07/2015		
Legal Name	RESEARCH AND EDUCATION LABORATORY IN INFORMATION TECHNOLOGIES	Participant Identity Code	999582382
Organisation Short Name	AIT	Beneficiary nr	4
Funding % for RTD activities (A)	75.0	If flat rate for indirect costs, specify %	N/A

1. Declaration of eligible costs/lump sum/flat-rate/scale of unit (in €)

	Type of Activity				Total (A+B+C+D)
	RTD (A)	Demonstration (B)	Management (C)	Other (D)	
Personnel costs	110,662	0	4,937	0	115,599
Subcontracting	0	0	0	0	0
Other direct costs	730	0	1,691	0	2,421
Indirect costs	66,397	0	2,962	0	69,359
Total costs	177,789	0	9,590	0	187,379
Maximum EU contribution	133,341	0	9,590	0	142,931
Requested EU contribution					142,931

2. Declaration of receipts

Did you receive any financial transfers or contributions in kind, free of charge from third parties or did the project generate any income which could be considered a receipt according to Art.II. 17 of the grant agreement ?
If yes, please mention the amount (in €)

No

4. Certificate on the methodology

Do you declare average personnel costs according to Art.II.14.1 ?

No

Is there a certificate on the methodology provided by an independent auditor and accepted by the Commission according to Art.II.4.4 ?

No

Name of the auditor		Cost of the certificate (in €), if charged under this project	
---------------------	--	--	--

5. Certificate on the financial statements

Is there a certificate on the financial statements provided by an independent auditor attached to this financial statement according to Art.II.4.4 ?

No

Name of the auditor		Cost of the certificate (in €)	
---------------------	--	--------------------------------	--

6. Beneficiary's declaration on its honour

We declare on our honour that:

- the costs declared above are directly related to the resources used to attain the objectives of the project and fall within the definition of eligible costs specified in Articles II.14 and II.15 of the grant agreement, and, if relevant, Annex III and Article 7 (special clauses) of the grant agreement;
- the receipts declared above are the only financial transfers or contributions in kind, free of charge, from third parties and the only income generated by the project which could be considered as receipts according to Art.II.17 of the grant agreement;
- the interest declared above is the only interest yielded by the pre-financing which falls within the definition of Art.II.19 of the grant agreement;
- there is full supporting documentation to justify the information hereby declared. It will be made available at the request of the Commission and in the event of an audit by the Commission and/or by the Court of Auditors and/or their authorised representatives.

Beneficiary's Stamp	Name of the Person(s) Authorised to sign this Financial Statement
	SPYRIDOULA PREVEDOUROU
	Date & signature

Form C for period 2 from UVEG

Form C - Financial Statement (to be filled in by each beneficiary)			
Project Number	288869	Funding scheme	Collaborative project
Project Acronym	NAVOLCHI		
Period from	01/05/2013	Is this an adjustment to a previous statement ?	No
To	31/07/2015		
Legal Name	UNIVERSITAT DE VALENCIA	Participant Identity Code	999953019
Organisation Short Name	UVEG	Beneficiary nr	5
Funding % for RTD activities (A)	75.0	If flat rate for indirect costs, specify %	60

1. Declaration of eligible costs/lump sum/flat-rate/scale of unit (in €)

	Type of Activity				Total (A+B+C+D)
	RTD (A)	Demonstration (B)	Management (C)	Other (D)	
Personnel costs	117,665	0	6,839	0	124,504
Subcontracting	0	0	0	0	0
Other direct costs	32,427	0	1,930	0	34,357
Indirect costs	90,055	0	5,261	0	95,316
Total costs	240,147	0	14,030	0	254,177
Maximum EU contribution	180,110	0	14,030	0	194,140
Requested EU contribution					194,140

2. Declaration of receipts

Did you receive any financial transfers or contributions in kind, free of charge from third parties or did the project generate any income which could be considered a receipt according to Art.II. 17 of the grant agreement ?
If yes, please mention the amount (in €)

No

4. Certificate on the methodology

Do you declare average personnel costs according to Art.II.14.1 ?

No

Is there a certificate on the methodology provided by an independent auditor and accepted by the Commission according to Art.II.4.4 ?

No

Name of the auditor	Cost of the certificate (in €), if charged under this project

5. Certificate on the financial statements

Is there a certificate on the financial statements provided by an independent auditor attached to this financial statement according to Art.II.4.4 ?

No

Name of the auditor	Cost of the certificate (in €)

6. Beneficiary's declaration on its honour

We declare on our honour that:

- the costs declared above are directly related to the resources used to attain the objectives of the project and fall within the definition of eligible costs specified in Articles II.14 and II.15 of the grant agreement, and, if relevant, Annex III and Article 7 (special clauses) of the grant agreement;
- the receipts declared above are the only financial transfers or contributions in kind, free of charge, from third parties and the only income generated by the project which could be considered as receipts according to Art.II.17 of the grant agreement;
- the interest declared above is the only interest yielded by the pre-financing which falls within the definition of Art.II.19 of the grant agreement;
- there is full supporting documentation to justify the information hereby declared. It will be made available at the request of the Commission and in the event of an audit by the Commission and/or by the Court of Auditors and/or their authorised representatives.

Beneficiary's Stamp	Name of the Person(s) Authorised to sign this Financial Statement
	Inmaculada Santaemilia Alcacer
	Date & signature

Form C for period 2 from ST

Form C - Financial Statement (to be filled in by each beneficiary)			
Project Number	288869	Funding scheme	Collaborative project
Project Acronym	NAVOLCHI		
Period from	01/05/2013	Is this an adjustment to a previous statement ?	No
To	31/07/2015		
Legal Name	STMICROELECTRONICS SRL	Participant Identity Code	999977657
Organisation Short Name	ST	Beneficiary nr	6
Funding % for RTD activities (A)	50.0	If flat rate for indirect costs, specify %	N/A

1. Declaration of eligible costs/lump sum/flat-rate/scale of unit (in €)

	Type of Activity				Total (A+B+C+D)
	RTD (A)	Demonstration (B)	Management (C)	Other (D)	
Personnel costs	19,049	0	2,195	0	21,244
Subcontracting	0	0	0	0	0
Other direct costs	0	0	0	0	0
Indirect costs	23,284	0	2,885	0	25,969
Total costs	42,333	0	4,880	0	47,213
Maximum EU contribution	21,166	0	4,880	0	26,046
Requested EU contribution					26,046

2. Declaration of receipts

Did you receive any financial transfers or contributions in kind, free of charge from third parties or did the project generate any income which could be considered a receipt according to Art.II. 17 of the grant agreement ?
If yes, please mention the amount (in €)

No

4. Certificate on the methodology

Do you declare average personnel costs according to Art.II.14.1 ?

No

Is there a certificate on the methodology provided by an independent auditor and accepted by the Commission according to Art.II.4.4 ?

No

Name of the auditor

Cost of the certificate (in €), if charged under this project

5. Certificate on the financial statements

Is there a certificate on the financial statements provided by an independent auditor attached to this financial statement according to Art.II.4.4 ?

No

Name of the auditor

Cost of the certificate (in €)

6. Beneficiary's declaration on its honour

We declare on our honour that:

- the costs declared above are directly related to the resources used to attain the objectives of the project and fall within the definition of eligible costs specified in Articles II.14 and II.15 of the grant agreement, and, if relevant, Annex III and Article 7 (special clauses) of the grant agreement;
- the receipts declared above are the only financial transfers or contributions in kind, free of charge, from third parties and the only income generated by the project which could be considered as receipts according to Art.II.17 of the grant agreement;
- the interest declared above is the only interest yielded by the pre-financing which falls within the definition of Art.II.19 of the grant agreement;
- there is full supporting documentation to justify the information hereby declared. It will be made available at the request of the Commission and in the event of an audit by the Commission and/or by the Court of Auditors and/or their authorised representatives.

Beneficiary's Stamp	Name of the Person(s) Authorised to sign this Financial Statement
	Roberto Silva
	Date & signature

Form C for period 2 from UGent

Form C - Financial Statement (to be filled in by each beneficiary)			
Project Number	288869	Funding scheme	Collaborative project
Project Acronym	NAVOLCHI		
Period from	01/05/2013	Is this an adjustment to a previous statement ?	No
To	31/07/2015		
Legal Name	UNIVERSITEIT GENT	Participant Identity Code	999988096
Organisation Short Name	Ugent	Beneficiary nr	7
Funding % for RTD activities (A)	75.0	If flat rate for indirect costs, specify %	60

1. Declaration of eligible costs/lump sum/flat-rate/scale of unit (in €)

	Type of Activity				Total (A+B+C+D)
	RTD (A)	Demonstration (B)	Management (C)	Other (D)	
Personnel costs	32,945	0	0	0	32,945
Subcontracting	0	0	0	0	0
Other direct costs	12,585	0	0	0	12,585
Indirect costs	27,318	0	0	0	27,318
Total costs	72,848	0	0	0	72,848
Maximum EU contribution	54,636	0	0	0	54,636
Requested EU contribution					54,635

2. Declaration of receipts

Did you receive any financial transfers or contributions in kind, free of charge from third parties or did the project generate any income which could be considered a receipt according to Art.II. 17 of the grant agreement ?
If yes, please mention the amount (in €)

No

4. Certificate on the methodology

Do you declare average personnel costs according to Art.II.14.1 ?

No

Is there a certificate on the methodology provided by an independent auditor and accepted by the Commission according to Art.II.4.4 ?

No

Name of the auditor

Cost of the certificate (in €), if charged under this project

5. Certificate on the financial statements

Is there a certificate on the financial statements provided by an independent auditor attached to this financial statement according to Art.II.4.4 ?

No

Name of the auditor

Cost of the certificate (in €)

6. Beneficiary's declaration on its honour

We declare on our honour that:

- the costs declared above are directly related to the resources used to attain the objectives of the project and fall within the definition of eligible costs specified in Articles II.14 and II.15 of the grant agreement, and, if relevant, Annex III and Article 7 (special clauses) of the grant agreement;
- the receipts declared above are the only financial transfers or contributions in kind, free of charge, from third parties and the only income generated by the project which could be considered as receipts according to Art.II.17 of the grant agreement;
- the interest declared above is the only interest yielded by the pre-financing which falls within the definition of Art.II.19 of the grant agreement;
- there is full supporting documentation to justify the information hereby declared. It will be made available at the request of the Commission and in the event of an audit by the Commission and/or by the Court of Auditors and/or their authorised representatives.

Beneficiary's Stamp	Name of the Person(s) Authorised to sign this Financial Statement
	Geert Van de Gucht
	Date & signature

Form C for period 2 from ETHZ

Form C - Financial Statement (to be filled in by each beneficiary)			
Project Number	288869	Funding scheme	Collaborative project
Project Acronym	NAVOLCHI		
Period from	01/05/2013	Is this an adjustment to a previous statement ?	No
To	31/07/2015		
Legal Name	EIDGENOESSISCHE TECHNISCHE HOCHSCHULE ZURICH	Participant Identity Code	999979015
Organisation Short Name	ETH Zürich	Beneficiary nr	8
Funding % for RTD activities (A)	75.0	If flat rate for indirect costs, specify %	60

1. Declaration of eligible costs/lump sum/flat-rate/scale of unit (in €)

	Type of Activity				Total (A+B+C+D)
	RTD (A)	Demonstration (B)	Management (C)	Other (D)	
Personnel costs	179,891	0	5,118	0	185,009
Subcontracting	0	0	0	0	0
Other direct costs	35,168	0	0	0	35,168
Indirect costs	129,034	0	3,070	0	132,104
Total costs	344,091	0	8,188	0	352,279
Maximum EU contribution	258,068	0	8,188	0	266,256
Requested EU contribution					266,256

2. Declaration of receipts

Did you receive any financial transfers or contributions in kind, free of charge from third parties or did the project generate any income which could be considered a receipt according to Art.II. 17 of the grant agreement ?
 If yes, please mention the amount (in €)

No

4. Certificate on the methodology

Do you declare average personnel costs according to Art.II.14.1 ?
 Is there a certificate on the methodology provided by an independent auditor and accepted by the Commission according to Art.II.4.4 ?

No
No

Name of the auditor	Cost of the certificate (in €), if charged under this project
---------------------	---

5. Certificate on the financial statements

Is there a certificate on the financial statements provided by an independent auditor attached to this financial statement according to Art.II.4.4 ?

No

Name of the auditor	Cost of the certificate (in €)
---------------------	--------------------------------

6. Beneficiary's declaration on its honour

We declare on our honour that:

- the costs declared above are directly related to the resources used to attain the objectives of the project and fall within the definition of eligible costs specified in Articles II.14 and II.15 of the grant agreement, and, if relevant, Annex III and Article 7 (special clauses) of the grant agreement;
- the receipts declared above are the only financial transfers or contributions in kind, free of charge, from third parties and the only income generated by the project which could be considered as receipts according to Art.II.17 of the grant agreement;
- the interest declared above is the only interest yielded by the pre-financing which falls within the definition of Art.II.19 of the grant agreement;
- there is full supporting documentation to justify the information hereby declared. It will be made available at the request of the Commission and in the event of an audit by the Commission and/or by the Court of Auditors and/or their authorised representatives.

Beneficiary's Stamp	Name of the Person(s) Authorised to sign this Financial Statement
	Juerg Leuthold / Anke Gravemann
	Date & signature